2012

Design, construction, and testing of a research quality electric machine testbed

Trever James Hassell
Michigan Technological University

DESIGN, CONSTRUCTION, AND TESTING OF A RESEARCH QUALITY ELECTRIC MACHINE TESTBED

BY

TREVER JAMES HASSELL

A REPORT

Submitted partial fulfillment of the requirements for the degree of

MASTER OF SCIENCE

(Electrical Engineering)

MICHIGAN TECHNOLOGICAL UNIVERSITY

This report, "Design, Construction, and Testing of a Research Quality Electric Machine TestBed" is hereby approved in partial fulfillment of the requirements for the Degree of MASTER OF SCIENCE IN ELECTRICAL ENGINEERING.

Department of Electrical and Computer Engineering

Signatures:

Report Advisor: _____

Dr. Wayne W Weaver

Committee Member: _____

Dr. Duane Bucheger

Committee Member: _____

Prof. John T. Lukowski

Committee Member: _____

Dr. Gordon G. Parker

Department Chair: _____

Dr. Daniel R. Fuhrmann

Date: _____

ABSTRACT

With energy demands and costs growing every day, the need for improving energy efficiency in electrical devices has become very important. Research into various methods of improving efficiency for all electrical components will be a key to meet future energy needs. This report documents the design, construction, and testing of a research quality electric machine dynamometer and test bed. This test cell system can be used for research in several areas including: electric drives systems, electric vehicle propulsion systems, power electronic converters, load/source element in an AC Microgrid, as well as many others. The test cell design criteria, and decisions, will be discussed in reference to user functionality and flexibility. The individual power components will be discussed in detail to how they relate to the project, highlighting any feature used in operation of the test cell. A project timeline will be discussed, clearly stating the work done by the different individuals involved in the project. In addition, the system will be parameterized and benchmark data will be used to provide the functional operation of the system.

ACKNOWLEDGMENTS

I am grateful to Dr. Weaver for his support and guidance throughout my Master's degree. Without his level of commitment to education and engineering, I would not have an excellent example of what a teacher and a researcher can be.

I am thankful to all of my colleagues and friends at Michigan Tech. Specifically Greg Vosters and Nishantha Ekneligoda for their helpful discussions. I would also like to thank Mark Sloat and Chuck Sannes for their guidance in my various research projects.

Lastly, and most importantly, I would like to express my gratitude to my entire family. This first starts with my parents and siblings for their unconditionally support allowing me to concentrate on my studies. I also would like to thank my wife, Aurenice Oliveira. Without her guidance and wisdom I would not have been able to achieve this goal of higher education. I would like to conclude by thanking my wife and my two beautiful daughters for giving me happiness, love, and motivation to achieve more.

TABLE OF CONTENTS

LIST OF TABLES

LIST OF FIGURES

TERMINOLOGY

Terminology helps reader to understand this Report without any difficulty with uncommon words. This report also involved several words and terms which is use in power electronics, power systems and control theory. This section defines these terms with small explanation.

Absorber: Electrical machine used to regenerate mechanical power into electrical power

Bus: A common connection point of electric power network

Fault: a discrete event that cause unacceptable changes in the power system

Filtering: Removing mechanism of unwanted component of a given information

Micro-grid: Small power system with small number of loads and sources, which can operate with or without connection to main grid

PI Controller: Proportional integral controller

Prime Mover: Electrical machine used in the traditional "motor" quadrant

States: Measurable or available information that can be used to define a physical system

Test Bed: a place equipped with instruments for testing components under working conditions

Transient: Changes that occur during a system response to an input

ACRONYMS

Acronyms help reader to understand this Report without any difficulty to find where the first definition is defined.

ADC: Analog to Digital Channel

AFE: Active Front End

APS: Applied Power System (Manufacture of Inverter)

CPS: Control Power Source

CTS: Current Trip Set-point

DTC: Direct Torque Control

ECE: Electrical and Computer Engineering department

EET: School of Technology – Electrical Engineering Technology department

EMI: Electro-Magnetic Interference

ESPB: Emergency Stop Push Button

HVAC: Heating, Ventilation, and Air conditioning

IFOC: Indirect Field-Oriented Control

IGBT: Insulated gate bipolar transistor

MADC: Multiplexed Analog to Digital Channel

MCSSE: Motor Controller and Safety System Enclosure

MPS: Main Power Source

NI: National Instruments

PC: Personal Computer

PI: Proportional Integral Control

PLC: Programmable Logic Controller

RFT: Reference Frame Theory

VFD: Variable Frequency Drive

VSI: Voltage Source Inverters

VTS: Voltage Trip Set-point

SUMMARY OF CHAPTERS

Summary of chapters will allow the readers to quickly access the content of the chapter and allow any of them to identify chapters of particular interest.

CHAPTER 1 "Introduction" discusses the motivation and background of the project, along with a basic theory of electric machines.

CHAPTER 2"Test Cell Design and Construction" discusses the test cell architecture design and construction.

CHAPTER 3 "Test Cell Component Discussion" discusses in detail all the relevant components in the systems and any feature used for test cell operation.

CHAPTER 4 "Test Cell System Parameterization" will discuss the parameterization of the test cell machines and control signals.

CHAPTER 5 "Test Cell Performance Review" will discuss the approach to obtaining component and system efficiency data along with torque and response data using slip control.

CHAPTER 6 "Conclusion" will present final conclusions and areas identified for future work.

CHAPTER 1. INTRODUCTION

For research purposes, a dynamometer test bed was designed and constructed in EERC SB31, shown in Figure 1.1. Proposed research topics could include system level testing, as well as component level testing of machines or power electronics. System level testing could be in the form of a load of a Microgrid or electrical propulsion drive system of an electric vehicle. A component level testing could include inverter and machine control, both individual and as a sub-system.

Part of this project was done in collaboration with the School of Technology-Electrical Engineering Technology (SoT-EET) as an EET senior design project. As part of Trever Hassell's responsibilities as a graduate student working in the Electrical and Computer Engineering department (ECE) under Dr. Wayne W. Weaver, he under took the roles of technical advisor and project engineer on the team. The team composition is listed in Table 1.1. The specific goal of the proposed senior design project was to investigate, design, build and commission a safety stop circuit and enclosure. An EET senior design team was established, under the advisement of Dr. Aurenice M. Oliveira and Trever Hassell. Dr. Oliveira served as the academic advisor, directing the teams work with regards to Senior Design/Capstone goals, and Trever Hassell served as the technical advisor, directing the teams individual and group tasks.

Table 1.1: EET Senior Design Team Composition

Title	Name	Affiliation
Sponsors:	Dr. Wayne W. Weaver	ECE MTU
	ABB Automation and Power	ABB Inc.
Advisors:	Dr. Aurenice Oliveira	EET, MTU
	Trever Hassell	ECE Graduate Student, MTU
Students:	Matt DeBarr	EET, MTU
	Ryan Paul	EET, MTU
	Raquiem Ali	EET, MTU

After the completion of the EET Senior Design team, Trever Hassell continued work on the test cell. The major work tasks completed were the electric machine parameterization, control signal gain tuning, system performance testing, and collection of system benchmark data. This included component efficiencies, power loss data, and slip-control performance testing. Figure 1.1 shows the completed electric machine test bed table.
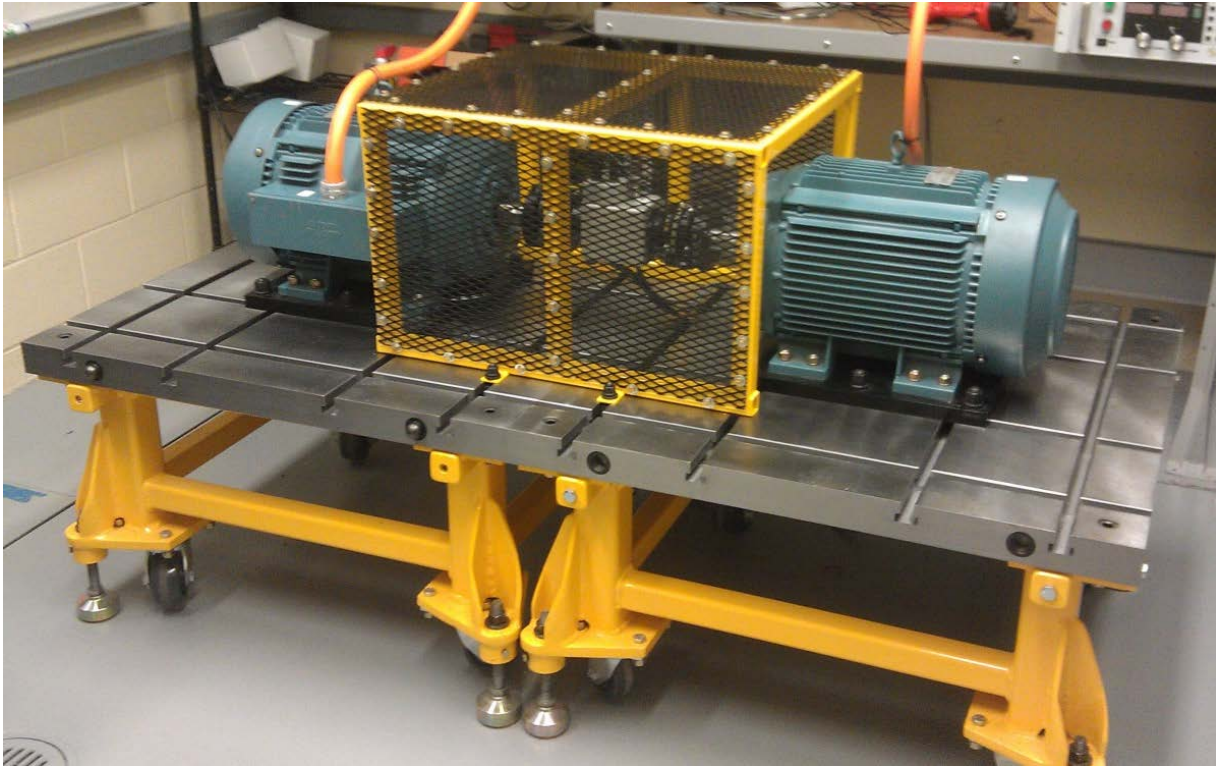
Figure 1.1: Dynamometer Test Bed Table

1.1 Motivation

The motivation for having the capability of electric machine, or electric drive propulsion system, comes from the increasing penetration of electric propulsion in the modern automobile [1] and Michigan Technological University growth in hybrid vehicle education [2]. Electric Vehicles (EV) and Hybrid Electric Vehicles (HEV) both use an electric machine for either full or partial traction of the vehicle. If a dynamometer Test Bed were developed with the expressed purpose of electric drive propulsions, and with flexibility to accommodate different machine types, this capability would be a great asset to have in the power electronics lab. Turning focus outside of the EV or HEV realm, a dynamometer test bed could also be used to model a load in a small AC Microgrid. This load could mimic the load cycle of hydraulic pump systems or a heating, ventilation, and air condition (HVAC) system of a small building.

1.2 Background

The project started as interest of Dr. Weaver to have the capability to test electric machines that were of moderate sizes. Before completion of this project, the scale of system

testing was limited to approximately ¼ HP machines. After discussing the idea with ABB Automation and Power group from New Berlin, WI; two 20 HP machines and a full four quadrant 50/40 HP Variable Frequency Drive (VFD) were donated. In addition a DC power supply and a couple of voltage source inverters (VSI), which had been previously purchased, were available for use in this project. All of these components served as the essential components in the test cell system; however system integration including some form of safety system was needed to safely control the behavior of the test cell.

The EET Senior Design project started in Fall of 2011 with the objective of to investigate, design, build and commission a safety stop circuit and enclosure. This involved the working knowledge of a how these components would integrate together, along with research into tools, techniques, and devices that could be incorporated into the test cell control system. Once a high level control and safety system was developed, the components had to be ordered and constructed. An electrical power and control enclosure was designed and constructed. The internal wiring and mounting was completed at the end of the Fall Semester. The enclosure was mounted and wired to the external components. Following that, a computer system was also specified and ordered, including a user PC and embedded controller, at this time

During the beginning of Spring 2012 semester the cell wiring was completed along with development of the software control packages used to control the test cell system. Also during this time a torque/speed sensor was selected and ordered. The cell became operational during mid-semester and the software control programs where refined to incorporate user functionality features. These features included a fault detection system, user control of torque and speed of the VFD, and DC power supply. A signal isolation system was researched and ordered. That would isolate any feedback signal to the embedded controller. Towards the end of the EET Senior Design project, the team had researched, designed, constructed, tested, and commissioned a functional safety stop system. A user manual was written to help future users of the test cell system to become familiar with it and troubleshoot it (if needed), as well as to change the test cell according to future research projects or needs.

After the completion of the EET senior design project, work was continued towards having a fully functional and known system. This included various testing and operational verification. The major tasks accomplished were the estimation of the electrical machine

parameters, the sensor signal gains were determined, and test cell operational efficiency data collected and analyzed.

1.3 Specific Individual and Team Project Contributions

This section will discuss the specific individual contributions that were accomplished outside the EET senior design team. As stated in the section 1.2, Trever Hassell participated on the team, both as a technical advisor and as a project engineer. With this dual role he contributed both to the completion on the EET senior design project and a successful commissioning of the test cell system. As the technical advisor of the team he led, he focused the group to concentrate critical task, meeting with them at least once a week both as a team and individually to discuss progress updates and answer any questions by the senior design team members. He also contributed considerably in a project engineering role. The contributions from the different project members are summarized in Table 1.2.

The project was completed in three phases: Phase I, during the fall semester of 2011, Phase II, during the spring of 2012, and Phase III, during the summer of 2012. During Phase I of the project, Trever Hassell was able accomplish the design, selection, ordering and oversee the construction of the MCSSE. The first task completed was the design of the test power architecture shown in Figure 2.1. This included working knowledge of the individual components and specific placement of the contactors to control electrical energy flow. He also researched and selected the components to be used in the MCSSE. This includes the Micrologix controller, contactors, fuses/fuseholders, safety relay, terminal blocks, enclosure fan, DIN rail mounts, DC power supply, and wire way. He also was responsible for the enclosure layout scheme and placement of the components on the back panel (see APPENDIX E. Drawing Files). He developed the wiring schematic used to construct the MCSSE and test cell cabling and guided the team with good practices in assembling the sub-plate and enclosure. He also researched and ordered many items from suppliers that are in use in the lab. This includes the isolation transformer, dSPACE embedded controller, operator station computer, and high voltage shielded power cables and connectors.

During Phase II of the project, I continued to research and order several components needed to complete the test cell. This would include the motor flexible coupling, torque sensor, motor coupling guard, and control signal isolation modules. In addition to this he bent the

conduit used for the ESPB enclosures and operations, guided the team to complete the wiring of the high voltage cables, communication cables. He also installed the analog control signal wiring between the work bench and controller station. Also during phase II he wrote the initial Micrologix program that allowed running the test cell system. That work was then continued by a senior design team member. He also worked very closely with the senior design team member who was responsible for the VFD communication LabVIEW program. Trever specifically set up the drive with the appropriate parameters to allow communication between controller station and VFD. Trever also completed approximately 75 percent of the test cell user's manual and documentation.

During Phase III of the project I continued working on several issues to complete the test cell project. These issues included control signal gain tuning, electrical machine parameter estimation, baseline system data collection, and test cell performance testing.

Table 1.2: Project Major Task Contribution

Phase	Task	EET Senior Design	Trever Hassell
I:	Cell Architecture Design		X
	Test Cell Safety Research	X	
	MCSSE Design		X
	MCSSE Parts Selection and Procurement	X	X
	MCSSE Construction	X	X
	Isolation Transformer		X
	Cabling and Connectors	X	X
	Embedded Controller/PC Station		X
II:	Initial Micrologix Program		X
	Expanded Micrologix Program w/ added features	X	
	Test Cell Power/Control Wiring	X	X
	ABB VFD Drive Configuration		X
	ABB VFD LabVIEW Program	X	
	Motor Coupling/Torque Sensor Specifications		X
	Test Cell User Manual	X	X
III:	Signal Isolation and Interface Board		X
	Signal Gain Tuning		X
	Electric Machine Parameter Estimation		X
	System Performance Characterization		X

X denotes at least 25% of work contributed to task

1.4   Electric Machine Control Theory

There will be three strategies discussed for induction machine drive system; volts per hertz, slip control, and field oriented control. The basic theory for developing the equivalent models and the control strategies are formulated from [3, 4]. The basic model begins with the a-b-c circuit equations for a general machine the per phase equivalent circuit, shown in Figure 1.2. This per phase equivalent has four major sections: the voltage input source (V_1), stator parameters (R_1, L_{l1}), the magnetic coupling (R_c, L_m), rotor parameters (R_2, L_{l2}), and rotor voltage source (V_{12}). The prime notation represents "as seen from the stator side".
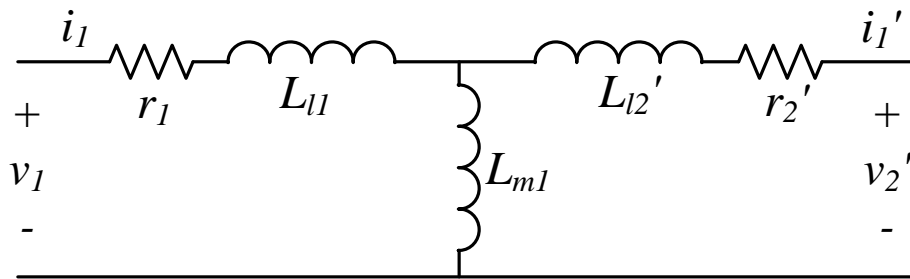
Figure 1.2: General Machine per Phase Equivalent

All per phase equivalent can also be expressed in terms of its equations as seen in (1.1). These voltage equations imply a seventh-order model which is already reduced considerably relative to actual rotor and stator construction. Also the stator and rotor circuits are split into separate equations that are coupled by the flux linkage between the respective phase and the stator/rotor. The torque of the machine is derived from the interaction of the flux linkage of the field and armature current. The interaction of these two quantities couple force to spin the rotor shaft. During steady state and conditions the flux linkage can be approximated to a constant, K as shown in (1.2). In addition the angle difference between the rotor current, I_r, and flux linkage needs to be taken into account. For maximum torque production, the angle difference, δ_r, that the rotor flux leads the rotor currents.

$$v_{as} = r_s i_{as} + \frac{d\lambda_{as}}{dt} \qquad v_{ar} = r_r i_{ar} + \frac{d\lambda_{ar}}{dt}$$
$$v_{bs} = r_s i_{bs} + \frac{d\lambda_{bs}}{dt} \qquad v_{br} = r_r i_{br} + \frac{d\lambda_{br}}{dt} \qquad (1.1)$$
$$v_{cs} = r_s i_{cs} + \frac{d\lambda_{cs}}{dt} \qquad v_{cr} = r_r i_{cr} + \frac{d\lambda_{cr}}{dt}$$

$$T = -K \, I_r \sin \delta_r \qquad (1.2)$$

To realize the volts per hertz control strategy, several key observations need to be considered. The first observation is the relationship of electrical frequency to electrical rotor frequency at rated conditions. Figure 1.3 shows the torque/speed curve for motors with NEMA Design A-C characteristics. It can be observed that in the region around full load speed, the torque slope is very steep. In this area, the electrical stator frequency and electrical rotor speed are very close to the same value. This implies that controlling the electrical rotor frequency can be accomplished from controlling the electrical stator frequency.
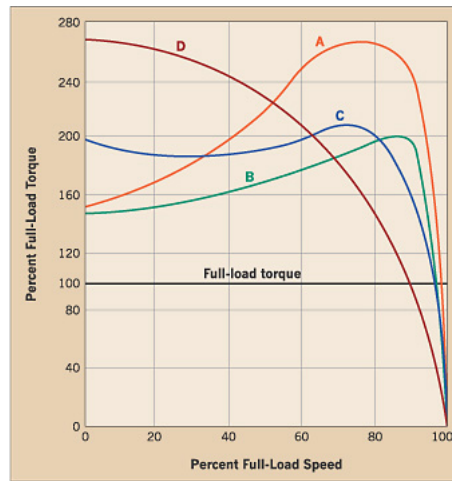
Figure 1.3: General shape of torque-speed curves for motors with NEMA Design A, B, C, and D characteristics [5]

Another key observation used for realizing volts per hertz is observing the behavior of (1.1). From this equation, it can be seen that the stator voltage is related to the flux linkage and voltage drop in the machine. At intermediate to high speeds the flux linkage term will dominate the stator voltage equation. At steady state the phase A voltage equation in (1.1) can be written as in (1.3), showing the magnitude of the voltage applied is related to the stator flux linkage by the electrical frequency [3]. This suggests that to maintain constant flux and therefore avoiding

7

saturation, the stator voltage magnitude should be proportional to the electrical frequency. The stator flux linkage can be set to the rated flux value as shown in (1.4).

$$V_s = \omega_e \Lambda_s \qquad (1.3)$$

$$\Lambda_{rated} = \frac{V_{a\text{-rated}}}{\omega_{e\text{-rated}}} \qquad (1.4)$$

As simple and easy it is to implement, there are some drawbacks to using volts per hertz. First, there is an inherent rotor speed difference from desired rotor speed to actual rotor speed. This is attributed the slope of torque-speed relationship. The more torque needed to be supplied to the load, the greater this difference in the two speeds. Second is that the relationship in (1.3) is only valid in steady state, so for dynamic behavior the response of the machine is not predicted.

To help address these two issues with volts per hertz control, slip control can be used. This strategy is also a simple method to implement. One approach to slip control is to assume a slip value based on machine parameters and compensate the commanded electrical frequency, as shown in (1.5). This method does not require any extra sensor feedback however requires knowledge of the slip speed which can vary with load or changes in machine performance, causing inaccurate steady state error. A second method of slip control would be to "close the loop" on speed. A proportional-integral (PI) controller could be used to automatically compensate for the difference in commanded frequency/speed and actual frequency/speed. The method requires a need for a speed sensor however the difference of the electrical rotor frequency and commanded reference frequency is driven to zero by the PI controller. Both forms of slip control result in better steady state performance when compared to volts per hertz control however the dynamic behavior is also governed by the PI controller gains.

$$\omega_e = \omega_r + \hat{\omega}_s \qquad (1.5)$$

The previously discussed methods involved controlling the speed of the machine to a command value. The next evolution in electric machine drive control is field-oriented control (FOC) [3]. FOC takes into the account the dynamic behavior inherent to the electrical machines and commands a electro-magnetic torque output of the machine, rather than a machine speed. However understanding these inherently time varying equations become difficult and computational intense when simulating in their native form. Because of this, reference frame theory (RFT) was employed to reduce this time varying equation to a "DC like" output. The idea

8

behind RFT is to fix the perspective of the equation with a spinning frame. This could be the actual rotor position, or in relation to the spinning rotor flux. The latter is the more important aspect in relation to torque and speed control. The precise control of torque is the goal of any motor drive system. For a more detailed explanation in RFT see chapters 3 and 4 of [3].

The general power invariant Park's transformations for the 3-phase system is shown in (1.6). This three-by-three matrix is design to transform a time varying values into some "DC like" output. This is highly dependent on the choice of reference angle (θ) chosen. The choice of angle for different transformations will be important.

$$\Gamma_{odq}(\theta) = \sqrt{\frac{2}{3}} \begin{pmatrix} \sqrt{\frac{1}{2}} & \sqrt{\frac{1}{2}} & \sqrt{\frac{1}{2}} \\ \cos(\theta) & \cos\left(\theta - \frac{2\pi}{3}\right) & \cos\left(\theta + \frac{2\pi}{3}\right) \\ -\sin(\theta) & -\sin\left(\theta - \frac{2\pi}{3}\right) & -\sin\left(\theta + \frac{2\pi}{3}\right) \end{pmatrix} \qquad (1.6)$$

The first step to get the rotor flux frame, is to transform the a-b-c equations into a 0-d-q reference frame. This new reference frame is intended to divide the voltages and currents into portion that contribute to pure loss, flux and torque. Choosing the reference frame angle equal to zero will $(\theta = 0)$ result in the appropriate transformation, see (1.7). The torque output of a machine is a function of q-axis current (torque input) and flux values, since the zero axis represents a pure loss, any current flowing on this axis does not contribute to torque contribution. The d-axis translates to the amount of flux that the machine is producing.

$$\Gamma_{012} = \sqrt{\frac{2}{3}} \begin{pmatrix} \frac{1}{\sqrt{2}} & \frac{1}{\sqrt{2}} & \frac{1}{\sqrt{2}} \\ 1 & -\frac{1}{2} & -\frac{1}{2} \\ 0 & \frac{\sqrt{3}}{2} & -\frac{\sqrt{3}}{2} \end{pmatrix} \qquad (1.7)$$

The 0-d-q domain equivalent circuits are shown in Figure 1.4. Theses equations are then transformed to the rotor flux frame. In this reference frame the output values of the machine have a constant value during steady state operation and will only varying during dynamic operation.

9
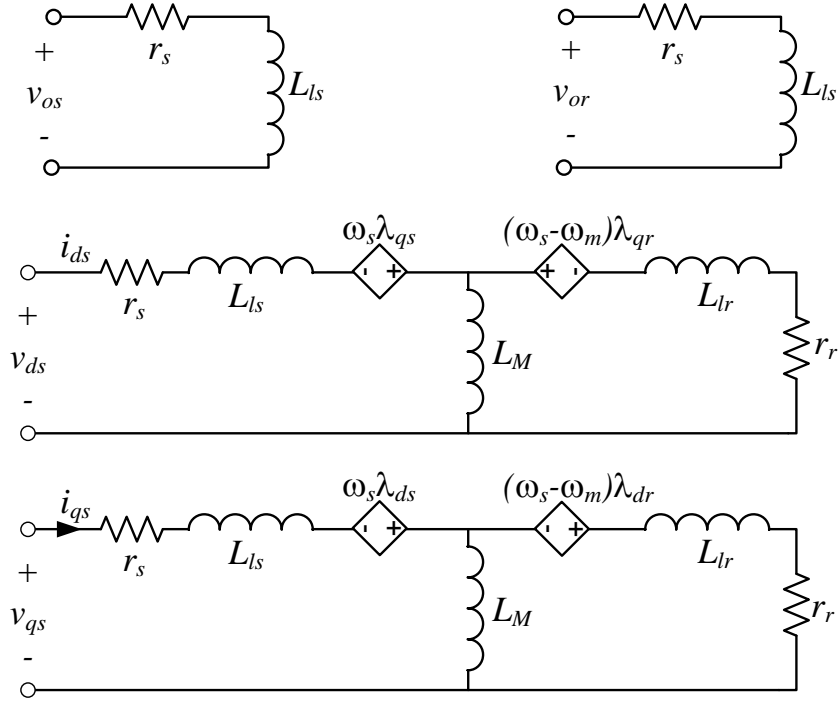
Figure 1.4: Induction Machine o-d-q equivalent circuits

In the rotor flux reference frame there are few quantities that would need to be known in order to properly work, most notably the magnitude and angle of the rotor flux. This can be accomplished through added hall-effort sensors to the machine, or via an estimator. The estimator takes known quantities of the machine operation and thru some mathematical relationship estimates the two components of rotor flux $(\lambda_{dr}, \lambda_{qr})$ that are used to find the rotor flux angle and magnitude. The estimator uses the d and q axis current, as well as the mechanical speed to estimate the respective flux linkage values. The estimator equations are shown in (1.8). With the known quantities of the rotor flux linkage d and q axis components the magnitude and angle of the rotor flux is found using (1.9).

$$\frac{d\lambda_{dr}}{dt} = -\frac{\lambda_{dr}}{\tau_r} - n_p \omega_m \lambda_{qr} + \frac{L_M}{\tau_r} i_{ds}$$

$$\frac{d\lambda_{qr}}{dt} = -\frac{\lambda_{qr}}{\tau_r} + n_p \omega_m \lambda_{dr} + \frac{L_M}{\tau_r} i_{qs}$$

(1.8)

$$\Psi = \sqrt{\lambda_{dr}^2 + \lambda_{qr}^2}$$

$$\rho = \tan^{-1}\left(\frac{\lambda_{qr}}{\lambda_{dr}}\right)$$

(1.9)

10

For the FOC control method, the machine equations are transformed entirely into the rotor flux frame, see (1.10) and (1.11). The control inputs are u_{flux} and u_{torque} values. These input values can be determined by many different means, however most easily by using a PI controller. The u_{flux} term represents the input that will result in changing the flux magnitude of the machine whereas the u_{torque} term contributes to the q-axis current, and the term that generates the most torque input. The actual torque produced by the machine is a consequence of the machine states and the input as shown in (1.12) or (1.13). The choice of which equation depends on the state chosen for flux linkage, however both of these equation shows that torque is produce from the interaction of the flux linkage (ψ or λ_{dr}, λ_{qr}) and the machine currents.

$$\begin{pmatrix} v_d \\ v_q \end{pmatrix} \overset{\Delta}{=} \sigma \begin{pmatrix} -n_p\omega_m i_q - \dfrac{L_m}{\tau_r\psi}i_q{}^2 - \dfrac{L_m}{\sigma L_r\tau_r}\psi + u_{flux} \\ \dfrac{n_p L_m}{\sigma L_r}\omega_r\psi + n_p\omega_m i_d + \dfrac{L_m i_q i_d}{\tau_r\psi} + u_{torque} \end{pmatrix} \tag{1.10}$$

$$L_s = L_{ls} + L_M$$

$$L_r = L_{lr} + L_M$$

$$\sigma = \frac{L_s L_r - L_M{}^2}{L_r}$$

$$\gamma = \frac{L_M{}^2 r_r + L_r{}^2 r_s}{\sigma L_r{}^2}$$

$$\tau_r = \frac{L_r}{r_r}$$

$$\frac{di_q}{dt} = -\left(\frac{L_m{}^2}{\sigma L_r\tau_r} + \frac{r_s}{\sigma}\right)i_q + u_{torque}$$

$$\frac{di_d}{dt} = -\left(\frac{L_m{}^2}{\sigma L_r\tau_r} + \frac{r_s}{\sigma}\right)i_d + \frac{L_m}{\tau_r}\psi + u_{flux}$$

$$\frac{d\psi}{dt} = -\frac{1}{\tau_r}\psi + \frac{L_m}{\tau_r}i_d \tag{1.11}$$

$$\frac{d\rho}{dt} = n_p\omega_m + \frac{L_m i_q}{\tau_r\psi}$$

$$\frac{d\omega_r}{dt} = \frac{n_p L_m}{JL_r}\psi i_q - \frac{T_{load}}{J}$$

$$T_{elec} = \frac{3}{2}\frac{L_M}{L_r}n_p\,\psi\,i_q \tag{1.12}$$

$$T_{elec} = \frac{3}{2}\frac{L_M}{L_r}n_p\,(\lambda_{dr}i_{qs} - \lambda_{qr}i_{ds}) \tag{1.13}$$

CHAPTER 2. TEST CELL DESIGN AND CONSTRUCTION

This chapter will discuss the design and construction of the test cell. The topics that will be discussed include; the approach to safety, system architecture designs, test cell room layout and wire/cable routing, and project timeline progress.

The test cell architecture was design for two machines "back to back" testing. A one-line schematic is shown in Figure 2.1. The two identical induction machines are mechanically coupled together via flexible motor couplings and torque sensor. There is only one source of electrical energy for the motors, a 208 VAC 50 Amp 3 phase receptacle, which is supplied from a power panel in the Electrical Energy Resource Center (EERC) SB31. This source would supply two "loads"; the magna DC power supply/inverter and an ABB frequency drive. The Magma DC power supply powers the APS inverter, which in-turns supplies power the "Prime Mover" electrical machine, M1. Because the frequency drive operates at a different voltage than the main source power a transformer is needed. The frequency drive would then supply the "Absorber" electrical machine, M2.
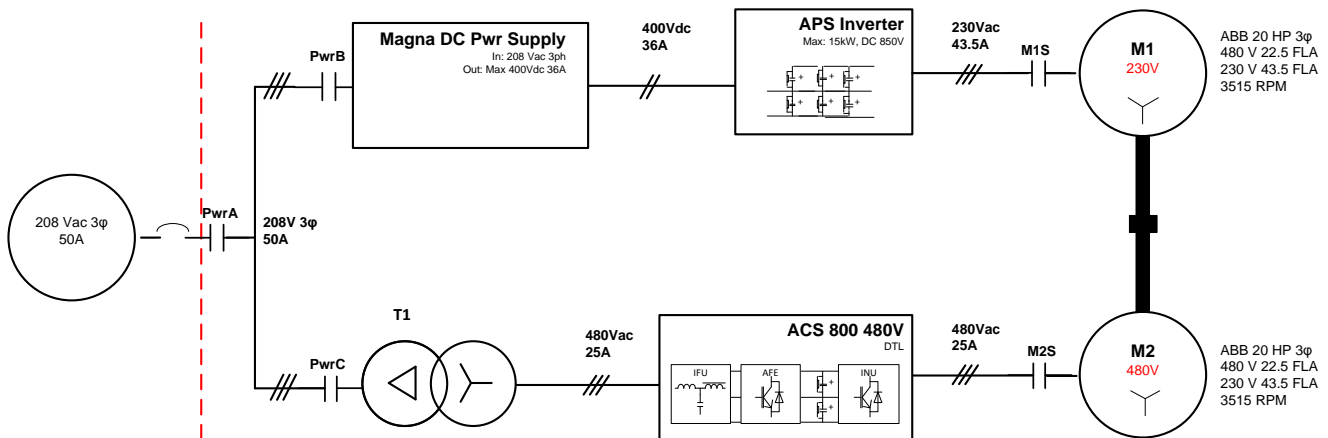
Figure 2.1: One Line Test Bed Circuit

The layout of test cell room is shown in Figure 2.2. This layout shows the operator station (PC Station), work benches, shelving, transformer, power panel, VFD, motor controller enclosure, and motor table. This layout allows the user to have access to all the different components.
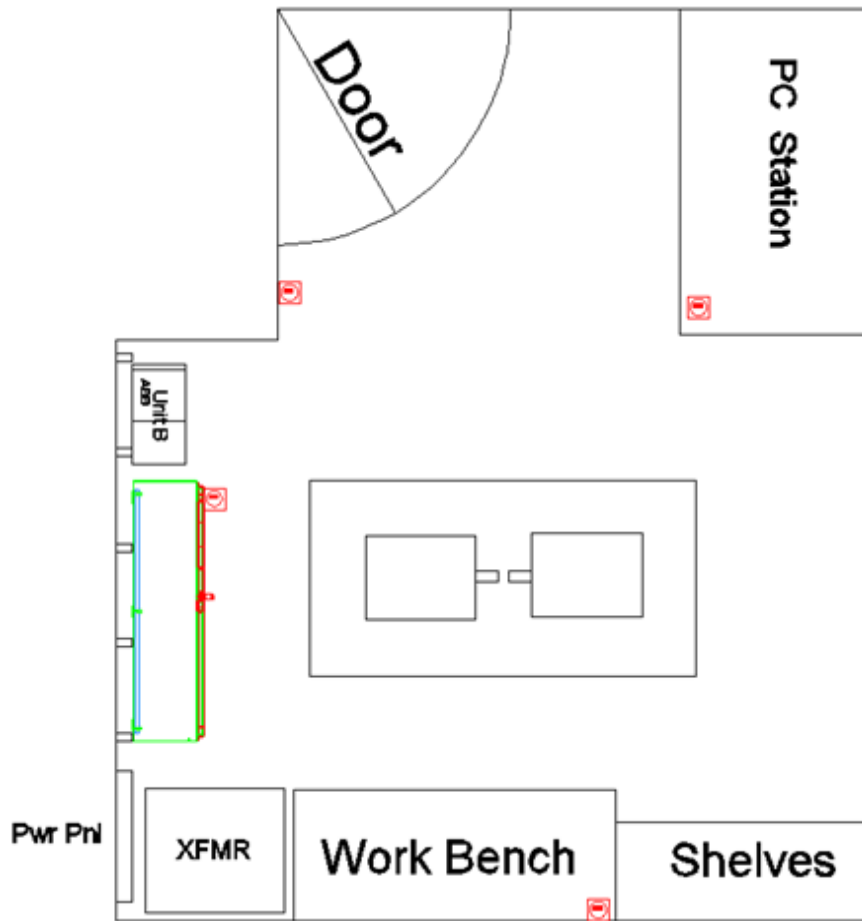
Figure 2.2: Test Cell Layout

2.1   Safety Considerations

While designing the dynamometer test bed, safety was a top concern. The test cell safety layout is shown in Figure 2.3 and it shows two zones of safety; the Green Zone and Red Zone. These zones are a mental construct used to indicate where the areas of concerns are for the test cell user. There are no physical barriers, or markings, in the test cell to differentiate the zones. The Green zone has virtually no added risk or safety concerns, whereas the red zone requires greater caution. The "Green Zone" is the intended area for the operator to be during any testing or computer use and has no greater risk due to the test cell components. The "Red Zone" has significantly greater risk of injury because of the Testbed table, cables and cable trays, and the exposed test cell electrical components; such as the inverter, DC power supply, transformer, dynamometer, and enclosure. These devices have adequate guarding to protect from injury, however the risk is greater around these components. To protect the torque sensor cables, a cable

tray was placed on the floor below the workbench. Users should observe caution to when working around the workbench. The work bench also has several electrical components that could cause risk of injury and the user should be cautious when working around this. For these reasons mentioned the "Red Zone" is determined to have an increased risk and heighten user caution is required.
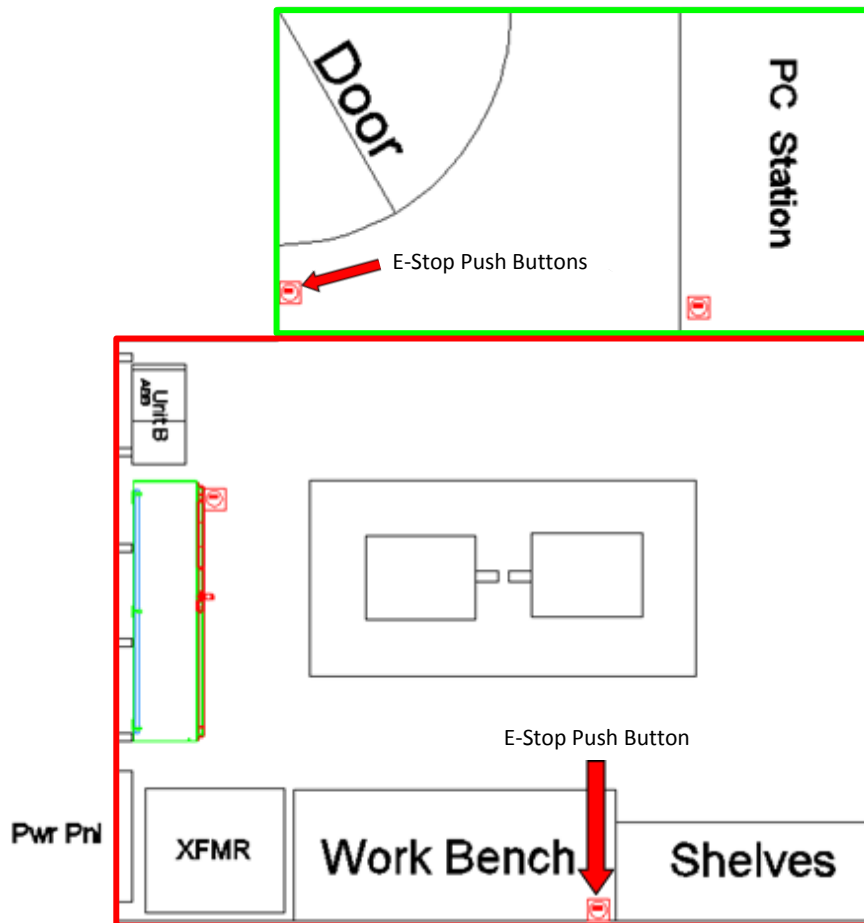
Figure 2.3: Test Cell Safety Area Layout

2.2   Design Considerations

Throughout the entire test cell system there are several varying power supplies with the majority of power supplies powering the inverter controls and control devices including 5 VDC and 15 VDC powers supplies to power the signal isolation and interface board. Turning attention to the MCSSE, it has only two external power sources. They are the "Main Power" source (MPS) (208 VAC 3ph) and the "Control Power" source (CPS) (120 VAC 1ph). Table 2.1 lists all of the

electrical energy levels present in the system and the rated maximum current carrying (fused limited) ability of the circuit.

Table 2.1: Test Cell Electrical Power Operation Levels

Name	Voltage	Max Current	Description
Main Power*	208 VAC3ph	50 A_{rms}	Line feeds to Motors
Motor 1	208 VAC 3ph	50 A_{rms}	Load feeds for Motor1 (Prime Mover)
Motor 2	480 VAC 3ph	30 A_{rms}	Load feeds for Motor2 (Absorber)
Control Power*	120 VAC 1ph	10 A_{rms}	Power for Micrologix, Aux Fans, DC Power Supply
Control System	24 VDC	10 A_{rms}	Power for Test Cell I/O, Stop PB, safety relay

*denotes external power source
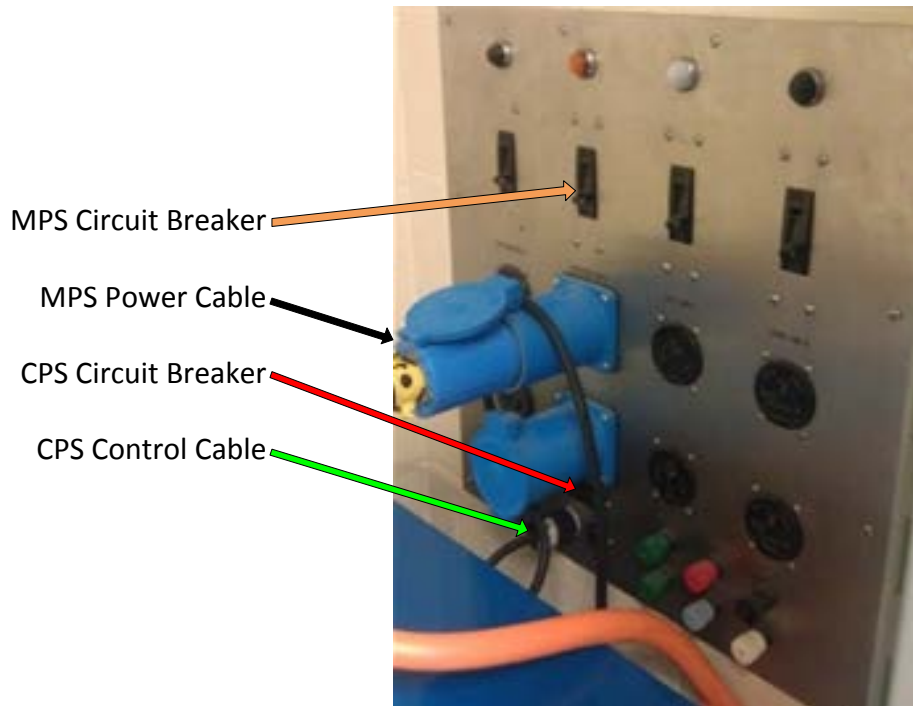
Figure 2.4: Power Panel Connections

The 120 VAC source CPS is independent of the MPS and supplies the 24 VDC power used for the safety control system (SCS). The SCS consists of several Emergency Stop pushbuttons (ESPB), test cell Input/output control, and a safety relay. This is done for both practicality and safety. Keeping the CPS separate from the high voltage MPS allows the SCS to be program, tested, and debugged. When testing the communication or MCSEE systems, the MPS is not required to be on, therefore to minimize the risk of injury the MPS is turned off. It

also allows a properly trained individual to work in the motor control cabinet with increase protection from the MPS.

2.2.1 Motor Controller and Safety System Enclosure

The Motor Controller and Safety System Enclosure (MCSSE) was design to house all of the test cell infrastructure controller hardware. The system includes five 60 A contactors that can control the flow of electrical energy in the test cell. They are controlled by a Allen-Bradley Micrologix controller and a Allen-Bradley safety relay. The reason both the devices control the operation of the contactors is for safety. The safety relay monitors the ESPB, using two different electrical circuits. If one of the contacts on the ESPB happens to malfunction, the safety relay will detect this and remove the electrical power to the outputs of the Micrologix, therefore open the contactors. If the safety relay does not detect an issue, the Micrologix controller has control on turning the contactors on and off, based on its user defined program. The advantages of having both devices controller the contactor operation is the reliability of the safety relay and functionality of the being able to program the Micrologix.

System level electrical schematics were developed (see Appendix E) and the MCSSE was design specifically to keep the high voltage AC power separate from the low voltage DC safety system power. Figure 2.5 shows the MCSSE with the enclosure doors open. The green box indicates the low voltage DC wiring. This is done to minimize any induced voltage on the DC Safety System control circuits which may cause undesired behavior. The presence of the low voltage AC (120 VAC single phase) is necessary to power the DC power supply, Micrologix controller, enclosure ventilation fan, and the inverter heat sink fan, it is located inside the green box (upper right hand corner). This location was chosen to again minimize any induced voltage the low voltage DC circuits will experience.
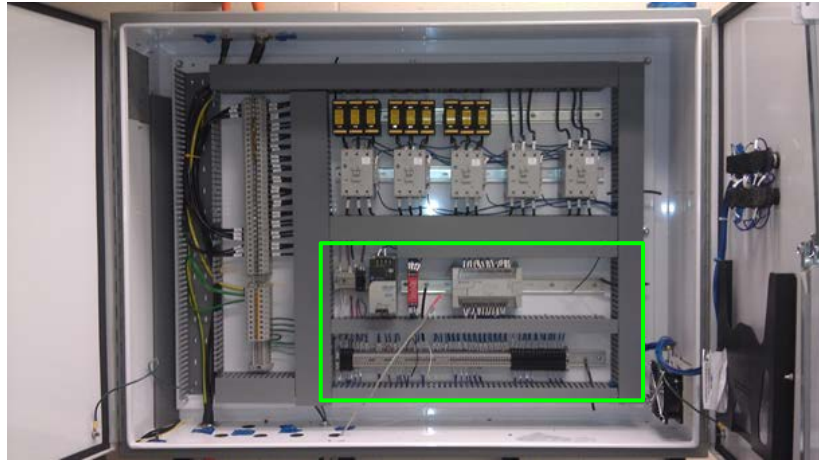
Figure 2.5: Enclosure Panel Payout

2.2.1 Test Cell Wire routing

The MCSSE was design to be the interface of the test cell power cable routing; therefore all of the power cables enter and exit this enclosure. Figure 2.6 shows the various cable routes in the test cell. There are four types of cable runs show; high voltage AC power, DC safety system circuit, communication, and control signals. The high voltage AC cables are specifically not routed right next to the low voltage cables. This again, is to minimize any induced voltage onto the low voltage cables. The high voltage AC power cables installed are shielded to also help to minimize any electro-magnetic interference (EMI) broadcasted from the inverter or ABB VFD. During installation of the high voltage cable shields were confirmed to have less than 0.5 Ω between shield and ground, most measured approximately 0.1 Ω.

The DC safety stop circuits were wired to the various ESPB enclosures via electric metallic conduit. This method protects the wiring both from physical damage and also serves to shield the wires from EMI that could be broadcast form the inverter or VFD. This also allows for seamless wiring from the enclosure to the ESPB enclosures.

Both the Modbus and Micrologix communication is accomplished via a shield communication cable from the PC station to the VFD and the enclosure. This cable is attached to the conduit and crosses the room via the ceiling. The control signals are routed from the PC station to the work bench via a 3 inch plastic wire way attached to wall. This serves to physically protect the cables from damage. The control signal cables are also shielded to protect from any EMI that could be present in the test cell room.
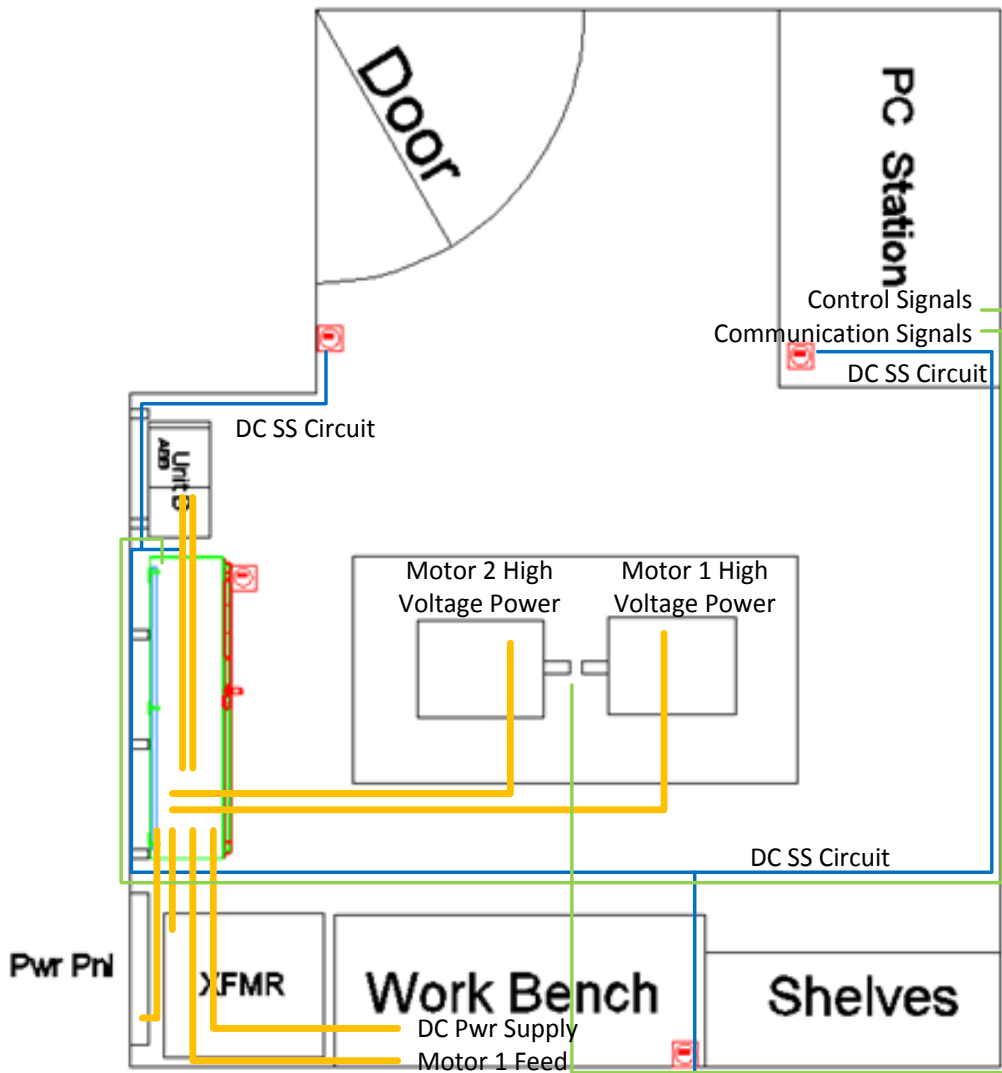
Figure 2.6: Test Cell Cable Routing

2.2.2 Control Signals

All of the analog and digital control signals that go from the embedded controller to the inverter are routed in plastic cable tray on the western and northern test cell walls. Part of the cable tray highlighted in Figure 2.7. Since the functionality of the test cell system may change, as much flexibility was built in the test cell design and the cable tray was installed to hold a high capacity of cables compared to was is being current used. As of the completion of the project, the cable tray holds 6 analog shielded cables, one 6 conductor digital shielded cable, and three cables for the torque sensor, and one CAT5 cable for communications. This cable tray allows for the addition of my several more cables if the system were to require more analog system channels. The location of the cable tray was chosen to allow for maximum user access and at the same

maximized the distance between the analog signals and power cables, helping to minimize any induced noise on the analog signals.
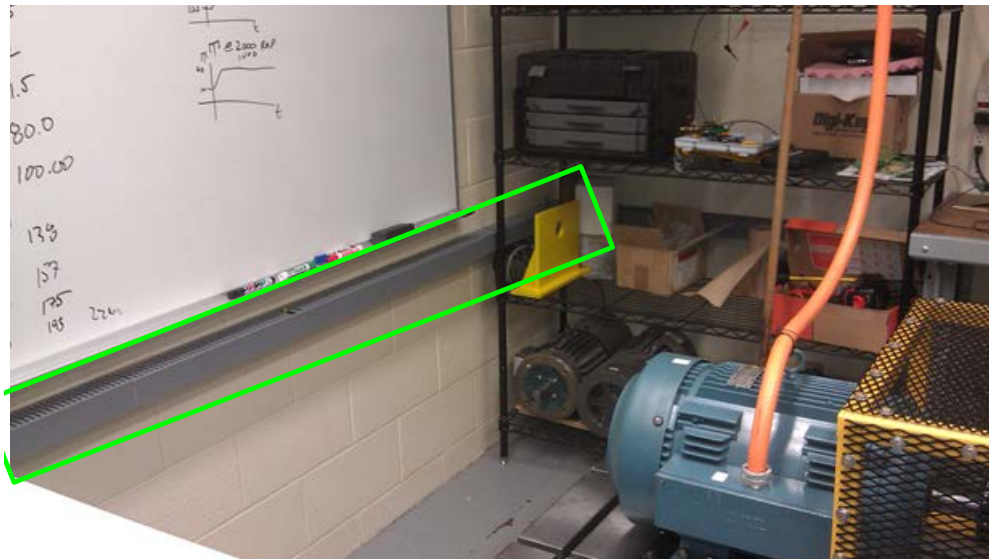
Figure 2.7: Control Signal Cable Tray

The analog cables used in the test cell were built with BNC connectors for flexibility and user convenience. Both the connections points, dSPACE and the signal interface board, have BNC female connectors, making reconfiguring and troubleshooting the signal channels easier for the test cell user. The analog signals are labeled with a channel number, in contrast to channel name, to allow for easy reconfiguration while maintaining easy of troubleshooting.

2.3   Project Progress Timeline

The project started at the beginning of Fall semester in September of 2011. At this time previous work had be done to; acquire donations for the electrical machines and VFD, tests cell electrical machine table was designed and constructed, mounting hardware attached to the wall, various components for use in the test cell purchased. The various components are comprised of DC power supply, several inverters, and electrical power meter with accessories. Figure 2.8 shows the state of the test cell at the start of the project.

Figure 2.8: Test Cell Photo – Start of Project

During the fall semester of 2011, Phase I of the project, the EET Senior Design team (including myself) researched and designed a architecture approach, ordered, and constructed the Test Cell Infrastructure Enclosure and Subpanel, as shown in Figure 2.9. Along with the enclosure and subpanel, the team ordered the materials necessary for the complete the test cell power cable routing. Several other components were also researched and ordered, including the isolation transformer, test cell computer, PLC, and safety relay.
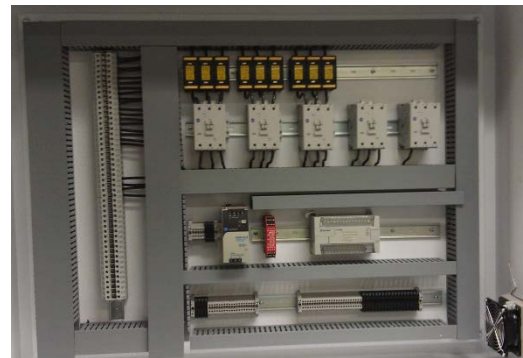
(a)   (b)

Figure 2.9: Test Cell Infrastructure (a) Enclosure and (b) Sub-panel

During the spring semester of 2012, Phase II of the project, the EET Senior Design team continued to procure parts for the test cell, program the test cell infrastructure control, develop the LabVIEW VFD control, complete the power and signal routing, and complete the safety items necessary for operation of the dynamometer. Some of the major components purchased

during this phase of construction were the embedded controller, flexible coupling, and torque sensor.

During the summer semester of 2012, Phase III of the project, the final items were completed to have a fully functional system. These final items include control signal isolation, control signal interfacing, system data and characterization, along with machine data and characterization. All of these items will be discussed in detail in CHAPTER 4. The completed test cell system photo is shown in Figure 2.10.

Figure 2.10: Completed Test Cell System

CHAPTER 3. TEST CELL COMPONENT DISCUSSION

This chapter will discuss the general operation of the major components, as well as any feature that is used specifically for the operation of the test cell. Each component will be discussed for general operational behavior as well as any relevant info gained during commissioning of the test cell. Figure 3.1 shows the system diagram in relation to the major individual components listed in Table 3.1, via the abbreviation letter.

Table 3.1: Test Cell Component Discussion

Abbreviation Letter	Component Name
A	Variable Frequency Drive
B	Induction Machines
C	Isolation Transformer
D	DC Power Supply
E	DC-AC Inverter
F	Motor Coupling Assembly
G	Controller Station
H	Control Signal Isolation and Interface
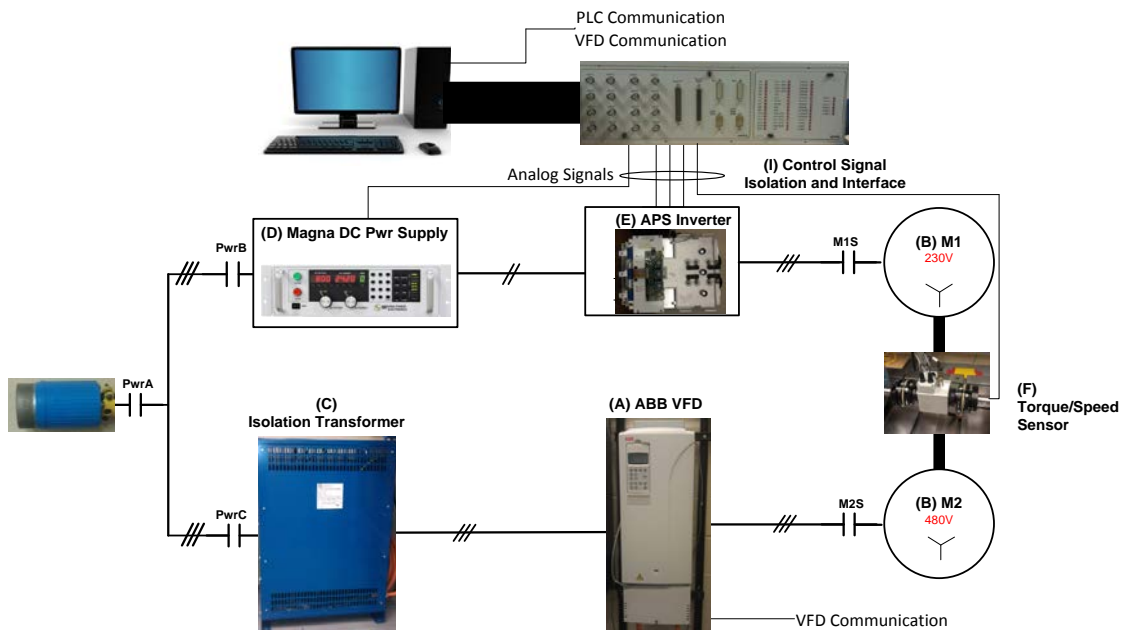
Figure 3.1: Test Cell System and Component Integration Overview

22

3.1   ABB Variable Frequency Drive

The ABB Variable Frequency Drive (VFD), see Figure 3.2, was donated from ABB Automation and Power based out of New Berlin, Wisconsin. It is intended to provide the load torque in the dynamometer system. It is an ultra-low harmonic (ULH) VFD, which minimizes the amount of harmonics injected from the grid or power supply. The VFD features insulated gate bipolar transistor (IGBT) controlling the supply side of the drive line connections to the DClink, known as an active front end (AFE). This is in contrast to the conventional diode bridge used in other VFD systems [6]. The AFE permits the ABB VFD to control the line current to sinusoidal waveform and the built in harmonic mitigation eliminates the need for additional, expensive equipment like transformers or line reactors. The AFE also ensures that the drives meet the harmonic distortion standards set by the IEEE 519-1992 standard. The ABB VFD features Direct Torque Control, and open-loop dynamic speed-control with accuracy matching AC drives using closed loop flux vector control, Start-up Assistant estimates motor parameters by the user entering nameplate info, and Adaptive Programming [6].

Figure 3.2: ABB Variable Frequency Drive

3.1.1   ABB VFD Specifications and Limits

The relevant VFD specifications are listed in Table 3.2. The ABB VFD is a full four-quadrant drive and has the capability to control up a 40 HP Continuous duty. It operates on 380-

500 VAC 3 phase power with a variation of input frequency of 48-63 Hz. The Drive has a max output frequency of 300 Hz. The drive is a deceivingly heavy, weighting around 150 lbs.

Table 3.2: ABB VFD Information

Description	Value
Part Number	ACS800-U31-0050-50
Serial Number	8112100765*
Nominal Power (ND/HD)	50/40 HP
Nominal Input Voltage (Normal Duty)	380-500 V
Input Frequency	48-63 Hz
Input Power Factor	0.99
Input Current (Cont/Max)	65/118 A
Motor Line Current (ND/HD)	67/57 A
Nominal Efficiency	97 %

3.1.2 ABB VFD Communications and Drive Setup

The VFD has several options for control input such as front panel keypad, and using a fieldbus adaptor the drive can communicate on various industry communication protocols. For the test cell setup, the VFD communicates via Modbus RTU receiving its commands from the test cell PC. If desired, the drive could also be easy configured to be controlled via the front panel simply by changing a few parameters.

The communication signal routing map is shown in Figure 3.3. This mapping illustrates how the signals sent on the Modbus network are sent to the appropriate internal VFD parameter. The right side of Figure 3.3 shows 3 major controlling input to the VFD; MAIN CW, EXT REF1, and EXT REF 2. The "MAIN CW" is the main control word and is used to control the drive to different operational states. These states of the VFD include; if the VFD is in "Ready On", "Ready Ref", "Ready Run", and "Fault". The "Ready On" state is when the VFD is powered with no Fault detected. If a fault is detected the VFD goes automatically goes into the "Fault". Once in "Ready On" state the VFD transition to "Ready Ref" after a few seconds and is awaiting the "Ready Run" command. When the "Ready Run" command is given, the VFD will then began executing the speed and torque references.

In Figure 3.3 the speed reference is read via the Modbus communication network and routed to EXT REF1. The torque reference value is mapped to 20.06 MAX TORQUE, an

internal parameter in the VFD. This VFD parameter limits the amount of torque the drive and machine will produce. Only during inverter or DC power supply faults will the VFD speed reference be the actual speed of the machine. During most operational points, the VFD will control the torque of the system, and the inverter will control the speed of the system.

Many parameters had to be set appropriately to result in successful operation in the test cell system. These parameters are listed Table 3.3. Most of these parameters determine which parameter locations the reference values are read from. Several features had to be changed from their default value. These included disabling the motor stall fault, utilizing the DTC control mode, and the maximum current values.
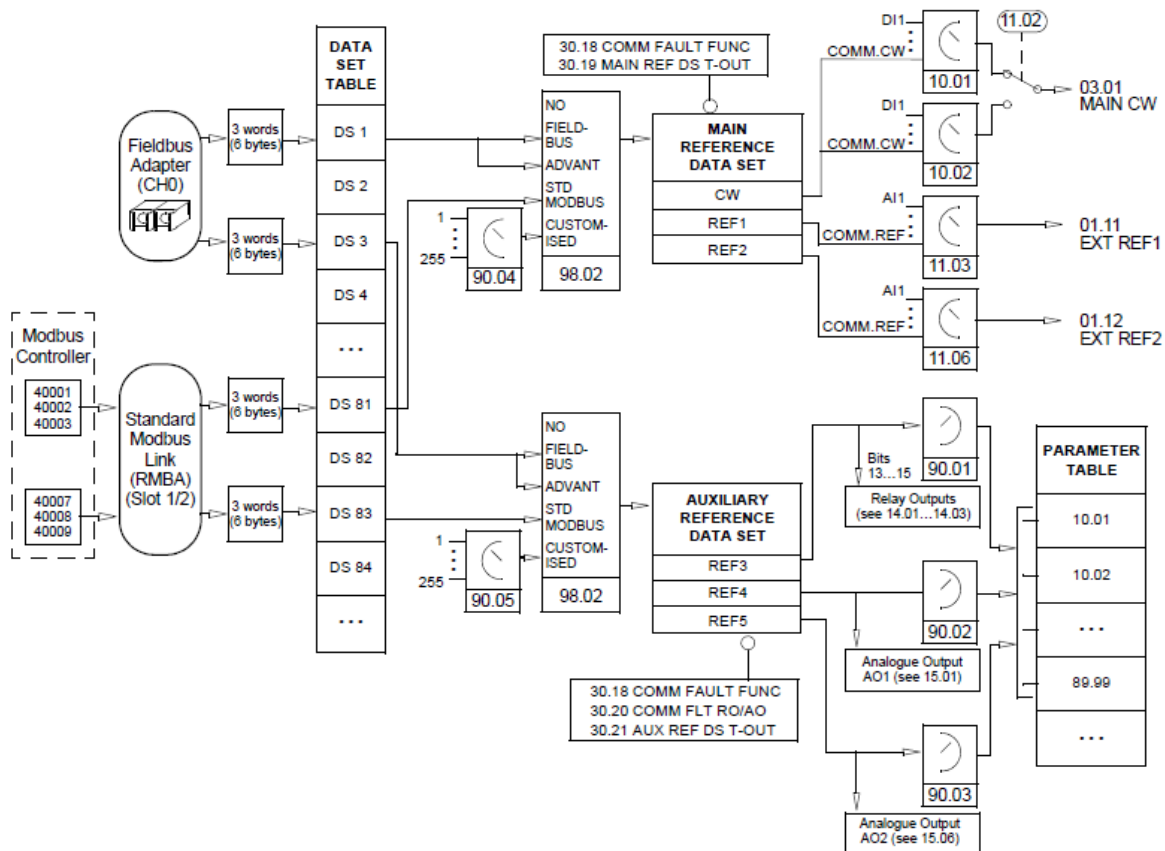
Figure 3.3: ABB Frequency Drive Parameter Mapping[7]

Table 3.3: VFD Parameter Config

Parameter	Value	Description
10.01	COMM.CW	EXT1 STRT/STP/DIR
10.02	COMM.CW	EXT2 STRT/STP/DIR
11.03	COMM.REF.	EXT REF1 SELECT
11.06	COMM.REF.	EXT REF2 SELECT
20.03	65	MAXIMUM CURRENT
20.04	0-100%	TORQ MAX LIM1
20.14	MAX LIM 1	MAX TORQ SEL
30.10	NO	STALL FUNCTION
90.01	2004	AUX DS REF3
99.04	DTC	MOTOR CTRL MODE

3.2   ABB Induction Machines

The ABB induction machines were also donated from ABB Automation and Power. The general machine info is shown in Table 3.4. These machines feature a dual wiring configuration that can be operated at either 230 VAC or 460 VAC 3 phase sources. The "Prime Mover" M1 machine is set up to operate at 230 VAC, which in low speed and high torque, is limited by the DC bus capabilities of the DC power Supply. The "Absorber" M2 motor is operated at 480 VAC, which is controlled via the ABB VFD.

Table 3.4: ABB Induction Motor Nameplate Information

Description	Name
Type	M1AA 256T-B2
Serial Number	M99B-09011
Nominal Power	20 HP
Nominal Frequency	60 Hz
Rated Speed	3515 RPM
Rated Voltage	460 VAC-Y
	230 VAC-Y //
Full-Load Current	22.5 A/45.0 A
Nominal Efficiency	90.2 %

Other than the name plate, no other information was provided. ABB and Baldor (subsidiary of ABB) was contacted to provide any factory data information, however, it was

stated that since "the M1AA motor series was discontinued several years ago and they are no longer able to bring up performance curves." Because of the future need of this knowledge, the machine parameters were estimated and thoroughly discussed in 4.1.

3.3   VFD Isolation Transformer

Since the VFD operates at a higher input and output voltage than what is supplied via the test cell infrastructure, a step-up transformer had to be purchased. The transformer was designed and build by Grand Transformer Inc.; a company that specializes in design and manufacture custom inductive components. The transformer is shown in Figure 3.4. The transformer was specified to be a 30 kVA 60Hz rating and to have several different voltage levels. The nameplate values are listed in Table 3.5. It can be configured for a 230 Vac or 460 Vac input voltage and either a 240 Vac or 480 Vac. This was done to allow for flexibility; if the need arises to be used in a different project or configuration.

Figure 3.4: Isolation Transformer

Table 3.5: Isolation Transfromer Nameplate Information

Description	Name
GTI Part Number	GT-H591E
Weight	475 lbs
Nominal Power	30 kVA
Nominal Frequency	60 Hz
Number of Phases	3
Temperature Rise	135°C
	@ 40°C Ambient
Insulation	Class N-1
Rated Voltage Primary	208/230/240 VAC-Series
	416/460/480 VAC-Parallel
Rated Voltage Secondary	240 VAC Wye-Series
	480 VAC Wye-Parallel

For the test cell specific configuration the transformer steps up the 208 Vac source voltage to 480 Vac needed to supply the VFD. The wiring connection information is shown in Table 3.6. This table shows how the isolation transformation was configured as a step up transformer.

Table 3.6: Isolation Transformer Test Cell Wiring Configuration Information

Description	Connection
Primary Lines Connections	L1-H1-13-36
	L2-H2-23-16
	L3-H3-33-26
Primary Aux Connections	14-13, 15-16
	24-23, 25-26
	33-34, 35-36
Secondary Line Connections	L1-X1
	L2-X2
	L3-X3
	N/C-X0 (Neutral)
Secondary Aux Connections	11-12, 21-22, 31-32

3.4 DC Power Supply

The DC power supply was purchased for prior lab use, with the intent to be used in a motor drive application. It is manufactured by Magna-Power Electronics and is available in a

variety of input and output configurations. The model used in the Dynamometer test cell is a TSA400-36 (see Figure 3.5). This particular module has a 240 volt, 3 phase input and is used to supply power to the inverter as discussed in section 3.5.

Figure 3.5: DC Power Supply

The DC power supply general specifications are summarized in Table 3.7. The DC power has three modes of operation; Normal, Constant Voltage, and Constant Current. For the "Normal" mode the TS series power supplies can be configure for control by rotary mode input, local sensing, internal control, and external control. With this configuration, the operator can select either a constant voltage or a constant current output using the front panel controls. The mode is determined by the limits of the voltage or current settings. During operation whichever limit is lower for that particular operating point it will determine the operation mode, either constant voltage or constant current, that will be governing the control.

Table 3.7: DC Power Supply General Specifications [8]

Value	Value
Nominal Power Output	15 kW
Max DC Bus Voltage	400 V
Max DC Current	36 A
Line Regulation: Voltage Mode	± 0.004 % FS
Current Mode	± 0.02 % FS
Load Regulation: Voltage Mode	± 0.01 % FS
Current Mode	± 0.04 % FS
Ripple Voltage	200 mV rms
Efficiency	>88 %
Input Voltage (3 phase)	208/240 V
Input Current (3 phase)	53 A

The DC power supply can be configured to receive its input from various input sources. The input setting can be easily changed from source to another with little operator input effort. For use in the test cell the DC power supply was setup to receive its reference value from a external source. This external programming source is analog output from the dSPACE embedded controller. This was done to allow for bus control via the embedded controller. It also has the ability to be controller via a Remote Web interface.

In order to properly operate in the external programming mode, some physical wiring had to be configured on the JS1, remote interfacing connector. This wiring ensures that the over current and voltage trip setpoint are set to their maximum allowed value. First the Voltage Trip Setpoint (VTS) and Current Trip Setpoint (CTS) were tied to a +10V dc ref (JS1-Pin 21). This set the value that the DC power supply would fault to 110% of the full-scaled value, as seen in Figure 3.6. Also shown in Figure 3.6 are the terminals for the reference voltage and current. For full operation, the current reference was also wired to the +10V dc reference value on the JS1. This would allow for max current output regardless of voltage bus setting.

TERM	PARM	DESCRIPTION	INPUT RANGE (V)	OUTPUT RANGE
3	VREF EXT	Voltage Set	0-10.0	0-100% FS Voltage
22	IREF EXT	Current Set	0-10.0	0-100% FS Current
4	TVREF EXT	Over Voltage Trip Set	0-10.0	0-110% FS Voltage
23	TIREF EXT	Over Current Trip Set	0-10.0	0-110% FS Current

Figure 3.6: DC Power Supply External Programming Parameters

3.5   Inverter

The inverter was purchased for prior lab use. It can be configure as either dc to dc power converter or a DC to AC single/three phase inverter. It main function is to power and control the "prime mover" machine. A picture can be seen in Figure 3.7. The unit is manufactured by Applied Power Systems, Inc (APS) located in Hicksville, NY. The inverter, part number **IAP75T120**, is a standard IGBT sixpack configuration consisting of 6 IGBT arranged in 3 phases, each containing two IGBTs, as shown in Figure 3.8. Some of the features of the inverter used are [9]:

- Compact Size –9.00” H X 11.00” W X 17.56” D

- DC Bus Voltages to 850VDC

- Snubber-less operation to 650VDC

- Switching frequencies to over 20kHz

- Protective circuitry with fail-safe opto-isolated fault annunciation, including:

OverCurrent	P.S. UnderVoltage
OverVoltage	Short circuit
OverTemperature	

- Opto-isolated or fiber-optic gate drive and fault signal output for electrical isolation and noise immunity

- Integrated cooling with temperature sensors and feedback
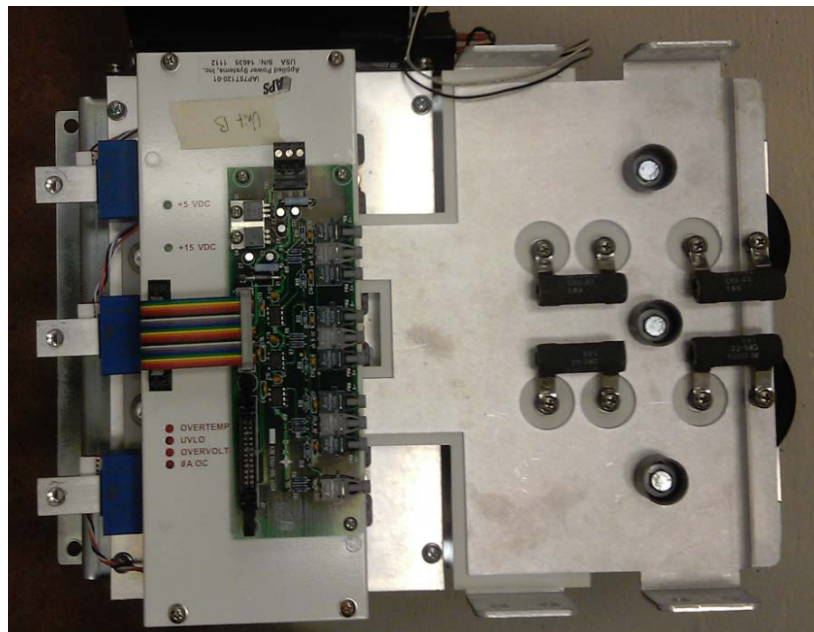
Figure 3.7: APS Inverter Picture
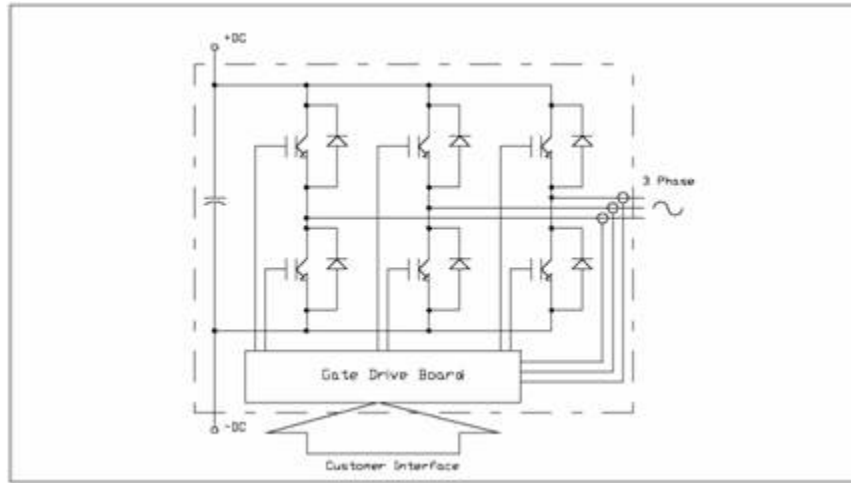
Figure 3.8: Inverter IGBT Six-Pack Configuration[9]

The relevant APS Inverter specifications are listed in Table 3.8. This listing is only a sample from the datasheet and the datasheet should be consulted in any inverter related issue. The dc inverter is a three level inverter, with a three phase output, however if desired the inverter could be configured for a dc to dc converter application.

Table 3.8: Inverter General Specifications [9]

Description	Value
Max DC Bus Voltage	800 V
Max Phase Current	75 W
DC Link Capacitance	3300 uF
Gate Driver Control Power	15/24 V
PWM Thresholds: On	12-15 V
Off	0-2 V
Output Over-current Trip Value	112.5
Over-temperature Trip Value	96-100 °C
Over-voltage Trip Value	900 V

3.6 Motor Coupling Assembly

The motor coupling assemble consists of the torque sensor and flexible coupling. A picture of the assembly is shown in Figure 3.9. The assembly is a "mechanically floating" system. This means there is no support to the sensor holding off the test bed. Excluding the shafts, the only means of mechanical connection is strap (cable) used to mechanically "ground"

and keep the sensor from spinning with motion of the shafts. The only force the mechanical "grounding" strap would need to provide is the frictional bearing force of the sensor.
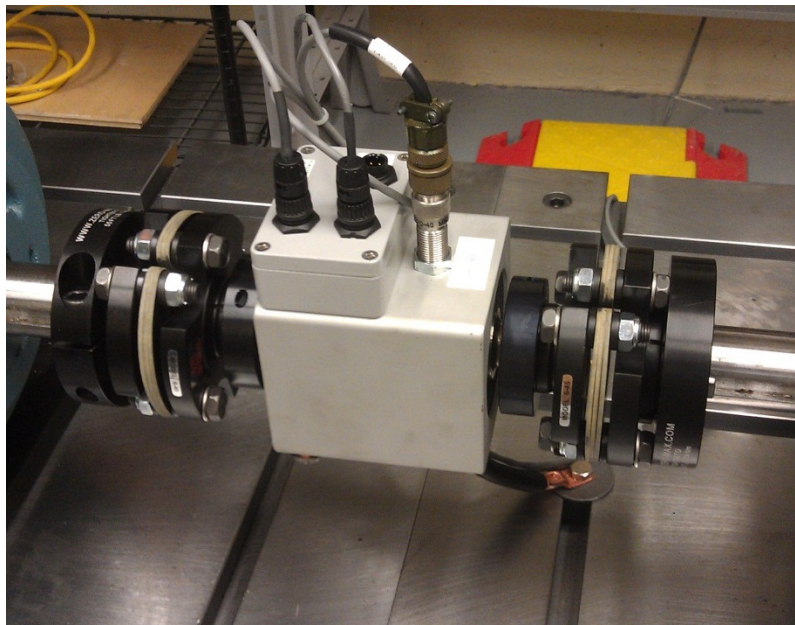
Figure 3.9: Torque Sensor and Flexible Coupling

3.6.1   Torque/Speed Sensor

The torque and speed sensor was purchased from S. Himmelstein and Company, which specializes in torque sensors of all type. The particular type used in the test cell dynamometer rotating, MCRT 48200 Compact Digital Torque Transducer (see Figure 3.9).

Table 3.9: Motor Coupling Assembly Part Number

Manufacture	Description	Part Number
Himmelstein	Torque/Speed Transducer	MCRT 48203V(1-3)CZ
Himmelstein	Display Instruments	Model 723
Himmelstein	50 foot length of torque and power cabling	P/N 224-8270-50
Himmelstein	50 foot length of speed cabling	P/N 224-5327V-50

Below is an excerpt from [10] which summarizes the capabilities of the torque sensor. "These Compact Digital Torque Transducers have high accuracy, low noise, high overload capacity, high over-range, inherent noise tolerance and a wide temperature range. Strain gage sensing and non-contact signal transfer make them well suited for control, laboratory and production use. They are offered in two accuracy grades, Code N standard performance and

Code C enhanced performance. Installation can be either floating or foot mounted with the integral mounting base."

The purchased torque sensor for use in the test cell is the enhanced performance model and also has an optional zero velocity speed sensor. The sensor was also purchase with an amplifier/digital read out. The readout displays torque, speed, and power as measure by the sensor. It also provides sensor signal excitation, amplification, conditioning, along with some electrical circuit protection. In addition provides scaled output voltage reading of two of the three measured quantities for a data acquisition system. However one important note regarding the speed sensor is there is no indication of direction from the sensor, just an absolute speed value.

Table 3.10: Himmelstein Torque Sensor Specifications

Description	Value
Full Scale Torque Rating	1,000 lbf-in (113 Nm)
Overload Rating	2,000 lbf-in
Speed Rating	8,500 RPM
Accuracy Class	±0.15% of full scale combined
Output Signal, Speed	60 pulses per revolution
Installed Options:	Enhanced performance (code C) Zero velocity speed pickup (code Z)

3.6.2 Flexible Motor Coupling

The torque sensor used is in conjunction with flexible couplings manufactured by Zero-Max, purchase from Motion Industries. Theses couplings are intend to minimize any misalignment in the horizontal direction which would translate to axially torque that could possible damage the torque sensor [11]. The flexibility comes from the composite discs that are a "clover" shape, which can compensate for misalignment of motor shafts. The flexible coupling specifications are listed in Table 3.11.

Table 3.11: Zero-Max Flexible Coupling Specifications

Description	Value
Coupling Single Flex Aluminum	6A45AC 1.625 X 1
Continuous Torque Rating	2,500 lbf-in (282 Nm)
Maximum Torque Rating	5,000 lbf-in (564 Nm)
Maximum Speed Rating	6,700 RPM
Misalignment: Angular	3°
Parallel	0.4 mm
Axial	2.3 mm
Bore: Max	1.75 in
Actual (Motor/Torque)	1.625 in / 1.000 in

3.7 Test Cell Infrastructure Controls

The test cell infrastructure controls was designed to be a standalone system, independent of the VFD and inverter controls. The test cell infrastructure essentially controls what components are supplied the primary 3 phase power from the main power source. The test cell infrastructure controls consist of the power wiring, fuses, contactors, and a programmable logic controller (PLC). The PLC is at the brain of the test cell infrastructure control. Based upon the user program, and the provided control inputs, the PLC decides the states of the outputs. Example of these control inputs are contactors, the safety relay, start/stop pushbuttons, fans, and indicator lights. The outputs of the system are the 3 phase power contactors as well as a few indicating lights

The high level control scheme of the test cell safety system puts the system in one of five states; "**Ready**", "**Enabled**", "**Powered**", "**ON**" and "**Fault**". In the "**Ready**" state the test cell has the external CPS applied and is awaiting the user to press the "System Start/ON". In this state the safety relay is off and no outputs are powered. The "**Enabled**" state verifies the user has pressed and released the "System Start/ON" pushbutton. When in this state, DC power is applied to the PLC contact outputs that can route power to the individual output devices. The only outputs powered during this state are the enclosure ventilation fan and external inverter fan. When the system is in the "**ON**" state all of the contactors are powered and closed. At this point the system is fully functional and the motor has the ability to turn. The "**Powered**" state allows

the motor drive components (DC power supply, inverter, ABB VFD) to be powered up however they are not electrically connected to the electric machines. This state ensures communication between these devices and the controller station but prevents shaft movement. The last state "**Fault**" is intended to automatically enters the system into the "**Powered**" state behaviors, with the added feature of indicating there is a system fault, via an indicator light. The implementation of this into a program was accomplished as part of the EET Senior Design Project; however the basis of the initial program was developed and implemented by Trever Hassell. After this initial program was developed, an EET Senior design team member continued the work incorporating many features not included in the initial functional program. These features include fault detection and indication, and E-Stop PB depressed detection.

3.8   User Interface Controller Station

The user interface controller station, see Figure 3.10, is the single point that interfaces all the different control systems. These interface consist of a LabVIEW GUI, dSPACE embedded controllers, Micrologix communication adaptor, and operator pushbuttons station. All of these systems can be monitored from this location in the test cell. However, these systems are not integrated into on control system and are monitored via several different, and separate, systems.
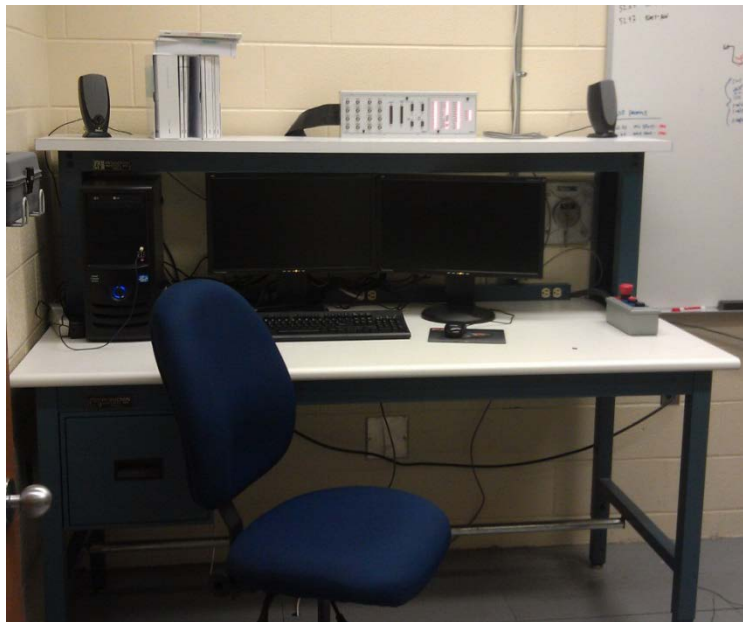
Figure 3.10: User Interface Controller Station

3.8.1 PC based Controls

The PC functions as the operator interface for both the embedded controller and ABB VFD. It also serves as the program and view the PLC located in the motor controller safety system enclosure (MCSSE). The ABB VFD is controlled via a National Instruments (NI) LabVIEW program that takes user input and reference values and sends them to the VFD via the Modbus RTU protocol. This protocol was chosen for its wide use industry, with ample documentation available. NI has both an excellent tutorial [12] and guide [13] for using LabVIEW in Modbus applications. The only hardware components needed were a USB to Serial Modbus adaptor, a RS-485 compatible communication cable, and a Modbus communication adaptor for the VFD donated by ABB Automation and Power. The embedded controller communicated via the PCI slot communication available on the backplane of the motherboard of the PC. The PLC communication is accomplished via a USB to Serial adaptor purchased from the manufacturer of the PLC.

3.8.2 Embedded Controller

A dSPACE DS1104 is used for the embedded controls of the inverter. This system was chosen for its already known behavior and its relative ease of use. This controller features two digital signal processors (DSP). The "primary" DSP performs the control algorithm execution therefore performing the majority of the calculations, and executes at a rate of about 100 μs. The other DSP, or "Slave" DSP, controls the switching action sent to the inverter via pulse width modulation (PWM). The slave DSP can operate at switching frequencies in excess of 100 kHz.

The DS1104 and breakout box features 8 ADC analog inputs (4 multiplexed, 4 parallel), 20 digital input/output (I/O), 8 channel DAC analog outputs, two DSP, Serial communication port, and Digital incremental encoder interface. The I/O channel list is shown in Table 3.12.

Table 3.12: Embedded Controller Input Output Channel List

Name	Type
Inverter Phase A Current	ADC
Inverter Phase B Current	ADC
Inverter Phase C Current	ADC
Inverter Heatsink Temperature	ADC
Inverter DC Bus Voltage Measure	ADC
DC Bus Voltage Command	DAC
Mechanical Rotor Angular Speed	ADC
Mechanical Rotor Torque	ADC
High Gate Switch Signal Phase A-1	PWMA1
High Gate Switch Signal Phase B-1	PWMB1
High Gate Switch Signal Phase C-1	PWMC1

3.9 Signal Isolation Modules

The signal isolation modules are intended to isolate any control signal input signal to that will be connected into the dSPACE embedded controller. There were two different modules, a 10 V [14] and 5 V [15] input voltage range, purchase for use with the test cell. The application of each signal will determine which isolation module will be used. The isolation are high bandwidth modules which have a 10 kHz range (-3 dB attenuation), shown in Figure 3.11. These modules are power via an external 5 Vdc power supply and can be purchased with a wide variety of backplanes or chassis. The particular chassis purchased for the test cell is a 16 slot however many configuration can be used.

Figure 3.11: Signal Isolation Module Chassis

Table 3.13: Signal Isolation Modules Specifications

Description	Value
Part Numbers	10V: ISO-5B40-02 5V: ISO-5B40-03
Voltage Input Range	10V: ±10V 5V: ±5V
Output Voltage Range	±5V
Bandwidth	3 dB @ 10 kHz
Nonlinearity	±0.02%
Isolation	1500 Vrms

3.10 Signal Interface Board

To easily and reliably interface with the various signals, an interface board was designed and constructed, as shown in Figure 3.12. It was designed based on the pin out of the inverter signal cable and terminal blocks that will allow the signals to connect to different external devices; such as the isolation modules and/or the dSPACE embedded controller. The signal interface board has a connector from the signal isolation module chassis to allow for easy BNC connection to the analog signal cables connected to the controller station.

The board was designed using Eagle. "The name EAGLE is an acronym, which stands for Easily Applicable Graphical Layout Editor. This award winning software offers user friendly, powerful and affordable solutions for PCB design, including Schematic Capture, Board Layout and Auto-router. User Language Programs enable features such as simulation and 3D-visualization." [16]. The board was also designed to incorporate the 5Vdc power supply need to power the signal isolation module chassis. This also reduces table-top space needed and reduces the probability of inadvertently shorting of the power supply to the signal interface board. It also allows for control power to be fused and routed to the signal isolation module chassis. The complete schematic and board layout is located in Appendix F.
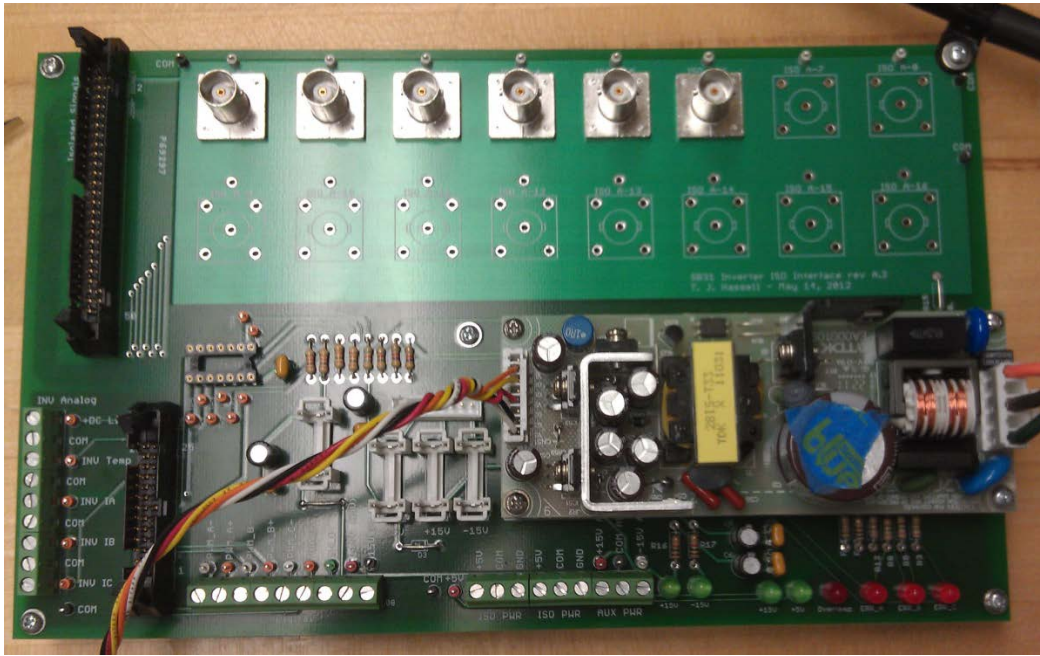
Figure 3.12: Signal Interface Board Rev A.3

CHAPTER 4. TEST CELL SYSTEM PARAMETERIZATION

This chapter will detail the work done to parameterized electric machines and test cell control signals. The major completed tasks were the estimation of the electrical machine parameters and all the control sensor gain signals feedback. The test cell system parameterization was necessary for future work that will be discussed in 6.2.

4.1   Electrical Machine Parameter Estimation

This section will discuss the methods that were used to derive the equivalent electrical machine parameters listed in Table 4.1. Several tests were performed to estimate the parameters of the ABB 20 HP induction machines; No-load and blocked rotor tests. These tests were conducted according to [17]. See Appendix D for more detail regarding how the electric machine parameters were calculated.

Table 4.1: Machine Parameter Estimation

Symbol	Name	Unit
R_s	Stator Resistance	Ω
R_r	Rotor Resistance	Ω
L_{ls}	Stator Leakage Inductance	H
L_{lr}	Rotor Leakage Inductance	H
L_m	Magnetizing Inductance	H
N_p	Number of Pole Pairs	--
J	Moment of Inertia	$Kg - m^2$

As detailed in [17], the moment of inertia the system was found by using (5.1). The system was spun to half of its rated speed (1797 RPM) and the torque was observed to be 2 in-lbs. The collected data is shown in Figure 4.1. By approximating the slope of the coast down data to be linear and solving the differential values for difference values, the moment of inertia was found by solving (5.1) for J, using the values in Table 4.2.
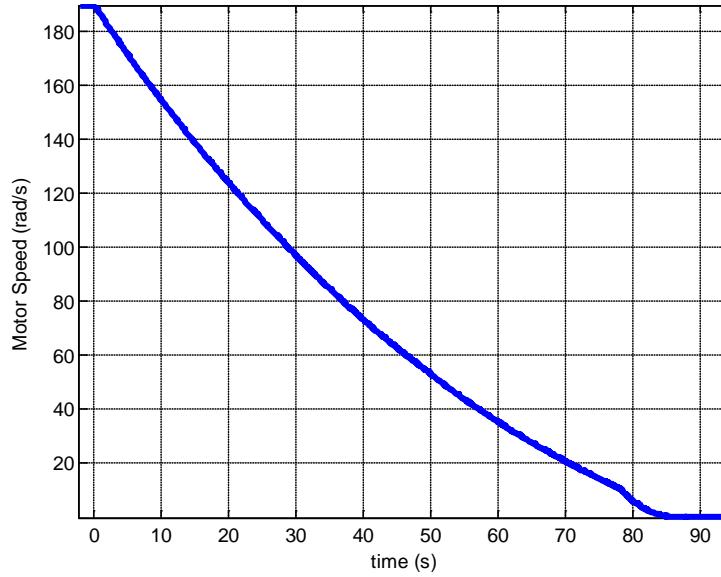
Figure 4.1: System Coast-Down Data

$$J\frac{d\omega}{dt} = -T_{rotational} \qquad (5.1)$$

Table 4.2: Coast-Down Data Calculation Values

Symbol	Name	Value	Units
$T_{rotational}$	Rotational Torque	0.22597	$N-m$
$d\omega_m$	Differential (Difference) Speed	188.181	$rad\!\!\Big/\!\!_s$
dt	Differential (Difference) Time	87.6	s
J	Moment of Inertia	105.191×10^{-3}	$Kg-m^2$

The pole calculation test was conducted to determine the number of the poles constructed in the machine. A fixed electrical frequency was applied to the motor and the rotor speed was observed. Based on the ratio of the electrical frequency divide by the mechanical frequency the number of pole pairs can be estimated.

Table 4.3: Number of Poles Pairs Data Values

Electrical Frequency	Speed (RPMs)	Speed (rad/s)	Mechanical Frequency	Poles Pairs*
15.0	898	94.04	15.0	1
30.0	1797	188.18	30.0	1
45.0	2695	282.22	44.9	1
60.0	3592	376.15	59.9	1

*denotes estimated value

The no-load test was conducted as described in section 6.6.1 of [17]. The electrical frequency of the machine was set to rated frequency and rated voltage; and the data was collected via the Yokogawa power meter. The captured data is displayed in Table 4.4 and Figure 4.2.

Table 4.4: No-Load Test Data Values

Line to Line Voltage (V_{rms})	Line Current (i_{rms})	Frequency (Hz)	Speed (RPM)	Average Real Power (W)	Apparent Power (VA)
220.04	7.463	60.044	3590	723	2808

Figure 4.2: No Load Test Data

The blocked rotor test was conducted as described in section 6.6.2 of [17]. To keep the rotor stationary, a rotor blocking device was design and built and is shown in Figure 4.3. Once the rotor blocking fixture was secured to the rotor of the electric machine via part of the flexible

motor coupling, the electrical frequency of the machine was set to 25% of the rated frequency and near rated line current and the data was collected via the Yokogawa power meter. The captured data is displayed in Table 4.5 and Figure 4.4. The testing method calls for conducting the test at line however the DC power supply could not source enough current to meet the rated line current.

Figure 4.3: Rotor Blocking Fixture

Table 4.5: Blocked Rotor Test Data Values

Line to Line Voltage (V_{rms})	Line Current (i_{rms})	Frequency (Hz)	Average Real Power (W)	Apparent Power (VA)
16.68	40.301	15	719	1148
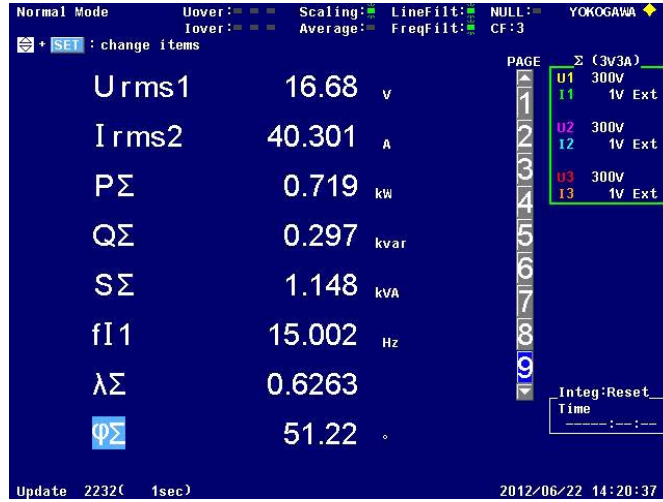
Figure 4.4: Blocked Rotor Test Data

Based on the data collected in Table 4.2 through Table 4.5, and the method described in Chapter 6 of [17], the machines were calculated. These estimated values are listed in Table 4.6.

Table 4.6: Estimated Machine Parameter Values

Symbol	Name	20 HP Value	75 HP Value [18]	Unit
R_s	Stator Resistance	150×10^{-3}	44.3×10^{-3}	Ω
R_r	Rotor Resistance	2.977×10^{-3}	31.1×10^{-3}	Ω
L_{ls}	Stator Leakage Inductance	303.57×10^{-6}	607.1×10^{-6}	H
L_{lr}	Rotor Leakage Inductance	202.38×10^{-6}	883.3×10^{-6}	H
L_m	Magnetizing Inductance	42.7712×10^{-3}	15.1993×10^{-3}	H
N_p	Number of Pole Pairs	1	1	--
J	Moment of Inertia	105.191×10^{-3}	5.86×10^{-3}	$Kg - m^2$

4.2 Control Sensor Signal Gain Feedback

The signal sensors that are available to be used in various control strategies are listed in Table 4.7. This list includes the three phase currents, the DC bus voltage measurement, and the heat sink temperature that are provided from the inverter. In addition, the list includes the DC bus command sent to the DC power supply and the torque and speed measurements from the torque sensor.

Table 4.7: Sensor Channel List

Name	Sense Value Range	Measured Value Range
Inverter Phase A Current*	-5 to 5 V	-200 to200 A
Inverter Phase B Current*	-5 to 5 V	-200 to200 A
Inverter Phase C Current*	-5 to 5 V	-200 to200 A
Inverter Heatsink Temperature *	-5 to 5 V	0 to120 °C
Inverter DC Bus Voltage Measure*	0 to 10 V	0 to1000 Vdc
DC Bus Voltage Command	0 to 10 V	0 to 400 Vdc
Mechanical Rotor Angular Speed	0 to 5 V	0 to 8500 RPM
Mechanical Rotor Torque	-5 to 5 V	0-1000 in-lbs

*denotes signal passed thru isolation module

4.2.1 Inverter Sensor Gains

The Applied Power Systems (APS) inverter supplies the signal measure of five of the eight signals read by the dSPACE embedded controller. The five signals are the three phase currents, heat sink temperature and the DC bus voltage measurement. Based on the datasheet provided by the manufacture [9], the gains were set up as shown in Table 4.8. All of these signals pass through the isolation modules described in section 3.9.

Table 4.8: Inverter Signal Channel Gain Values

Name	Full Scale Value	Isolation Module Voltages	Gain Value
Inverter Phase A Current*	200 A	5 V to 5V	20×1
Inverter Phase B Current*	200 A	5 V to 5V	20×1
Inverter Phase C Current*	200 A	5 V to 5V	20×1
Inverter Heatsink Temperature*	120° C	10 V to 5V	12×2
Inverter DC Bus Voltage Measure*	1000V	10 V to 5V	100×2

*denotes signal passed thru isolation module

Figure 4.5 shows the Simulink block diagram representation of the control signal feedback gain. One should notice that the current signals has an adjustment for a DC offset that is being observed on the actual signal. The analog control signal coming from the inverter has a slight DC offset and requires compensation.
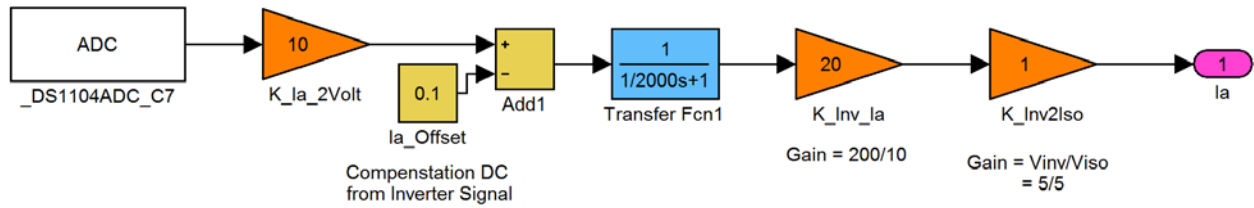
Figure 4.5: Inverter Current Sensor Gain Diagram

Figure 4.6 shows the DC bus measure sensor gain diagram. This is read from the multiplexed analog to digital channel (ADC) on the on the dSPACE embedded controller. Since the DC bus changes relatively slowly, when compared to the phase currents, there is a much slower response filter. This allows for a more consistent display and controllability. There is also an adjust table that compensates for any difference between actual bus voltage and measure bus voltage and is based upon collected data (see Appendix B).
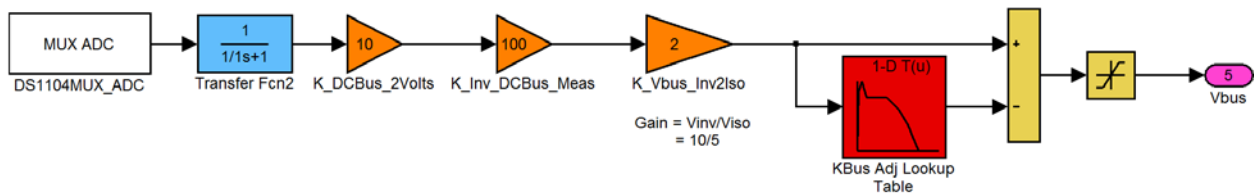
Figure 4.6: Inverter DC Bus Measurement Sensor Gain Diagram

Figure 4.7 shows the inverter heat sink temperature sensor gain diagram. This is can be read from a multiplexed analog to digital channel (MADC) or a regular ADC on the dSPACE embedded controller. Since the Inverter heat sink will also change relatively slowly, a slower response filter is placed on the signal to keep the value consistent.
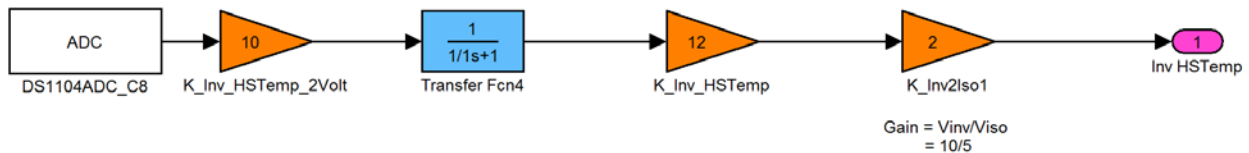
Figure 4.7: Inverter Heat Sink Temperature Sensor Gain Diagram

4.2.2 DC Power Supply Bus Voltage Command Sensor Gain

The Magna DC Power Supply, as explained in section 3.4, has the ability to have the DC bus controlled via an external controller. The DC power supply reads an analog voltage on sent

from the dSPACE embedded controller. This allows for the dynamic control of the DC bus via some control scheme. Table 4.9 lists the sensor gain values based on the manufacture's data sheet [8]. Figure 4.8 shows the Simulink block diagram of the sensor value path. Important to note is the adjustment table that is located to the left of the diagram. This compensates for the measured error from the command to read value on the power supply (see Appendix B). This error could be due to noise induced onto the analog signal from either the inverter or power supply.

Table 4.9: DC Power Supply Bus Command Channel Gain Values

Name	Full Scale Value	Input Voltage	Gain Value
DC Power Supply Bus Command	400V	0 V to 10V	40
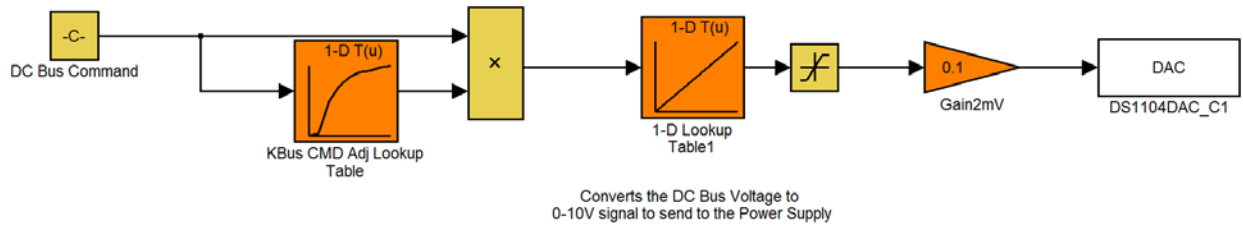
Figure 4.8: DC Power Supply Bus Command Sensor Gain Diagram

4.2.3   Mechanical Rotor Angular Speed and Torque Sensor Gain

The mechanical rotor angular speed sensor signal is supplied by the S. Himmelstein and Company digital compact torque/speed sensor and the signal conditioner module. The 700 series multi-channel signal conditioner display and controller supplies both the torque and speed analog signals. The channels are factory configured to use a ±5 volt signal range. The signal feedback channels are based from the full scaled reading of each respected channels. The channel gain values are summarized in Table 4.10. The Series 700 analog channels do not go thru an isolation module and therefore do not need any additional scaling factors. Figure 4.9 and Figure 4.10 show the block diagram for the torque and speed sensor signals.

Table 4.10: Himmelstein Torque and Speed Sensor Channel Gain Values

Name	Full Scale Value	Gain Value
Mechanical Rotor Angular Speed	8500 RPM	1700
Mechanical Rotor Torque	1000 in-lbs	200
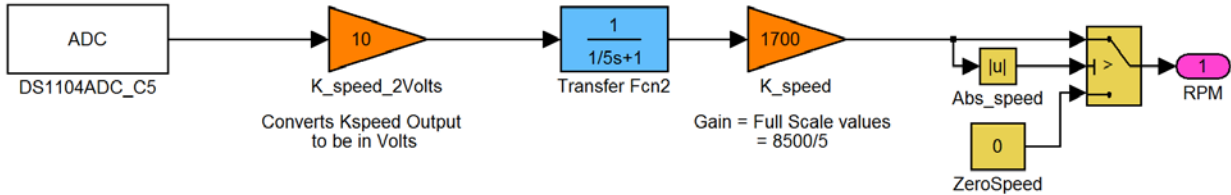
Figure 4.9: Mechanical Rotor Angular Speed Sensor Gain Diagram
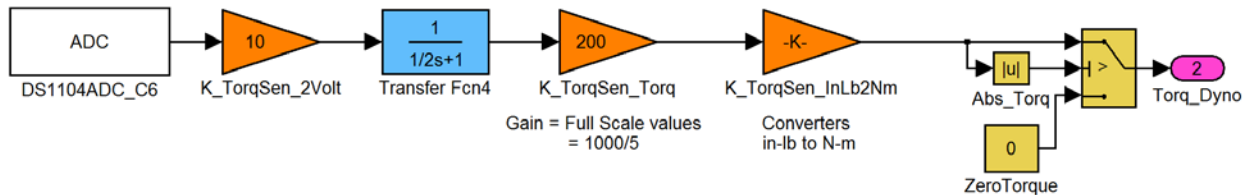
Figure 4.10: Mechanical Rotor Torque Sensor Gain Diagram

The final sensor gain values are listed in Table 4.11. This listed does not included the empirical adjust date that was need for several channels to read the independently measured data.

Table 4.11: Sensor Channel Gain Values

Name	Gain Name	Gain Value
Inverter Phase A Current*	K_inv_phA_curr	20
Inverter Phase B Current*	K_inv_phB_curr	20
Inverter Phase C Current*	K_inv_phC_curr	20
Inverter Heatsink Temperature *	K_inv_hs_temp	12
Inverter DC Bus Voltage Measure*	K_inv_dcbus_meas	100
DC Bus Voltage Command	K_dcps_dcbus_cmd	40
Mechanical Rotor Angular Speed	K_torqsense_torq	1700
Mechanical Rotor Torque	K_torqsense_speed	200

*denotes signal passed thru isolation module

CHAPTER 5. TEST CELL PERFORMANCE REVIEW

This chapter will discuss the criteria used to verify the operation of the test cell. First, data was gathered for each component in the system in efforts to quantify the efficiency of the components during a given operational region. The subsequent sections will discuss the test cases and conditions in which the data was collected.

5.1 Component Efficiency Characterization

Relative system/component data were gathered using the Yokogawa power meter in order to characterize the system. The data obtained data is shown in Table 5.1. From this data the system power losses and efficiencies were calculated. The Yokogawa WT500 was wired in accordance to [19] for the three phase, three wire; (3V3A mode). The wiring configuration is shown in Figure 5.1. This configuration utilizes three voltage and three current measurements. The voltage measurements are three phase to phase measurements and are listed in Table 5.2. The power meter was also setup up to obtain measure data every 0.5 seconds and utilized a built in 8 point averaging function. This allowed to dampening out any oscillations in the displayed measurements.

Table 5.1: Gathered Component Measurement Quantities

Name	Abbreviation	Units
Volts per Hertz Value	V/Hz	V-s
Line-Line RMS Voltage	Urms1	V
Line-Line RMS Voltage Current	Irms1	A
Total Real Power	$P\Sigma$	kW
Total Reactive Power	$S\Sigma$	kVAR
Total Apparent Power	$Q\Sigma$	kVA
Power Factor	$\lambda\Sigma$	--
Power Factor Angle	$\varphi\Sigma$	degrees
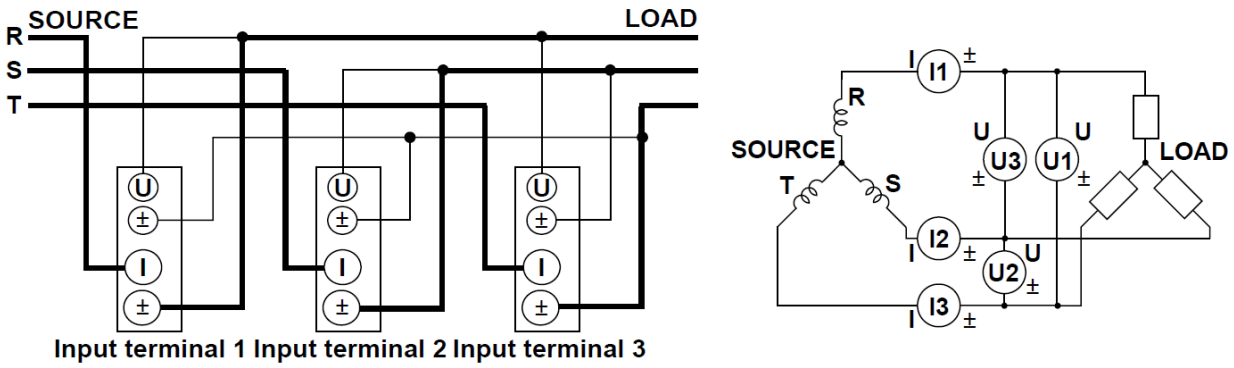
Figure 5.1: Yokogawa WT500 Wiring Diagram [19]

Table 5.2: Yokogawa Voltage/Current Measurement Configuration

Description	Line Connection
Element 1 Voltage (U1)	R-T (A-C)
Element 2 Voltage (U2)	S-T (B-C)
Element 3 Voltage (U3)	R-S (A_B)
Element 1 Current (I1)	R (A)
Element 2 Current (I2)	S (B)
Element 3 Current (I3)	T (C)

Figure 5.2 shows a sample of data collection image. Displayed in this figure are columns consisting of the three individual elements, as well as the sum total. Viewing Figure 5.2 closely will show the total does not equal the sum of the individual elements; however this is correct for the setup of the power meter. When wired for the 3V3A-3W (3-wire) the meter uses two of the measurements (elements 1 and 2) to find the overall power. This is done so that the last element could be used to measure the DC input to an inverter. The power meter could be setup up to measure 3phase, 4 wire (3V3A-4W) by accessing the neutral point in the system. If this was done, the sum of the individual element values would match the last column on the power meter. This was not done because of the add complexity of the physical setup to the power meter and also because of the lack of neutral point access. Since both the 3V3A-3W and 3V3A-4W methods will produce the same total values, the 3V3A-3W setup was preferred due to its less complicated setup.

Normal Mode   Uover:☐ ☐ ☐   Scaling:■ LineFilt:■ NULL:☐   YOKOGAWA ◆
                   Iover:☐ ☐ ☐   Average:☐ FreqFilt:■ CF:3
⬙ + SET : change items

           ___Element1_____ ___Element2_____ ___Element3_____ __Σ (3V3A)__
          U1   300V   U2   300V   U3   300V
          I1   1V Ext   I2   1V Ext   I3   1V Ext
Urms [V]   208.26   208.27   208.32   208.28
Irms [A]   25.934   26.638   26.928   26.500
P   [W]   3.993ₖ   4.536ₖ   -0.427ₖ   8.529ₖ
Q   [var]   3.637ₖ   -3.195ₖ   5.593ₖ   0.443ₖ
S   [VA]   5.401ₖ   5.548ₖ   5.609ₖ   9.560ₖ
λ   [ ]   0.7392   0.8176   -0.0762   0.8921
φ   [°]   G42.33   D35.16   G94.37   26.86
fI   [Hz]   59.985   59.983   59.984
fI   [Hz]   59.985   59.983   59.984
                                                      Integ:Reset
⬙PAGE⬙ 1/9   Time
                                                      ─────:──:──

Update 6402(1sec)   2012/07/06 11:44:13

Figure 5.2: Sample Power Meter Data Collection Image

With the power meter properly configured data was collected at prescribed operational points, see Table 5.3 and Table 5.4 . At each torque and speed operation point, data was collected via the power meter (see Figure 5.2) for all components in the systems. In total, each component had 36 operational points that were collected and are summarized in table located in APPENDIX C. System Parameter Data.

Table 5.3: System Components Characterization Components

Component Name
DC Power Supply
DC-AC Inverter
Machine1
Machine2
Variable Frequency Drive
Isolation Transformer

Table 5.4: Operational Data Collection Points

Speed (RPM)	Torque (%)
500	0
1000	10
2000	20
3000	30
4000	40
5000	50

From the collected data, power losses (5.2) and efficiency (5.3) values were calculated for each component. These equations are relatively straight forward for most operational points however there are few occurrences when the power output is zero. This happens at low speed and torque, when the regeneration power is low and a particular component (transformer, VFD, electric machine 2) has a fixed loss at that given operating point. Another issue is that the power flowing in each component changes direction. This occurs when transitioning from lower speeds and torques, where the both the prime mover and the absorber components are supplying power, to higher speeds and torques, where the absorber regenerates power back to the power supply. These calculation were performed using Matlab and is shown in APPENDIX C. System Parameter Data.

$$P_{loss} = P_{in} - P_{out} \tag{5.2}$$

$$\eta = \frac{P_{out}}{P_{in}} \tag{5.3}$$

The DC power supply efficiency and power contour plots are shown in Figure 5.3. This figure shows that the DC power supply has generally increasing losses with both speed and torque. Referring to Table 3.7, the DC power supplies efficiency is stated to be greater than 88%. This closely matches Figure 5.3. There is a large area that the calculated efficiency is near or exceeding that value.
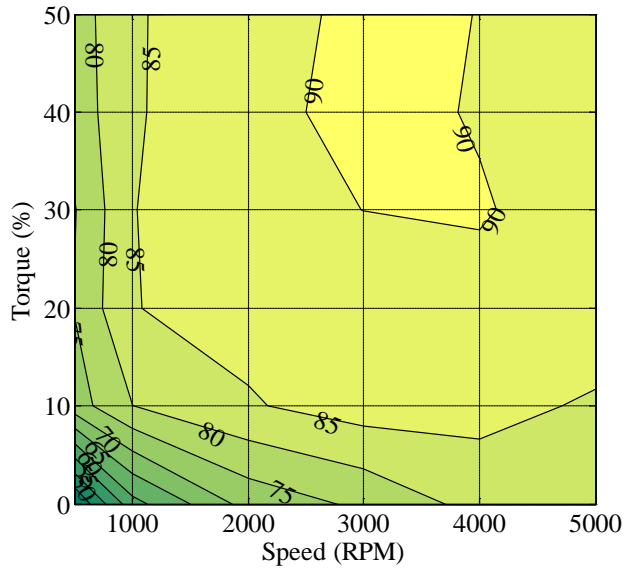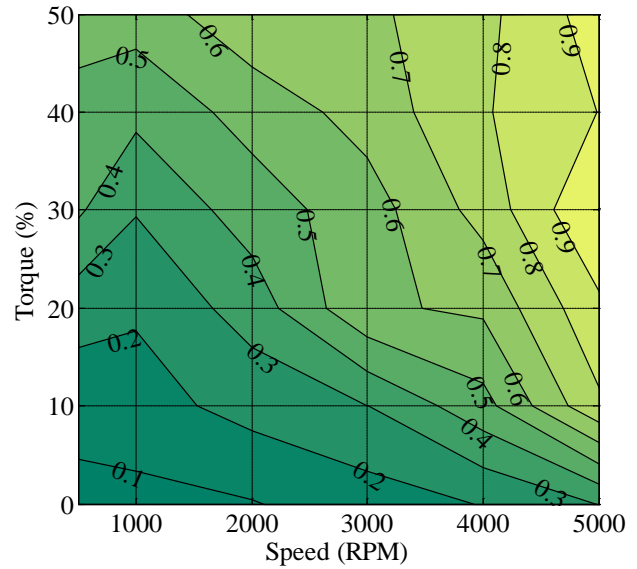
(a)   **(b)**

Figure 5.3: DC Power Supply (a) Efficiency and (b) Power Loss Map

The inverter efficiency and power contour plots are shown in Figure 5.4 This figure shows that the inverter has a very high efficiency region over most of the operational points. The manufacturer does not list efficiency data with the information on this inverter but when comparing this to other inverter efficiency data greater than 60-80% [20, 21], it can be seen that this inverter is very efficient. This fact is also reflected in power losses shown in Figure 5.4. This shows that in the maximum loss case is around 250 W.
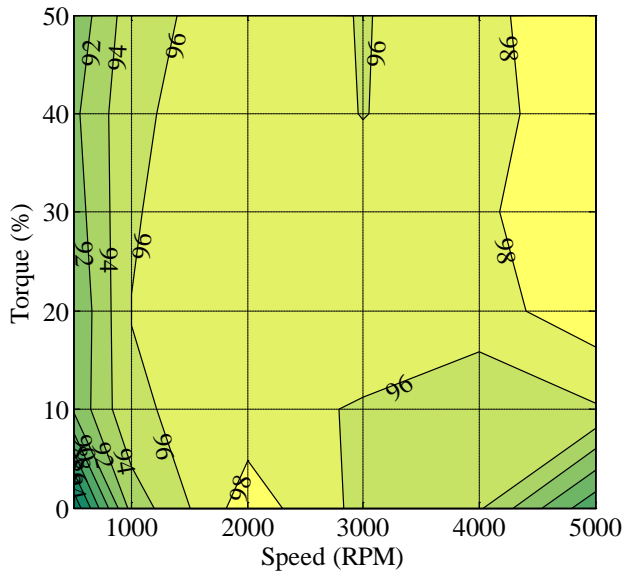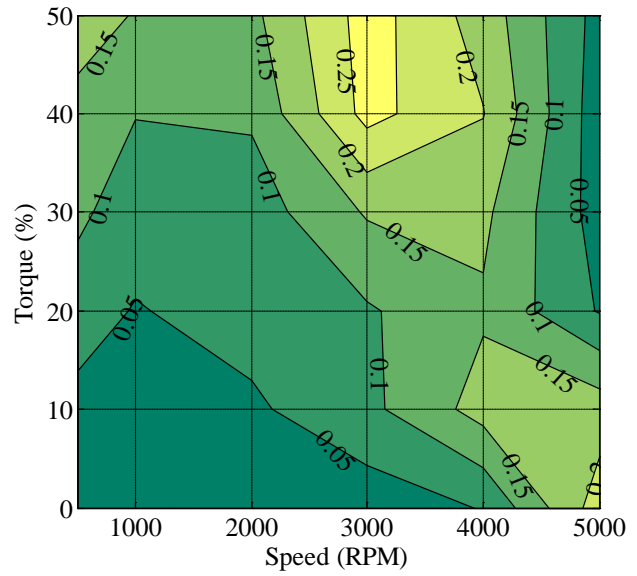
Figure 5.4: Inverter (a) Efficiency% and (b) Power Loss Map kW

The prime mover machine efficiency and power contour plots are shown in Figure 5.5. This figure shows that the prime mover machine has the worst efficiency of the prime mover circuit components. Not only is the maximum efficiency lower that DC power supply and inverter, but the size of the operational region in which that occurs is smaller. When comparing to the manufacture claim of 90.2% at nominal conditions (see Table 3.4), it can be seen that smaller values were calculated. There are a few explanations for this. The first is that the machine is not operating at nominal conditions. For most of the operation region the machine is operating at 1/3 of rated or nominal power. The second reason for lower than claimed efficiency, is that control scheme of the machine will have significant influence over the efficiency, however, the control scheme was not optimize, which would result is higher losses and lower efficiency.
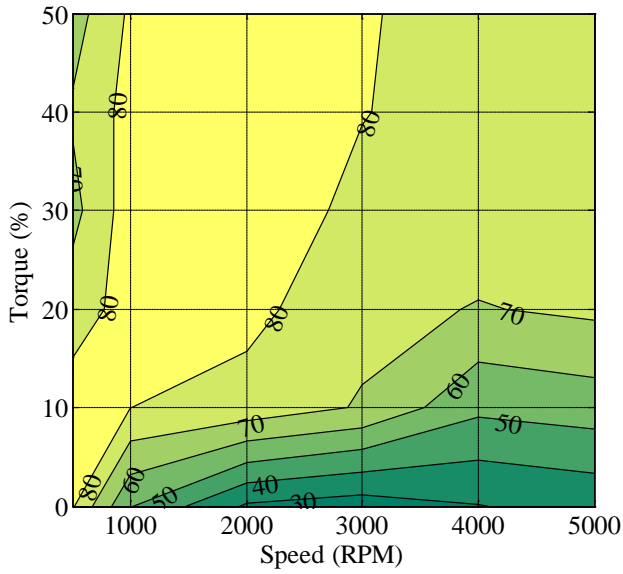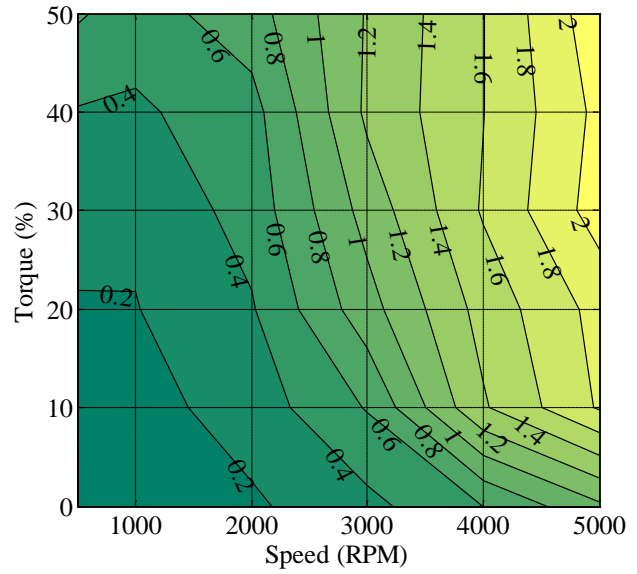
Figure 5.5: Machine1 (a) Efficiency% and (b) Power Loss Map kW

The absorber efficiency and power contour plots are shown in Figure 5.6. This figure shows that when the machine operated to optimized for lowering power losses, can achieve very high efficiencies. These very high efficiencies are a result of the VFD operating to optimize for flux. Most of the operational region of the absorber machine has 90% or better efficiency value. It can also be observed that the losses are significantly reduced from the prime mover machine to the absorber machine.
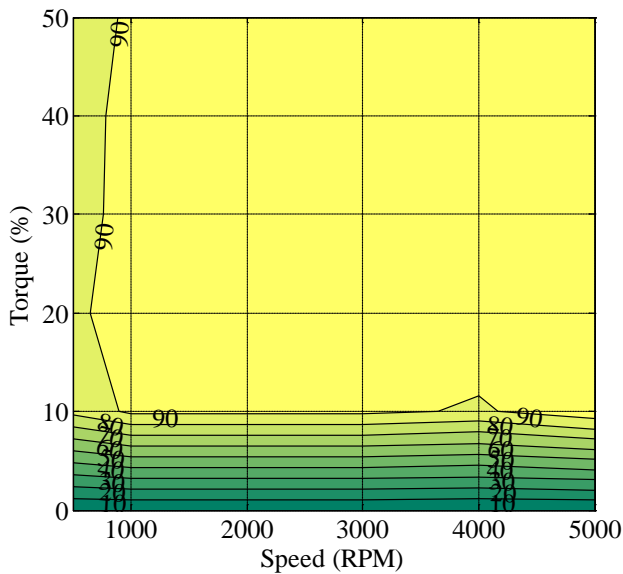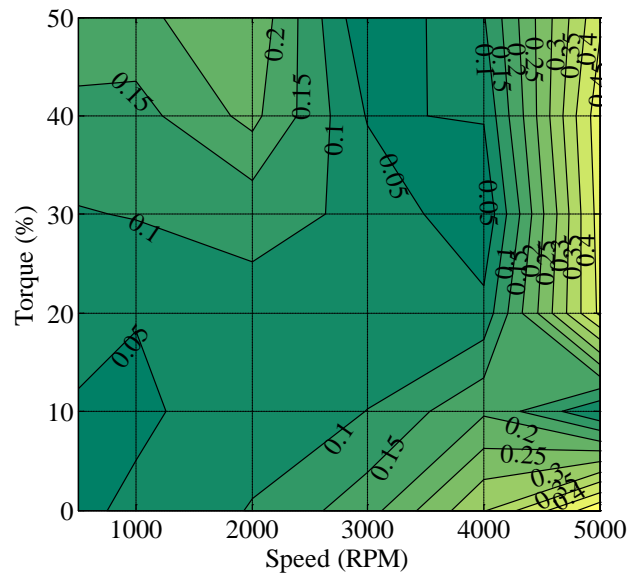
Figure 5.6: Machine2 (a) Efficiency% and (b) Power Loss Map kW

56

The VFD efficiency and power contour plots are shown in Figure 5.7. This figure shows that the VFD has a wider variance of efficiencies. During high power operation regions the VFD operates at greater than 80% efficiency. This varies from the manufacture claims 97% efficiency, referring to Table 3.2; however that claim is at nominal conditions of 40 HP. This can be explained by looking at the operation power point that the system was operating at. Our machine is only a 20 HP, with only a maximum power of around 7 HP.
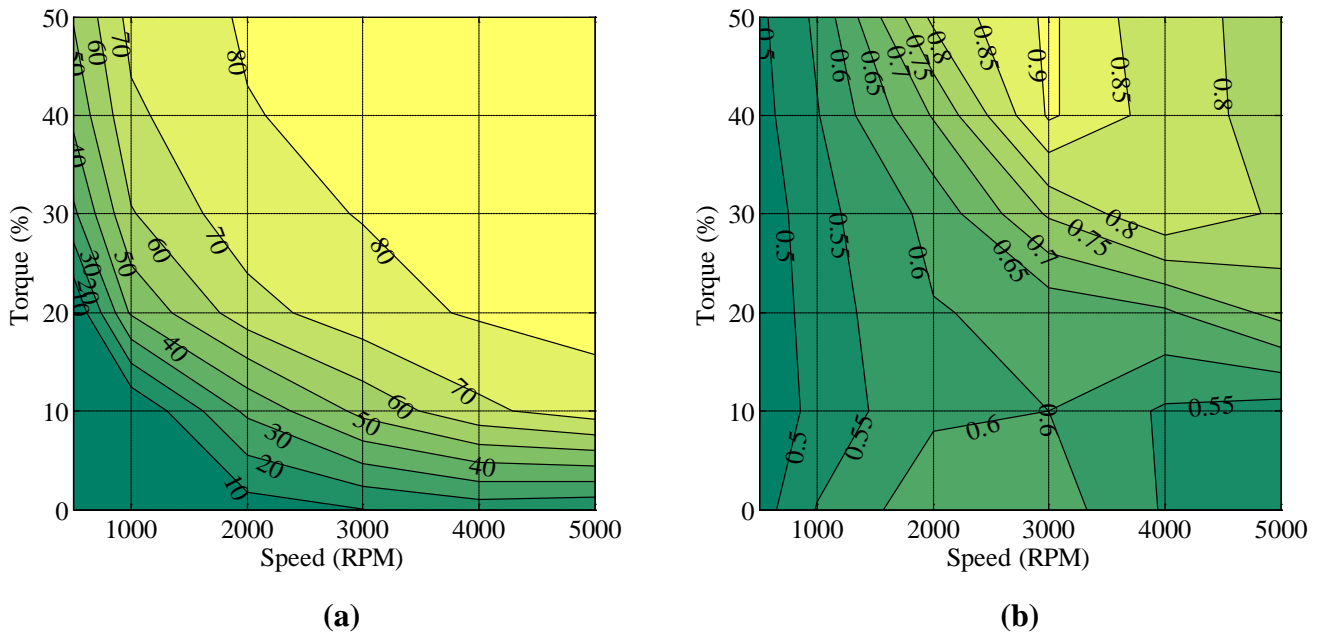
Figure 5.7: Variable Frequency Drive (a) Efficiency% and (b) Power Loss Map kW

The transformer efficiency and power contour plots are shown in Figure 5.8. This figure shows that the transformer also has a wider variance of efficiencies. During high power operation regions the transformer operates at greater than 90% efficiency. The manufacture did not supply efficiency data however when comparing typical transformer efficiency [22] values this seems reasonable. One notable area of operation is the 2000 RPM and 10 % torque has an extremely high efficiency value. This is because around that condition there is very lower power needed since the absorber machine is regenerating. Also at this time the regenerative power is just enough to cover the VFD losses. This point is effectively, from the point of view of the transformer a no load condition.
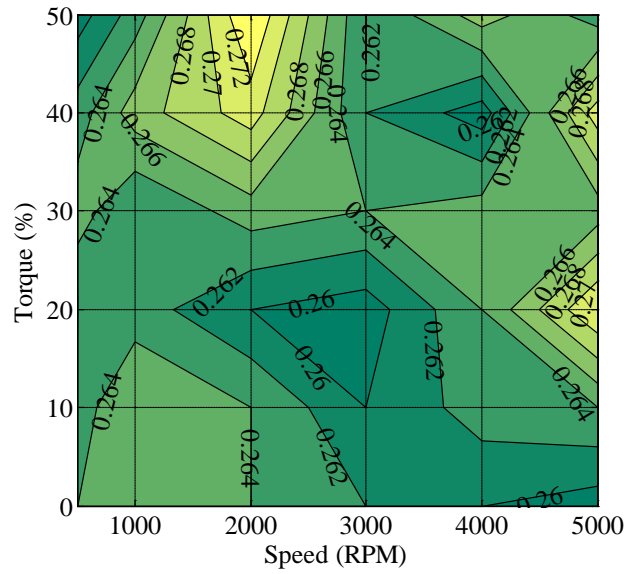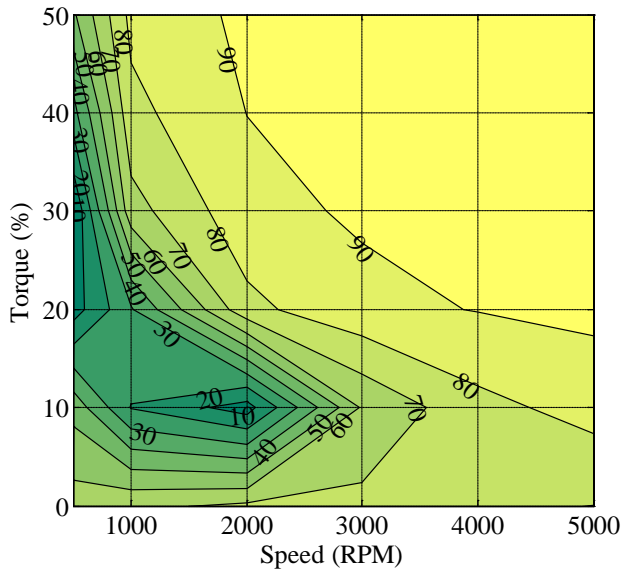
(a)   **(b)**

Figure 5.8: Transformer (a) Efficiency % and (b) Power Loss Map kW

The total system efficiency and power contour plots are shown in Figure 5.8. This figure shows that the system has an increase of efficiency and losses, with an increase in shaft power. During high power operation regions the system operates at greater than 50% efficiency with losses up to 4 kW at high speed and torque.
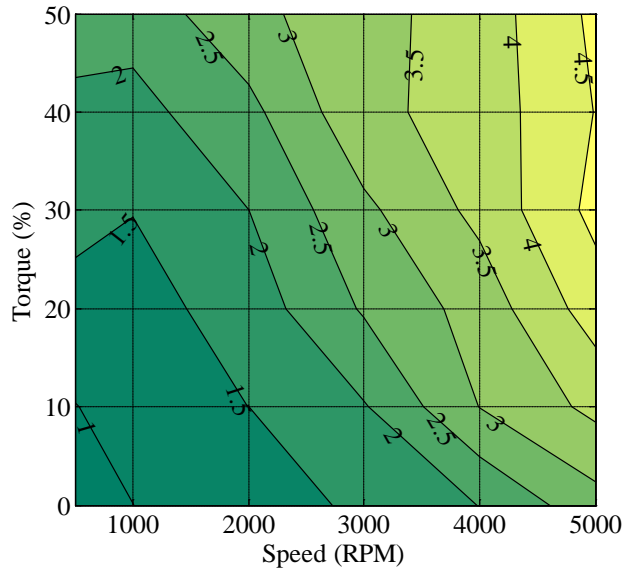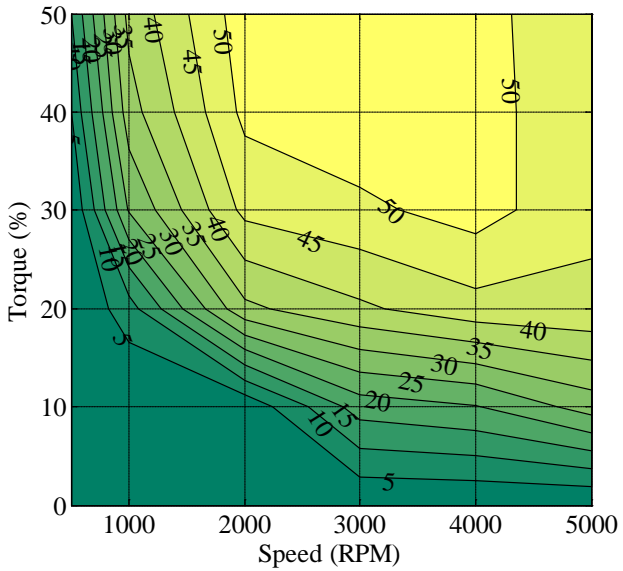
(a)   **(b)**

Figure 5.9: Total System (a) Efficiency% and (b) Power Loss Map kW

5.2 Slip Control Performance

The control scheme for the APS inverter used for testing and validation was primarily a closed loop volts per hertz speed controller or slip control. A block diagram of this control scheme is shown in Figure 5.10. However during some portions of testing, the user can use volts per hertz via a direct frequency command for troubleshooting. The slip control controller utilized analog speed feedback via the torque sensor to get a measured value of speed. From the speed command and feedback, the speed error was determined and supplied to a PI controller. The output of the controller was essentially the volts per hertz value in RPM. This was then converted to a frequency and a peak voltage value. From these two quantities, along with the bus voltage, the duty cycle and switching signals were sent to the inverter.
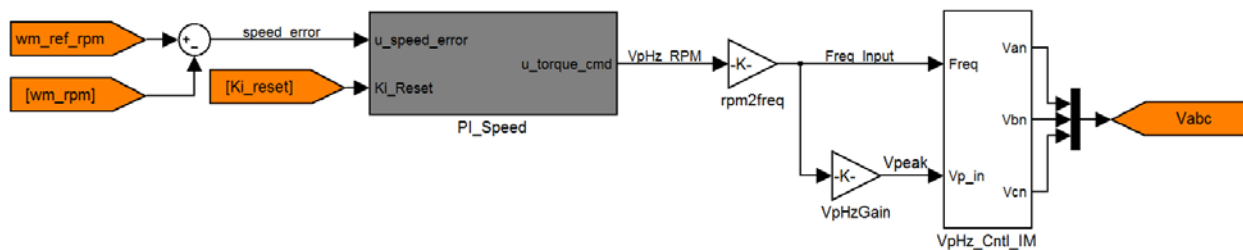
Figure 5.10: Volts per Hertz Control Scheme

Utilizing this close loop speed controller has advantages and disadvantages that were previously discussed in section 1.4 of this Report. The main advantage, however, is the automatic torque compensation to meet the required torque of the load while operating at the command speed. This control scheme was used to collect system performance data and verify system operation. A series of torque and speed step changes were executed and data was collected. A summary of the test points are shown in Table 5.5. For all tests the Volts per Hertz gain was calculated to in accordance to(5.4). The PI controller gains were determined from experimental operation and are shown in Table 5.6

Table 5.5: System Performance Data Collection Points

Test	Speed (RPM)	Torque (%)
Speed Step Change	1000-3000	10
Speed Step Change	1000-3000	40
Speed Step Change	1000-3000	50
Torque Step Change	1000	10-40
Torque Step Change	2000	10-75
Torque Step Change	5000	10-40

$$K_{VpHz} = \frac{V_{rated:l-n(peak)}}{f_{rated}} \tag{5.4}$$

Table 5.6: System Performance Controller Parameters

Name	Value
Proportional Gain	0.5
Integral Gain	0.5
K_{VpHz}	3

The speed response change test was executed to show the response time of a speed changed at various load torque values. Figure 5.11 and Figure 5.12 shows that the increase torque required (Δ 5 N-m) to accelerate the system is relatively the same in both the low and high load torque test cases. It can also be seen that the response time that the system reaches steady state speed is also the same in both cases (~10 s). Figure 5.13 shows the same speed response time, however, a notable aspect to discussion is the fact that the steady state torque value changed from the low speed (~ 21 N-m) to high speed (~ 16 N-m) step change. This can be attributed to the VFD keeping a constant max power of approximately 7 HP and limiting the torque output of the absorber machine.
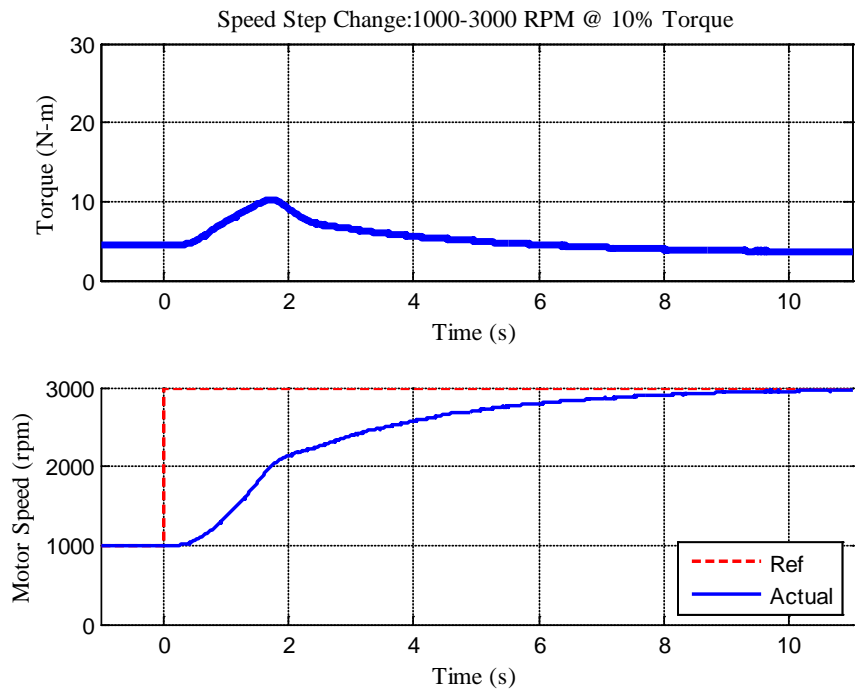
Figure 5.11: Speed Step Change 1000-3000 RPM @ 10% Torque
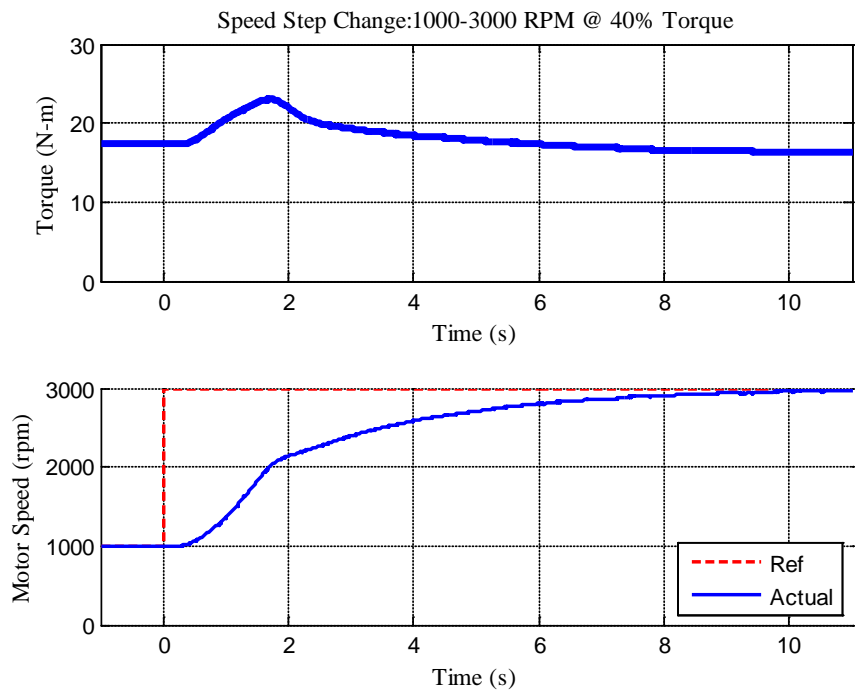
Figure 5.12: Speed Step Change 1000-3000 RPM @ 40% Torque

61
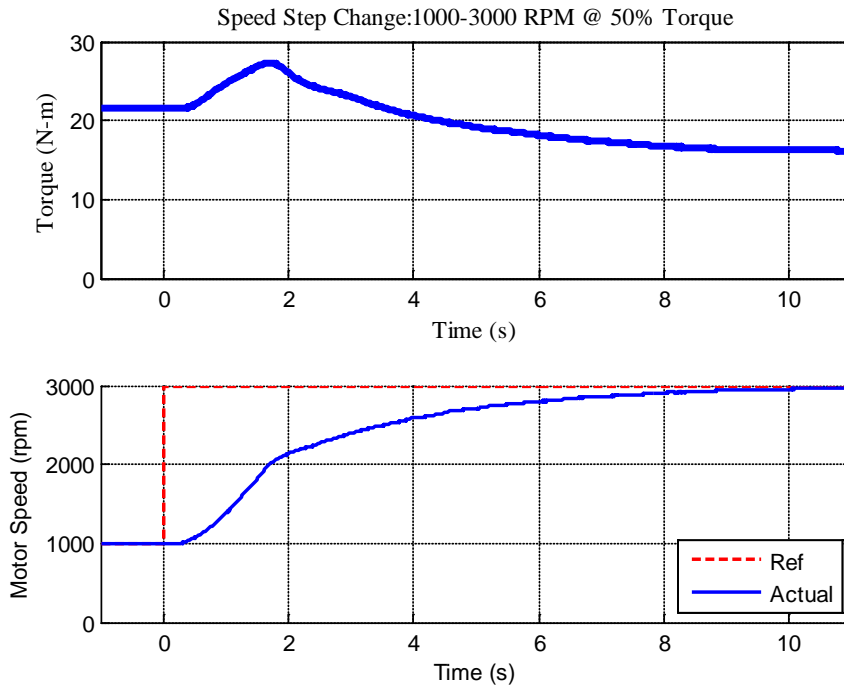
Figure 5.13: Speed Step Change 1000-3000 RPM @ 50% Torque

The torque response change test was executed to show the response time of the torque changed at various shaft speed values. Figure 5.14 and Figure 5.15 shows that the decrease speed when the added torque is applied from the VFD (Δ 30 RPM). It can also be seen that the response time that the system reaches steady state speed is also the same in both cases (~5 s). Figure 5.16 shows this same behavior however at a much higher torque step change. One notable difference is that at this higher torque operation, there are more speed oscillations around the reference value.
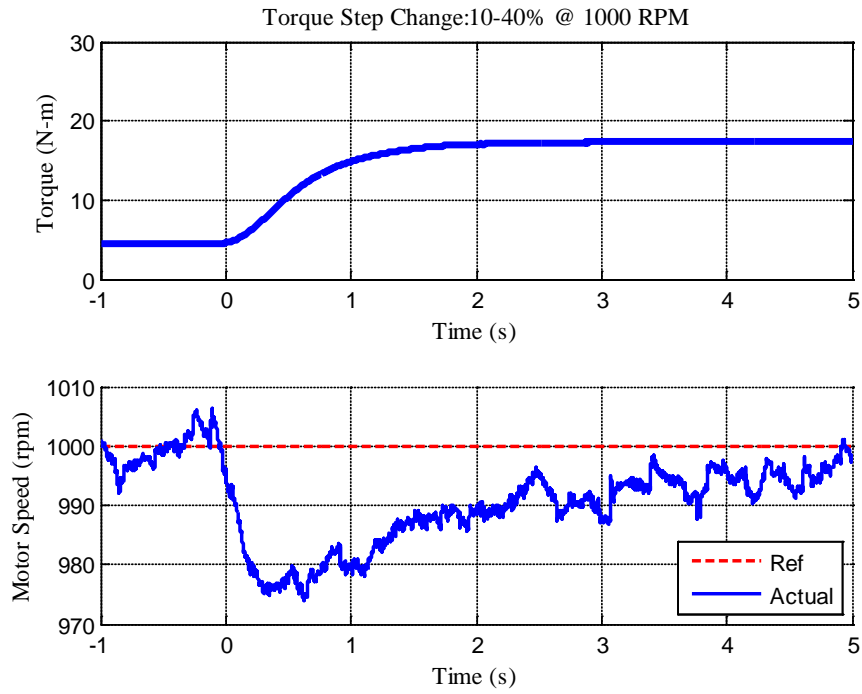
Figure 5.14: Torque Step Change 10 to 40% @ 1000 RPM
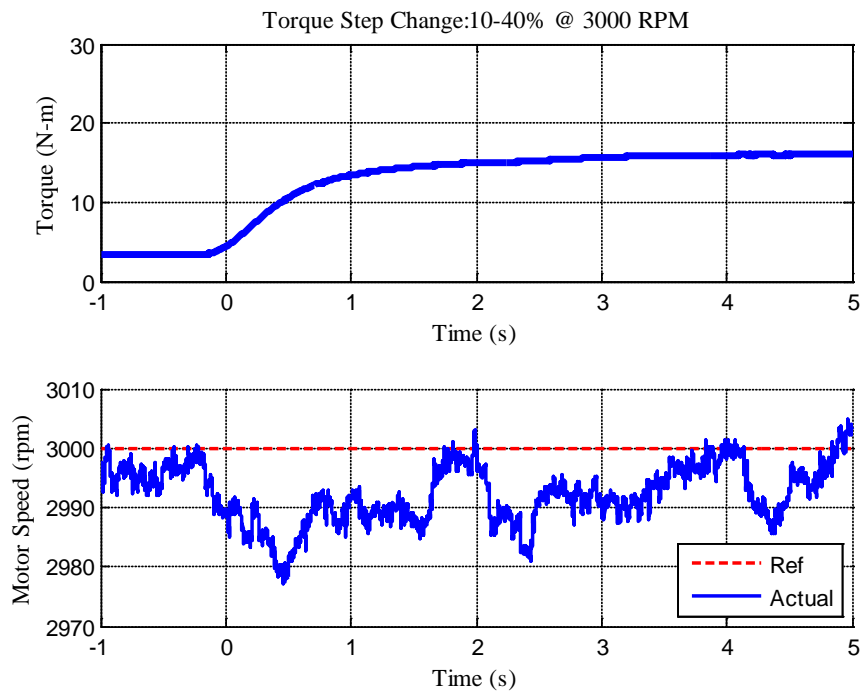
Figure 5.15: Torque Step Change 10 to 40% @ 3000 RPM
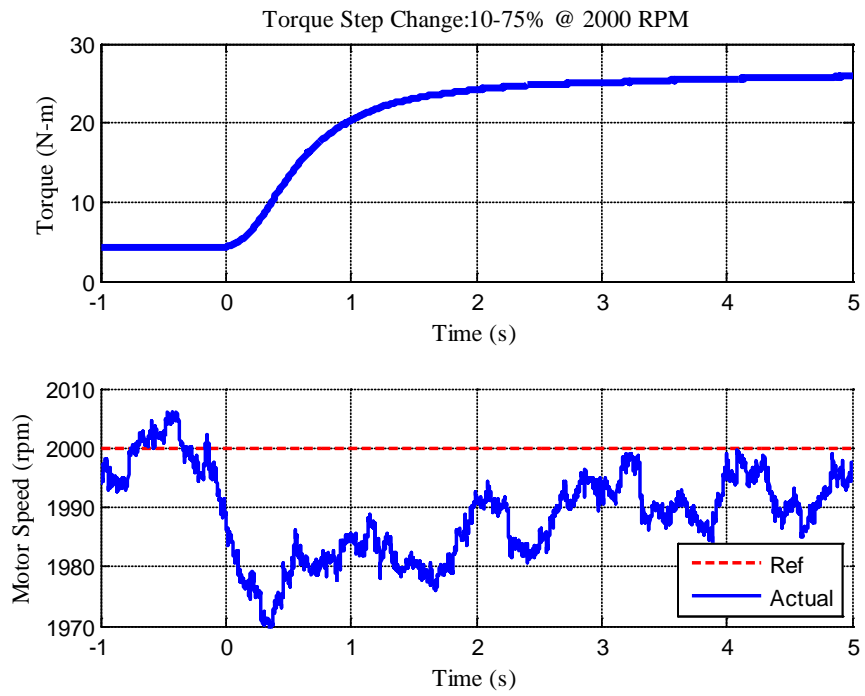
Figure 5.16: Torque Step Change 10 to 75% @ 2000 RPM

CHAPTER 6. CONCLUSION

This chapter will summarize and present closing thoughts on the project report and test cell system. It will also present areas of future work, along with areas of research that could utilize the test cell system.

6.1   Summary

A research quality electric machine test bed was designed, constructed, and commissioned. The project background was discussed stating the work that was completed by the EET Senior Design team and my individual contributions to the project. The selection of the test cell architecture and components were also discussed. The major test cell power components were discussed in detail and key features of the equipment were highlighted in regards to their specific use in the test cell.

The control sensors gain feedback signal routing were developed for use in data acquisition and measurement purposes. No load and blocked rotor tests were conducted in order to get estimates of the induction machines equivalent circuit parameter values. The performance of the test cell was also presented. This involved system characterization with regards to efficiency and power losses. Both component and system level values were found for use as baseline information in future testing. Torque and speed step changes were conducted in order to get system responses from the basic volts per hertz, slip control scheme.

6.2   Future Work

While the test cell is fully functional there have been several areas that were identified to increase the test cell's usability and expand its research capabilities. They are listed in order of complexity to complete, least being first.

- <u>Optimized volts per hertz gain determination</u> – During the collection of system characterization data, the volts per hertz gain (K_{VpHz}) value was selected via experimental determination. The values used during system characterization where not optimized. Simple test procedures could be conducted where the optimal value could be found at each torque/speed load point, leading to lower steady state power losses.

- Control Signal Noise Reduction – All of the analog signals are susceptible to induced noise voltage from the inverter and VFD. For higher performance control strategies this extra noise may skew the actual value and cause less than optimal performance. The inverter current signals have increased sensitivity to this effect when used in higher performance control strategies, such as field oriented control or direct torque control schemes.

- Integration of different control systems – Integration of the inverter embedded controls, VFD control, and test cell infrastructure control would be a key asset to automated testing. Currently, the speed (frequency) ref to the inverter and torque request to VFD, are controlled via two different controllers. The test cell infrastructure controls sends no information on its state to the other system. Incorporating them into a single control system, or have a communication link between the three, would serve to allow for simultaneous, and dynamic, control of the test bed machines.

- Investigation into limited regenerative power – The combination of the VFD and absorber machine limits the absorbing power to approximately 7 HP (5.2 kW). Further investigation into is necessary to determine whether this is limited by the physical hardware or the VFD control strategy.

- Implementation of high performance control scheme – Indirect field oriented control (IFOC) or direct torque control (DTC) schemes have greater system response [23, 24]. The implementation of either IFOC or DTC allow the test cell to have a greater performance, allowing for expanded system functionality when performing system level testing, as an electric propulsion power train, or use as a load source for use in a AC Microgrid.

6.3   Possible Research Areas Projects

The test cell has many research areas in which it could serve as the hardware component with little to no modifications needed.

- Electric Machine Controls and Hardware Development – The test cell has all the necessary power and control signals needed to begin research into high performance controls or hardware development. To realize this area of research the test cell

configuration would not need modification. However, most of the items listed in section 6.2 would need to be completed.

- Electric Vehicle Propulsion Systems – To utilize the test cell as an EV propulsion system, the dc power supply would need to be replaced by a battery pack, or a simulated battery voltage/current profile from the output of the dc power supply. The electric machine would either be replaced with differing machines, or kept as the currently installed induction machine, as needed by the EV architecture.

- AC MicroGrid – To utilize the test cell for a 3 phase AC MicroGrid, it would need to be modified according to whether it was used as a combination source and load, or an individual source and load. For either, the combination or individual source load setup, minimal hardware configuration would need to be completed, however the control scheme would require substantial development, most notably if the test cell was not used as a machine type load.

- Power Electronic Converter – The test cell may be configured for an using a AFE rather than the dc power supply by switching the power supply and controlling the dc bus, via another inverter. This is AFE architecture is common to several modern motor drive systems. This would require little configuration change however would need moderate control scheme and signal work.

REFERENCES

[1]   C. C. W. Chan, Y.S.; Bouscayrol, A.; Keyu Chen, "Powering Sustainable Mobility: Roadmaps of Electric, Hybrid, and Fuel Cell Vehicles [Point of View]," *Proceedings of the IEEE* vol. 97, pp. 603-607, 2009.

[2]   (2012). *Hybrid Electric Vehicle Curriculum (HEV)*. Available: http://www.mtu.edu/hybrid/

[3]   O. W. P. Krause, S. Sudhoff, *Analysis of Elctric Machinery and Drive Systems*, Second ed.: IEEE Press, 2002.

[4]   "Class Lecture Notes," ed. EE5221 Advance Electric Machine: Michigan Technological University.

[5]   *Understanding Induction Motor Nameplate Information*. Available: http://ecmweb.com/motors/understanding-induction-motor-nameplate-information

[6]   *Wall-mounted low harmonic drives, ACS800-31*. Available: http://www.abb.com/product/seitp322/d615ea11e114f520c125789a00372d2f.aspx?productLanguage=us&country=US

[7]   "ACS800-U31 Drives 7.5 to 125 HP Hardware Manual," ed: ABB Inc.

[8]   *Programmable DC Power Supplies*. Available: http://www.magna-power.com/products/programmable-dc-power-supplies/ts-series

[9]   *IAP75T120 SixPac*. Available: http://www.appliedps.com/newweb/Datasheets/AP-75T120/AP-75T120.htm

[10]   *MCRT® 48200V Compact Digital Torque Transducers*. Available: http://www.himmelstein.com/Compact_Digital_Torque_Transducers_MCRT_48200V_Series.asp

[11]   (June 29, 2012). *Zero-Max Composite Disc Couplings*. Available: http://www.zero-max.com/flexible-shaft-couplings-composite-disc-couplings-c-1_2-l-en.html

[12]   *Introduction to Modbus*. Available: http://www.ni.com/white-paper/7675/en

[13]   *NI Modbus Library for LabVIEW*. Available: http://sine.ni.com/nips/cds/view/p/lang/en/nid/201711

[14]   *Analog Isolation Module, Voltage Input (10 kHz), ±10 V Input, ±5 V Output*. Available: http://www.mccdaq.com/signal-conditioning/ISO-5B41-03.aspx

[15]   *Analog Isolation Module, Voltage/Current Input, ±5 V Input, ±5 V Output*. Available: http://www.mccdaq.com/signal-conditioning/ISO-5B41-02.aspx

[16]   *EAGLE PCB DESIGN SOFTWARE*. Available: http://www.cadsoftusa.com/

[17]   A. E. F. K. Fitzgerald, Charles;Umans, Stephen D., *Electric Machinery* Sixth ed.: McGraw-Hill Science Engineering, 2003.

[18]   Baldor, "Product Information Packet IDBRPM25754," 1 ed: Baldor Electric Company, 2006.

[19]   (7/12/2012). *WT 500 Power Analyzer User's Manual*.

[20]   I. Wilmore Electronics Co. *DC-TO-AC POWER INVERTERS*. Available: www.wilmoreelectronics.com/Prodlit/1400dc-ac.pdf

[21]   Solar-Facts.com. *Inverter Efficiency*. Available: http://www.solar-facts.com/inverters/inverter-efficiency.php

[22]   K. D. Harden, "OPTIMIZING ENERGY EFFICIENCY STANDARDS FOR LOW VOLTAGE DISTRIBUTION TRANSFORMERS," Master of Science in Engineering, Purdue University, Fort Wayne, Indiana, 2011.

[23]   M. Depenbrock, "Direct self-control (DSC) of inverter-fed induction machine," *Power Electronics, IEEE Transactions on,* vol. 3, pp. 420-429, 1988.

[24]   I. Takahashi and T. Noguchi, "A New Quick-Response and High-Efficiency Control Strategy of an Induction Motor," *Industry Applications, IEEE Transactions on,* vol. IA-22, pp. 820-827, 1986.

[25]   "Experiment 13: Volts per Hertz Control of a Three Phase Induction Motor," ed. EE3221 Introduction to Motor Drives Lab: Michigan Technological University.

APPENDIX A. DATASHEETS

A.1 Himmelstein Series 700 Instrument Summary

S. HIMMELSTEIN AND COMPANY

Series 700 Instrument Summary

Serial Number: 723 - 3961

Model Number: 723

Factory Reference Number: 31881-VE

Channel 1:

Chan 1 Signal Conditioner: DCVA

Display Full Scale: 1000.0

Display Resolution: 1

Display Legend: LB-IN

Measured Parameter: Torque

Transducer Used: MCRT 48203V

Installed Shunt Cal Resistor: N/A

Channel 2:

Chan 2 Signal Conditioner: CTUA

Display Full Scale: 8500

Display Resolution: 10

Display Legend: RPM

Measured Parameter: Speed

Transducer Used: C/F

Installed Shunt Cal Resistor: N/A

Channel 3:

Calculation: (Ch1*Ch2)/Const

Calculation Constant: 63025

Display Full Scale: 134

Display Resolution: 0.1

Display Legend: HP

Measured Parameter: Horsepower

Analog Outputs:

Analog Output 1: +/-5 V   Assigned to Channel No. 1

Analog Output 2: +/-5 V   Assigned to Channel No. 2

NOTES:

1. C/F denotes customer furnished material or data.
2. N/A denotes the parameter or data is not applicable.
3. When applicable, shunt calibration resistors are installed for Himmelstein furnished transducers.
4. See Section 3.0 for transducer calibration values.
5. Instrument shipped as indicated. Programmable items not listed are at their default values. User may change legends, calculations, scaling, etc.;see attached instructions.

APPENDIX B. SENSOR CALIBRATIONS

B.1 DC Bus Command Adjustment Table Calibration

Bus CMD	DC Bus	AI Value	K
0.1	0	0	0.95
50	52.6	1.25	0.95057
100	103.3	2.5	0.968054
150	153.8	3.76	0.975293
200	204.2	4.99	0.979432
250	254.6	6.25	0.981932
300	305.1	7.5	0.983284
350	355.5	8.75	0.984529
400	405.8	9.95	0.985707

B.2 DC Bus Measurement Adjustment Table Calibration

DC Bus Cmd	DC Bus	Diff(Cmd-Act)
0.1	0.1	0
10	10	7
25	25	4.5
50	50	3
100	100	0
150	150	-2
200	200	-8
250	250	-11
300	300	-15
350	350	-20
400	400	-25

APPENDIX C. SYSTEM PARAMETER DATA

C.1 DC Power Supply System Data

				Torque (%)						
				0						
Speed (RPM)	V/f	Urms1	Irms1	PΣ (kW)	QΣ (kVAR)	SΣ (kVA)	λΣ	φΣ (°)	T (in-lbs)	P(HP)
500	1.0	209.36	0.685	0.116	-0.250	0.284	0.4678	62.11	4.0	0.030
1000	1.0	209.73	0.922	0.165	0.065	0.335	0.4940	60.39	3.8	0.060
2000	1.0	209.15	1.644	0.332	0.535	0.596	0.5580	56.08	2.7	0.080
3000	1.0	209.33	2.777	0.627	0.876	1.007	0.6227	51.48	3.5	0.140
4000	1.0	209.42	4.557	1.110	1.418	1.653	0.6713	47.83	6.2	0.380
5000	1.0	208.86	7.518	1.951	2.292	2.720	0.7172	44.18	12.5	0.880

				10						
Speed (RPM)	V/f	Urms1	Irms1	PΣ (kW)	QΣ (kVAR)	SΣ (kVA)	λΣ	φΣ (°)	T (in-lbs)	P(HP)
500	2.5	209.39	2.290	0.499	0.726	0.831	0.6006	53.08	44.2	0.350
1000	2.5	209.71	3.443	0.803	1.084	1.251	0.6416	50.09	41.9	0.650
2000	2.5	208.86	6.022	1.516	1.865	2.179	0.6960	45.89	39.3	1.260
3000	2.5	209.15	8.933	2.373	2.725	3.236	0.7332	42.85	38.0	1.810
4000	2.5	209.07	12.617	3.503	3.765	4.569	0.7667	39.94	33.0	2.000
5000	2.5	208.44	17.190	4.980	4.994	6.206	0.8025	36.63	39.7	3.000

				20						
Speed (RPM)	V/f	Urms1	Irms1	PΣ (kW)	QΣ (kVAR)	SΣ (kVA)	λΣ	φΣ (°)	T (in-lbs)	P (HP)
500	2.5	209.79	4.079	0.983	1.272	1.482	0.6633	48.45	84.0	0.670
1000	3.0	209.58	5.584	1.398	1.730	2.027	0.6897	46.40	79.5	1.270
2000	3.0	208.86	9.750	2.623	2.958	3.527	0.7437	41.95	77.0	2.450
3000	3.0	209.01	14.426	4.095	4.240	5.223	0.7841	38.36	68.9	3.300
4000	3.0	208.89	18.535	5.574	0.349	6.706	0.8312	33.78	70.2	4.500
5000	3.0	208.34	23.887	7.552	0.415	8.620	0.8761	28.82	77.0	6.100

				30						
Speed (RPM)	V/f	Urms1	Irms1	PΣ (kW)	QΣ (kVAR)	SΣ (kVA)	λΣ	φΣ (°)	T (in-lbs)	P (HP)
500	2.5	209.40	6.428	1.646	1.970	2.331	0.7060	45.09	123.9	0.980
1000	3.0	209.72	7.744	2.027	2.368	2.813	0.7205	43.90	116.0	1.860
2000	3.0	208.82	13.248	3.723	3.926	4.792	0.7769	39.02	115.0	3.680
3000	3.0	208.91	18.537	5.569	0.358	6.707	0.8303	33.87	105.0	5.030
4000	3.0	208.78	23.887	7.593	0.421	8.638	0.8790	28.47	106.9	6.800
5000	3.0	208.80	26.673	8.580	0.439	9.613	0.8925	26.81	91.0	7.150

40										
Speed (RPM)	V/f	Urms1	Irms1	PΣ (kW)	QΣ (kVAR)	SΣ (kVA)	λΣ	φΣ (°)	T (in-lbs)	P (HP)
500	3.0	209.41	7.371	1.922	2.241	2.673	0.7190	44.03	160.0	1.280
1000	3.0	208.98	10.124	2.735	3.048	3.665	0.7463	41.73	154.9	2.460
2000	3.0	208.72	16.613	4.833	0.280	6.006	0.8048	36.41	153.5	4.860
3000	3.0	208.55	22.890	7.212	0.408	8.268	0.8722	29.23	141.8	6.770
4000	3.0	208.61	24.219	7.711	0.421	8.751	0.8811	28.22	107.2	6.870
5000	3.0	208.33	26.392	8.494	0.433	9.523	0.8920	26.88	90.0	7.200

50										
Speed (RPM)	V/f	Urms1	Irms1	PΣ (kW)	QΣ (kVAR)	SΣ (kVA)	λΣ	φΣ (°)	T (in-lbs)	P (HP)
500	3.0	209.45	9.512	2.564	2.878	3.451	0.7430	42.01	196.2	1.570
1000	3.0	209.29	12.445	3.467	3.692	4.511	0.7684	39.79	192.0	3.050
2000	3.0	208.74	19.794	6.034	0.391	7.156	0.8432	32.52	191.0	6.050
3000	3.0	208.50	23.081	7.287	0.415	8.335	0.8742	29.05	142.8	6.850
4000	3.0	208.74	24.163	7.694	0.419	8.736	0.8807	28.27	107.0	6.800
5000	3.0	208.28	26.500	8.529	0.443	9.560	0.8921	26.86	90.0	7.200

Efficiency								
	Torque (%)						Average	Median
Speed (RPM)	0	10	20	30	40	50	82.62%	85.30%
500	39.66%	72.75%	75.28%	74.79%	77.11%	77.57%		
1000	58.18%	79.95%	84.84%	84.85%	84.46%	84.40%		
2000	71.69%	84.50%	86.89%	87.94%	88.87%	88.83%		
3000	75.92%	87.40%	85.74%	90.05%	91.14%	90.68%		
4000	81.62%	86.73%	88.91%	90.28%	89.74%	89.95%		
5000	84.52%	84.30%	88.35%	88.33%	89.38%	88.87%		

Power Losses (kW)								
	Torque (%)						Average	Median
Speed (RPM)	0	10	20	30	40	50	0.479	0.457
500	0.070	0.136	0.243	0.415	0.440	0.575		
1000	0.069	0.161	0.212	0.307	0.425	0.541		
2000	0.094	0.235	0.344	0.449	0.538	0.674		
3000	0.151	0.299	0.584	0.554	0.639	0.679		
4000	0.204	0.465	0.618	0.738	0.791	0.773		
5000	0.302	0.782	0.880	1.001	0.902	0.949		

C.2 Inverter System Data

					Torque (%)					
					0					
Speed (RPM)	V/f	Urms1	Irms1	PΣ (kW)	QΣ (kVAR)	SΣ (kVA)	λΣ	φΣ (°)	T (in-lbs)	P(HP)
500	1.0	22.76	2.030	0.046	-0.006	0.046	0.9901	8.07	3.5	0.030
1000	1.0	42.41	2.271	0.096	-0.009	0.096	0.9952	5.60	3.4	0.060
2000	1.0	82.39	2.888	0.238	-0.014	0.238	0.9983	3.35	2.4	0.070
3000	1.0	122.84	3.879	0.476	-0.026	0.477	0.9984	3.27	3.3	0.160
4000	1.0	163.19	5.565	0.906	-0.059	0.908	0.9979	3.75	5.5	0.330
5000	1.0	203.83	8.103	1.649	-0.090	1.652	0.9984	3.24	9.8	0.770

					10					
Speed (RPM)	V/f	Urms1	Irms1	PΣ (kW)	QΣ (kVAR)	SΣ (kVA)	λΣ	φΣ (°)	T (in-lbs)	P(HP)
500	2.5	54.49	6.671	0.363	-0.024	0.363	0.9979	3.72	44.0	0.350
1000	2.5	103.81	6.195	0.642	0.031	0.643	0.9987	2.88	40.7	0.650
2000	2.5	203.19	6.326	1.281	-0.100	1.285	0.9967	4.67	39.0	1.240
3000	2.5	303.23	6.885	2.074	-0.234	2.088	0.9934	6.60	37.9	1.790
4000	2.5	385.27	7.938	3.038	-0.349	3.058	0.9932	6.71	30.4	1.940
5000	2.5	385.27	10.964	4.198	-0.453	4.224	0.9938	6.39	35.0	2.790

					20					
Speed (RPM)	V/f	Urms1	Irms1	PΣ (kW)	QΣ (kVAR)	SΣ (kVA)	λΣ	φΣ (°)	T (in-lbs)	P (HP)
500	2.5	57.07	12.977	0.740	-0.028	0.741	0.9993	2.17	84.2	0.670
1000	3.0	124.55	9.534	1.186	-0.048	1.187	0.9991	2.40	79.5	1.270
2000	3.0	244.24	9.351	2.279	-0.152	2.284	0.9978	3.84	77.0	2.430
3000	3.0	304.85	11.545	3.511	-0.239	3.520	0.9976	3.96	75.8	3.610
4000	3.0	385.47	12.923	4.956	-0.493	4.982	0.9949	5.78	69.6	4.400
5000	3.0	385.47	17.367	6.672	-0.535	6.694	0.9967	4.64	75.7	6.000

					30					
Speed (RPM)	V/f	Urms1	Irms1	PΣ (kW)	QΣ (kVAR)	SΣ (kVA)	λΣ	φΣ (°)	T (in-lbs)	P (HP)
500	2.5	60.66	20.312	1.231	-0.041	1.232	0.9994	1.90	123.5	0.990
1000	3.0	126.18	13.631	1.720	0.040	1.720	0.9997	2.38	116.0	1.870
2000	3.0	245.49	13.353	3.274	-0.153	3.278	0.9989	2.71	115.0	3.660
3000	3.0	306.23	16.394	5.015	-0.229	5.020	0.9989	2.64	113.0	5.380
4000	3.0	385.52	17.826	6.855	-0.475	6.873	0.9974	4.11	106.0	6.780
5000	3.0	385.51	19.714	7.579	-0.551	7.600	0.9972	4.28	88.1	7.090

40										
Speed (RPM)	V/f	Urms1	Irms1	PΣ (kW)	QΣ (kVAR)	SΣ (kVA)	λΣ	φΣ (°)	T (in-lbs)	P (HP)
500	3.0	70.26	21.100	1.482	-0.043	1.482	0.9996	1.65	161.0	1.290
1000	3.0	127.61	18.108	2.310	0.053	2.311	0.9997	1.35	155.0	2.470
2000	3.0	246.47	17.436	4.295	-0.143	4.297	0.9994	1.94	153.1	4.880
3000	3.0	307.95	21.358	6.573	-0.218	6.577	0.9994	1.96	149.0	7.070
4000	3.0	385.51	17.993	6.920	-0.455	6.937	0.9976	3.93	106.0	6.840
5000	3.0	385.53	19.745	7.592	-0.536	7.612	0.9973	4.21	87.9	7.100

50										
Speed (RPM)	V/f	Urms1	Irms1	PΣ (kW)	QΣ (kVAR)	SΣ (kVA)	λΣ	φΣ (°)	T (in-lbs)	P (HP)
500	3.0	73.47	27.088	1.989	-0.055	1.990	0.9996	1.60	196.8	1.570
1000	3.0	129.22	22.648	2.926	0.027	2.926	0.9999	0.58	192.0	3.050
2000	3.0	247.79	21.640	5.360	-0.149	5.362	0.9996	1.60	190.4	6.060
3000	3.0	307.95	21.471	6.608	-0.217	6.612	0.9994	1.93	150.5	7.190
4000	3.0	385.52	18.001	6.921	-0.494	6.940	0.9973	4.20	107.0	6.830
5000	3.0	385.54	19.715	7.580	-0.538	7.601	0.9973	4.24	88.7	6.990

Efficiency							
Torque (%)						Average	Median
Speed (RPM)	0	10	20	30	40	50	95.17%	95.90%
500	80.43%	90.36%	90.14%	90.98%	91.50%	90.60%		
1000	92.71%	95.79%	96.04%	95.81%	95.58%	95.04%		
2000	99.16%	96.72%	96.97%	97.71%	97.51%	97.44%		
3000	95.38%	95.81%	97.32%	96.91%	95.94%	95.87%		
4000	94.26%	94.40%	97.11%	97.65%	97.08%	97.43%		
5000	86.42%	95.78%	99.30%	99.63%	99.68%	99.57%		

Power Losses (kW)							
Torque (%)						Average	Median
Speed (RPM)	0	10	20	30	40	50	0.100	0.091
500	0.009	0.035	0.073	0.111	0.126	0.187		
1000	0.007	0.027	0.047	0.072	0.102	0.145		
2000	0.002	0.042	0.069	0.075	0.107	0.137		
3000	0.022	0.087	0.094	0.155	0.267	0.273		
4000	0.052	0.170	0.143	0.161	0.202	0.178		
5000	0.224	0.177	0.047	-0.028	0.024	-0.033		

C.3 Machine1 System Data

							Torque (%)				
							0				
Speed (RPM)	V/f	Urms1	Irms1	PΣ (kW)	QΣ (kVAR)	SΣ (kVA)	λΣ	ϕΣ (°)	T (in-lbs)	P(HP)	
500	1.0	11.74	3.152	0.037	0.021	0.064	0.5793	54.60	5.3	0.040	
1000	1.0	16.07	3.890	0.089	0.049	0.108	0.8224	34.68	3.8	0.060	
2000	1.0	34.15	4.751	0.236	0.125	0.281	0.8387	33.00	2.7	0.090	
3000	1.0	53.42	5.685	0.454	0.237	0.526	0.8634	30.30	3.1	0.150	
4000	1.0	74.43	7.490	0.854	0.416	0.966	0.8842	27.85	5.2	0.340	
5000	1.0	97.30	9.467	1.425	0.665	1.595	0.8932	26.72	7.3	0.625	

						10				
Speed (RPM)	V/f	Urms1	Irms1	PΣ (kW)	QΣ (kVAR)	SΣ (kVA)	λΣ	ϕΣ (°)	T (in-lbs)	P(HP)
500	2.5	20.74	10.359	0.328	0.163	0.372	0.8808	28.27	45.8	0.370
1000	2.5	43.87	9.755	0.615	0.334	0.741	0.8291	33.99	41.4	0.660
2000	2.5	98.27	9.415	1.239	1.041	1.603	0.7730	39.38	39.8	1.270
3000	2.5	140.28	10.146	1.987	1.521	2.465	0.8062	36.27	38.5	1.840
4000	2.5	183.82	10.842	2.868	2.038	3.452	0.8308	33.82	31.2	2.000
5000	2.5	220.60	12.291	4.021	2.774	4.696	0.8561	31.12	38.5	2.950

						20				
Speed (RPM)	V/f	Urms1	Irms1	PΣ (kW)	QΣ (kVAR)	SΣ (kVA)	λΣ	ϕΣ (°)	T (in-lbs)	P (HP)
500	2.5	21.59	19.160	0.667	0.256	0.717	0.9309	21.43	85.8	0.680
1000	3.0	53.51	14.136	1.139	0.587	1.310	0.8690	26.65	79.9	1.270
2000	3.0	111.93	13.586	2.210	1.177	2.634	0.8392	32.94	77.5	2.450
3000	3.0	166.02	14.010	3.417	2.289	4.029	0.8483	31.98	69.7	3.350
4000	3.0	216.24	14.917	4.813	3.143	5.587	0.8615	30.51	70.5	4.480
5000	3.0	234.25	18.141	6.625	4.089	7.360	0.9001	25.83	79.2	6.380

						30				
Speed (RPM)	V/f	Urms1	Irms1	PΣ (kW)	QΣ (kVAR)	SΣ (kVA)	λΣ	ϕΣ (°)	T (in-lbs)	P (HP)
500	2.5	22.93	30.356	1.120	0.437	1.205	0.9293	21.68	125.00	1.00
1000	3.0	54.07	19.320	1.648	0.724	1.809	0.9110	24.36	117.50	1.89
2000	3.0	111.23	18.513	3.199	1.506	3.566	0.8971	26.22	115.50	3.65
3000	3.0	165.38	18.897	4.860	2.261	5.413	0.8979	26.12	106.30	5.08
4000	3.0	215.15	19.840	6.694	2.911	7.431	0.9008	25.74	106.50	6.80
5000	3.0	234.27	20.598	7.607	4.577	8.358	0.9102	24.47	94.00	7.40

40										
Speed (RPM)	V/f	Urms1	Irms1	PΣ (kW)	QΣ (kVAR)	SΣ (kVA)	λΣ	φΣ (°)	T (in-lbs)	P (HP)
500	3.0	27.40	30.427	1.356	0.492	1.444	0.9386	20.13	162.20	1.30
1000	3.0	54.43	25.256	2.208	0.876	2.381	0.9272	22.00	155.30	2.47
2000	3.0	112.20	23.533	4.188	1.786	4.573	0.9157	23.70	153.50	4.91
3000	3.0	165.68	23.992	6.306	2.666	6.885	0.9159	23.66	143.00	6.79
4000	3.0	215.66	19.970	6.718	2.906	7.460	0.9005	25.77	108.50	6.87
5000	3.0	233.89	20.532	7.568	3.041	8.318	0.9098	24.52	93.50	7.40

50										
Speed (RPM)	V/f	Urms1	Irms1	PΣ (kW)	QΣ (kVAR)	SΣ (kVA)	λΣ	φΣ (°)	T (in-lbs)	P (HP)
500	3.0	28.70	38.863	1.802	0.684	1.932	0.9329	21.10	198.00	1.58
1000	3.0	55.48	31.039	2.781	1.065	2.982	0.9324	21.19	191.90	3.05
2000	3.0	112.09	29.076	5.223	2.096	5.646	0.9251	22.31	190.50	6.05
3000	3.0	165.78	24.075	6.335	2.678	6.913	0.9165	23.58	142.00	6.86
4000	3.0	215.68	20.028	6.743	2.931	7.482	0.9012	25.68	108.00	6.90
5000	3.0	234.01	20.627	7.613	4.588	8.360	0.9106	24.41	93.40	7.35

Efficiency							Average	Median
	Torque (%)							
Speed (RPM)	0	10	20	30	40	50	69.92%	75.91%
500	80.64%	84.14%	76.04%	66.60%	71.51%	65.40%		
1000	50.29%	80.05%	83.17%	85.54%	83.44%	81.80%		
2000	28.45%	76.46%	82.69%	85.11%	87.45%	86.40%		
3000	24.64%	69.07%	73.13%	77.89%	80.31%	80.77%		
4000	29.70%	52.02%	69.43%	75.77%	76.28%	76.33%		
5000	32.71%	54.72%	71.83%	72.56%	72.93%	72.01%		

Power Losses (kW)							Average	Median
	Torque (%)							
Speed (RPM)	0	10	20	30	40	50	0.839	0.607
500	0.007	0.052	0.160	0.374	0.386	0.623		
1000	0.044	0.123	0.192	0.238	0.366	0.506		
2000	0.169	0.292	0.383	0.476	0.526	0.710		
3000	0.342	0.615	0.918	1.075	1.241	1.218		
4000	0.600	1.376	1.471	1.622	1.594	1.596		
5000	0.959	1.821	1.866	2.087	2.048	2.131		

C.4 Machine2 System Data

					Torque (%)					
					0					
Speed (RPM)	V/f	Urms1	Irms1	PΣ (kW)	QΣ (kVAR)	SΣ (kVA)	λΣ	ϕΣ (°)	T (in-lbs)	P(HP)
500	1.0	71.50	4.122	0.010	0.510	0.511	-0.0192	88.90	3.9	0.030
1000	1.0	136.36	3.842	0.015	0.907	0.907	-0.0163	89.07	3.4	0.500
2000	1.0	262.00	3.731	0.036	1.693	1.693	-0.0211	88.79	2.0	0.070
3000	1.0	387.59	3.636	0.068	2.440	2.411	-0.0269	88.46	3.1	0.150
4000	1.0	496.48	3.437	0.093	2.954	2.956	-0.0314	88.20	5.9	0.360
5000	1.0	496.66	2.655	0.070	2.283	2.284	-0.0305	88.25	10.4	0.830

					10					
Speed (RPM)	V/f	Urms1	Irms1	PΣ (kW)	QΣ (kVAR)	SΣ (kVA)	λΣ	ϕΣ (°)	T (in-lbs)	P(HP)
500	2.5	69.25	4.677	-0.229	0.512	0.561	0.4091	114.15	43.8	0.350
1000	2.5	133.86	4.482	-0.452	0.935	1.039	0.4354	115.81	41.0	0.650
2000	2.5	260.01	4.311	-0.870	1.735	1.941	0.4483	116.64	39.0	1.240
3000	2.5	385.66	4.238	-1.272	2.529	2.831	0.4494	116.71	38.1	1.800
4000	2.5	498.95	4.169	-1.685	3.185	3.603	0.4676	117.88	30.5	1.900
5000	2.5	500.59	3.862	-2.145	2.572	3.349	0.6406	129.83	38.0	3.060

					20					
Speed (RPM)	V/f	Urms1	Irms1	PΣ (kW)	QΣ (kVAR)	SΣ (kVA)	λΣ	ϕΣ (°)	T (in-lbs)	P (HP)
500	2.5	66.90	5.919	-0.447	0.520	0.686	0.6516	130.66	83.5	0.670
1000	3.0	131.47	5.777	-0.895	0.964	1.316	0.6805	132.89	80.0	1.270
2000	3.0	257.57	5.638	-1.745	1.812	2.515	0.6936	133.92	76.8	2.450
3000	3.0	383.62	5.582	-2.581	2.663	3.709	0.6959	134.10	68.5	3.290
4000	3.0	508.94	5.554	-3.408	3.515	4.896	0.6962	134.12	70.5	4.460
5000	3.0	567.72	5.697	-4.297	3.595	5.602	0.7670	140.08	75.0	6.060

					30					
Speed (RPM)	V/f	Urms1	Irms1	PΣ (kW)	QΣ (kVAR)	SΣ (kVA)	λΣ	ϕΣ (°)	T (in-lbs)	P (HP)
500	2.5	64.35	7.546	-0.649	0.535	0.841	0.7713	140.48	122.3	0.980
1000	3.0	128.84	7.400	-1.307	1.009	1.651	0.7916	142.33	117.6	1.880
2000	3.0	255.11	7.388	-2.606	1.928	3.242	0.8039	143.51	115.0	3.660
3000	3.0	380.98	7.279	-3.876	2.837	4.803	0.8069	143.79	105.0	5.040
4000	3.0	506.28	7.164	-5.066	3.715	6.283	0.8064	143.75	106.0	6.710
5000	3.0	592.65	6.363	-5.047	4.146	6.531	0.7727	140.59	89.0	7.120

40										
Speed (RPM)	V/f	Urms1	Irms1	PΣ (kW)	QΣ (kVAR)	SΣ (kVA)	λΣ	φΣ (°)	T (in-lbs)	P (HP)
500	3.0	61.95	9.358	-0.836	0.557	1.004	0.8322	146.32	160.8	1.290
1000	3.0	126.09	9.235	-1.712	1.066	2.017	0.8489	148.09	155.0	2.470
2000	3.0	252.23	9.190	-3.447	2.059	4.015	0.8584	149.14	152.8	4.850
3000	3.0	378.63	9.071	-5.110	3.046	5.949	0.8589	149.20	140.0	6.680
4000	3.0	571.04	7.037	-5.070	4.769	6.961	0.7284	136.75	106.8	6.780
5000	3.0	589.25	6.403	-5.035	4.165	6.535	0.7705	140.40	89.5	7.150

50										
Speed (RPM)	V/f	Urms1	Irms1	PΣ (kW)	QΣ (kVAR)	SΣ (kVA)	λΣ	φΣ (°)	T (in-lbs)	P (HP)
500	3.0	58.84	11.249	-0.990	0.578	1.147	0.8636	149.70	196.9	1.570
1000	3.0	122.97	11.161	-2.089	1.135	2.377	0.8787	151.49	191.5	3.060
2000	3.0	249.70	11.135	-4.268	2.230	4.816	0.8864	152.42	190.0	6.070
3000	3.0	413.88	8.737	-5.121	3.601	6.260	0.8180	144.88	140.0	6.720
4000	3.0	590.86	7.055	-5.052	5.159	7.221	0.6997	134.40	106.2	6.770
5000	3.0	590.88	6.409	-5.041	4.196	6.559	0.7686	140.23	89.0	7.150

Efficiency								
Torque (%)							Average	Median
Speed (RPM)	0	10	20	30	40	50	77.67%	91.90%
500	0.00%	82.98%	88.13%	87.01%	86.21%	84.00%		
1000	0.00%	91.82%	94.48%	92.71%	92.92%	91.82%		
2000	0.00%	91.84%	95.49%	95.72%	94.12%	94.58%		
3000	0.00%	92.68%	96.81%	97.66%	99.11%	99.92%		
4000	0.00%	88.53%	98.05%	99.88%	98.94%	98.16%		
5000	0.00%	97.48%	90.30%	91.44%	91.22%	91.95%		

Power Losses (kW)								
Torque (%)							Average	Median
Speed (RPM)	0	10	20	30	40	50	0.839	0.607
500	0.040	0.047	0.060	0.097	0.134	0.189		
1000	0.060	0.040	0.052	0.103	0.130	0.186		
2000	0.103	0.077	0.082	0.117	0.215	0.245		
3000	0.180	0.100	0.082	0.091	0.045	0.004		
4000	0.347	0.193	0.066	0.006	0.054	0.095		
5000	0.536	0.055	0.462	0.473	0.485	0.441		

C.5 Variable Frequency Drive System Data

					Torque (%)					
					0					
Speed (RPM)	V/f	Urms1	Irms1	PΣ (kW)	QΣ (kVAR)	SΣ (kVA)	λΣ	φΣ (°)	T (in-lbs)	P(HP)
500	1.0	494.60	1.781	0.488	1.445	1.525	0.3196	71.36	4.1	0.030
1000	1.0	494.20	1.801	0.568	1.433	1.542	0.3686	68.37	3.5	0.050
2000	1.0	493.90	1.848	0.672	1.431	1.581	0.4253	64.83	1.9	0.060
3000	1.0	494.03	1.893	0.695	1.463	1.620	0.4290	64.59	2.8	0.150
4000	1.0	494.47	1.924	0.638	1.519	1.648	0.3873	67.21	6.2	0.390
5000	1.0	493.35	2.062	0.601	1.656	1.762	0.3409	70.07	10.3	0.790

					10					
Speed (RPM)	V/f	Urms1	Irms1	PΣ (kW)	QΣ (kVAR)	SΣ (kVA)	λΣ	φΣ (°)	T (in-lbs)	P(HP)
500	2.5	494.73	1.695	0.229	1.434	1.452	0.1577	80.93	44.3	0.360
1000	2.5	493.50	1.732	0.065	1.479	1.480	0.0440	87.48	41.0	0.650
2000	2.5	494.15	1.922	-0.279	1.621	1.645	-0.1699	99.78	39.2	1.250
3000	2.5	494.68	2.203	-0.672	1.764	1.888	-0.3562	110.86	38.1	1.810
4000	2.5	494.28	2.464	-1.142	1.773	2.109	-0.5413	122.77	30.7	1.950
5000	2.5	494.05	2.770	-1.619	1.731	2.370	-0.6831	133.08	37.5	2.870

					20					
Speed (RPM)	V/f	Urms1	Irms1	PΣ (kW)	QΣ (kVAR)	SΣ (kVA)	λΣ	φΣ (°)	T (in-lbs)	P (HP)
500	2.5	494.26	1.773	0.014	1.518	1.518	0.0093	89.46	84.0	0.670
1000	3.0	493.75	1.922	-0.370	1.601	1.643	-0.2252	103.02	79.7	1.260
2000	3.0	494.51	2.414	-1.148	1.720	2.068	-0.5552	123.72	77.0	2.460
3000	3.0	495.42	2.925	-1.968	1.558	2.510	-0.7839	141.62	68.3	3.270
4000	3.0	495.28	3.519	-2.766	1.209	3.019	-0.9162	156.38	70.0	4.430
5000	3.0	494.89	4.394	-3.580	1.170	3.767	-0.9505	161.90	76.2	6.060

					30					
Speed (RPM)	V/f	Urms1	Irms1	PΣ (kW)	QΣ (kVAR)	SΣ (kVA)	λΣ	φΣ (°)	T (in-lbs)	P (HP)
500	2.5	494.39	1.917	-0.182	1.632	1.642	-0.1106	96.35	123.2	0.990
1000	3.0	494.22	2.185	-0.774	1.703	1.870	-0.4138	114.45	117.0	1.870
2000	3.0	494.93	2.908	-1.991	1.500	2.493	-0.7986	142.99	114.9	3.650
3000	3.0	495.68	3.889	-3.119	1.191	3.338	-0.9342	159.10	104.5	5.020
4000	3.0	495.44	5.100	-4.222	1.151	4.376	-0.9648	164.75	106.7	6.690
5000	3.0	494.85	5.146	-4.256	1.156	4.411	-0.9650	164.80	89.6	7.070

40										
Speed (RPM)	V/f	Urms1	Irms1	PΣ (kW)	QΣ (kVAR)	SΣ (kVA)	λΣ	φΣ (°)	T (in-lbs)	P (HP)
500	3.0	494.39	1.994	-0.355	1.670	1.708	-0.2079	102.00	161.0	1.280
1000	3.0	493.87	2.455	-1.165	1.747	2.100	-0.5546	123.69	154.0	2.450
2000	3.0	495.26	3.486	-2.743	1.191	2.990	-0.9173	156.53	152.7	4.840
3000	3.0	496.23	5.081	-4.203	1.186	4.367	-0.9624	164.24	140.8	6.720
4000	3.0	495.22	5.130	-4.244	1.162	4.400	-0.9645	164.69	108.0	6.780
5000	3.0	495.01	5.147	-4.256	1.165	4.413	-0.9645	164.69	89.0	7.120

50										
Speed (RPM)	V/f	Urms1	Irms1	PΣ (kW)	QΣ (kVAR)	SΣ (kVA)	λΣ	φΣ (°)	T (in-lbs)	P (HP)
500	3.0	494.09	2.202	-0.502	1.816	1.884	-0.2667	105.46	197.0	1.570
1000	3.0	493.93	2.666	-1.528	1.684	2.281	-0.6700	132.06	192.0	3.050
2000	3.0	495.43	4.255	-3.456	1.177	3.651	-0.9466	161.20	190.5	6.050
3000	3.0	495.92	5.089	-4.212	1.169	4.372	-0.9636	164.49	141.0	6.700
4000	3.0	495.17	5.128	-4.242	1.162	4.398	-0.9645	164.68	106.8	6.880
5000	3.0	494.83	5.143	-4.251	1.167	4.408	-0.9643	164.65	89.0	7.070

Efficiency								
Torque (%)							Average	Median
Speed (RPM)	0	10	20	30	40	50	53.61%	67.91%
500	2.05%	0.00%	0.00%	28.04%	42.46%	50.71%		
1000	2.64%	0.00%	41.34%	59.22%	68.05%	73.15%		
2000	5.36%	32.07%	65.79%	76.40%	79.58%	80.97%		
3000	9.78%	52.83%	76.25%	80.47%	82.25%	82.25%		
4000	14.58%	67.77%	81.16%	83.34%	83.71%	83.97%		
5000	11.65%	75.48%	83.31%	84.33%	84.53%	84.33%		

Power Losses (kW)								
Torque (%)							Average	Median
Speed (RPM)	0	10	20	30	40	50	0.633	0.599
500	0.478	0.458	0.461	0.467	0.481	0.488		
1000	0.553	0.517	0.525	0.533	0.547	0.561		
2000	0.636	0.591	0.597	0.615	0.704	0.812		
3000	0.627	0.600	0.613	0.757	0.907	0.909		
4000	0.545	0.543	0.642	0.844	0.826	0.810		
5000	0.531	0.526	0.717	0.791	0.779	0.790		

C.6 Transformer System Data

					Torque (%)					
					0					
Speed (RPM)	V/f	Urms1	Irms1	PΣ (kW)	QΣ (kVAR)	SΣ (kVA)	λΣ	φΣ (°)	T (in-lbs)	P(HP)
500	1.0	209.59	4.907	0.752	1.615	1.781	0.4220	65.04	4.4	0.030
1000	1.0	209.61	4.968	0.833	1.600	1.803	0.4618	62.50	3.5	0.060
2000	1.0	209.51	5.144	0.936	1.615	1.866	0.5013	59.91	2.6	0.090
3000	1.0	209.33	5.054	0.957	1.563	1.832	0.5224	58.51	3.3	0.160
4000	1.0	209.30	5.176	0.898	1.648	1.876	0.4786	61.41	6.3	0.340
5000	1.0	209.23	5.537	0.860	1.813	2.006	0.4285	64.63	10.4	0.830

					10					
Speed (RPM)	V/f	Urms1	Irms1	PΣ (kW)	QΣ (kVAR)	SΣ (kVA)	λΣ	φΣ (°)	T (in-lbs)	P(HP)
500	2.5	209.67	4.662	0.492	1.620	1.693	0.2909	73.09	44.5	0.360
1000	2.5	209.27	4.641	0.331	1.649	1.682	0.1966	78.66	41.2	0.660
2000	2.5	209.42	4.854	-0.015	1.760	1.760	-0.0085	90.49	39.9	1.240
3000	2.5	209.05	5.342	-0.412	1.890	1.934	-0.2129	102.29	38.2	1.850
4000	2.5	209.33	5.837	-0.879	1.925	2.116	-0.4153	114.54	31.5	2.000
5000	2.5	209.16	6.392	-1.355	1.878	2.316	-0.5853	125.82	36.0	3.000

					20					
Speed (RPM)	V/f	Urms1	Irms1	PΣ (kW)	QΣ (kVAR)	SΣ (kVA)	λΣ	φΣ (°)	T (in-lbs)	P (HP)
500	2.5	209.61	4.728	0.276	1.694	1.716	0.1611	80.73	83.7	0.670
1000	3.0	209.48	4.842	-0.107	1.754	1.754	-0.0607	93.48	79.5	1.270
2000	3.0	209.30	5.736	-0.888	1.880	2.079	-0.4269	115.27	77.5	2.440
3000	3.0	209.00	6.692	-1.709	1.717	2.423	-0.7056	134.88	68.3	3.300
4000	3.0	209.04	7.941	-2.502	1.417	2.875	-0.8701	150.47	69.7	4.450
5000	3.0	209.10	9.903	-3.308	1.384	3.585	-0.9226	157.32	75.7	6.060

					30					
Speed (RPM)	V/f	Urms1	Irms1	PΣ (kW)	QΣ (kVAR)	SΣ (kVA)	λΣ	φΣ (°)	T (in-lbs)	P (HP)
500	2.5	209.53	4.966	0.083	1.800	1.802	0.0458	87.37	123.8	0.990
1000	3.0	209.50	5.280	-0.512	1.846	1.916	-0.2672	105.50	116.8	1.880
2000	3.0	209.34	6.696	-1.726	1.708	2.428	-0.7108	135.30	115.0	3.680
3000	3.0	208.93	8.790	-2.855	1.403	3.181	-0.8974	153.82	105.2	5.040
4000	3.0	209.15	11.596	-3.957	1.411	4.201	-0.9419	160.37	107.0	6.860
5000	3.0	209.01	11.663	-3.991	1.377	4.222	-0.9454	160.97	90.6	7.220

					40					
Speed (RPM)	V/f	Urms1	Irms1	PΣ (kW)	QΣ (kVAR)	SΣ (kVA)	λΣ	φΣ (°)	T (in-lbs)	P (HP)
500	3.0	209.41	4.935	-0.092	1.787	1.790	-0.0512	92.94	160.0	1.300
1000	3.0	209.48	5.747	-0.898	1.882	2.085	-0.4307	115.51	153.8	2.450
2000	3.0	209.32	7.855	-2.472	1.414	2.848	-0.8681	150.24	153.8	4.860
3000	3.0	208.91	11.538	-3.941	1.378	4.175	-0.9439	160.72	141.2	6.760
4000	3.0	209.03	11.656	-3.985	1.390	4.220	-0.9442	160.77	108.2	6.800
5000	3.0	209.06	11.654	-3.985	1.388	4.220	-0.9444	160.80	90.0	7.150

					50					
Speed (RPM)	V/f	Urms1	Irms1	PΣ (kW)	QΣ (kVAR)	SΣ (kVA)	λΣ	φΣ (°)	T (in-lbs)	P (HP)
500	3.0	209.35	5.334	-0.243	1.919	1.934	-0.1258	97.23	196.4	1.580
1000	3.0	209.39	6.169	-1.265	1.846	2.237	-0.5654	124.43	191.3	3.050
2000	3.0	209.10	9.563	-3.182	1.367	3.463	-0.9189	156.76	190.5	6.040
3000	3.0	208.73	11.567	-3.950	1.374	4.182	-0.9445	160.82	141.0	6.780
4000	3.0	209.10	11.624	-3.975	1.387	4.210	-0.9442	160.60	108.0	6.850
5000	3.0	208.95	11.653	-3.988	1.373	4.217	-0.9455	161.00	90.0	7.120

			Efficiency					
			Torque (%)				Average	Median
Speed (RPM)	0	10	20	30	40	50	69.55%	77.22%
500	64.89%	46.54%	5.07%	0.00%	25.92%	48.41%		
1000	68.19%	19.64%	28.92%	66.15%	77.08%	82.79%		
2000	71.79%	5.38%	77.35%	86.69%	90.12%	92.07%		
3000	72.62%	61.31%	86.84%	91.54%	93.77%	93.78%		
4000	71.05%	76.97%	90.46%	93.72%	93.90%	93.71%		
5000	69.88%	83.69%	92.40%	93.77%	93.63%	93.81%		

			Power Losses (kW)					
			Torque (%)				Average	Median
Speed (RPM)	0	10	20	30	40	50	0.264	0.264
500	0.264	0.263	0.262	0.265	0.263	0.259		
1000	0.265	0.266	0.263	0.262	0.267	0.263		
2000	0.264	0.264	0.260	0.265	0.271	0.274		
3000	0.262	0.260	0.259	0.264	0.262	0.262		
4000	0.260	0.263	0.264	0.265	0.259	0.267		
5000	0.259	0.264	0.272	0.265	0.271	0.263		

C.7 Matlab Script to Calculate Efficiency data and Power Losses

```matlab
%% System Charaterization Calc File()
% Initialization
clc
clear all
close all
format compact
format short g
tic

FileName='SystemCharData.xlsx';

% Set Up SheetName Container
SheetNames={'1-DCPwrSupply', '2-Inverter', '3-Machine1', '4-Machine2', '5-
VFD', '6-Xfmr'};

%% Setup Data Containers
if 1
    % Torque/Speed Data
    SheetName=char(SheetNames(1));          % Converter Charater Array to
String
    Data.Speed.RPM=xlsread(FileName,SheetName,'B4:B9')';

    % Defines the start of the row in the worksheet for the corresponding
    % Torque Value
    Torque.HeaderRow=[2+0*9,2+1*9,2+2*9,2+3*9,2+4*9,2+5*9];
    Torque.StartRow=Torque.HeaderRow+2;

    % Read in Values

Torque.percent(1)=xlsread(FileName,SheetName,['C',num2str(Torque.HeaderRow(1)
)]);

Torque.percent(2)=xlsread(FileName,SheetName,['C',num2str(Torque.HeaderRow(2)
)]);

Torque.percent(3)=xlsread(FileName,SheetName,['C',num2str(Torque.HeaderRow(3)
)]);

Torque.percent(4)=xlsread(FileName,SheetName,['C',num2str(Torque.HeaderRow(4)
)]);

Torque.percent(5)=xlsread(FileName,SheetName,['C',num2str(Torque.HeaderRow(5)
)]);

Torque.percent(6)=xlsread(FileName,SheetName,['C',num2str(Torque.HeaderRow(6)
)]);

    % Write to Data Structure
    Data.Torque.percent = Torque.percent;
end

save('B4AssembleData.mat')

%% Call Sub-Function to Assemble Data
```

```matlab
% clc
% clear
% close all

load('B4AssembleData.mat')

ExcelDataCols = ['C','D','E','F','G','H','I','J','K','L'];
CatNames = {'VpHz','V_{rms} (V)','I_{rms}(A)','P (kW)', 'Q (kVAR)','S
(kVA)','\lambda','\phi (\circ)','T_{shaft} (in-lbs)', 'P_{shaft} (Hp)'};
CatVarNames = {'VpHz','Vin_V','Iin_A','Pwr_kW',
'Q_kVAR','S_kVA','lambda','phi_deg','Trq_shaft_inlbs', 'Pwr_shaft_Hp'};

% Set Up SheetName Container
Data=AssembleDataFunc(Data,FileName,SheetNames,ExcelDataCols,length(SheetName
s),length(CatNames),Torque.HeaderRow);
save('AfterAssembleData.mat')
toc

%% Calc different values
close all
clc
clear
load('AfterAssembleData.mat')
tic

[Data]=CalcEff(FileName,SheetNames,Data);
save('AfterEffCalcData.mat')

disp(sprintf('DONE'));
toc

%-----------------------------------------------------------------------------------------
function [Data]=CalcEff(FileName,SheetNames,Data)
%% Calc different values
ExcelDataCols = ['C','D','E','F','G','H','I','J','K','L'];
CatNames = {'VpHz','V_{rms} (V)','I_{rms}(A)','P (kW)', 'Q (kVAR)','S
(kVA)','\lambda','\phi (\circ)','T_{shaft} (in-lbs)', 'P_{shaft} (Hp)'};
CatVarNames = {'VpHz','Vin_V','Iin_A','Pwr_kW',
'Q_kVAR','S_kVA','lambda','phi_deg','Trq_shaft_inlbs', 'Pwr_shaft_Hp'};

CatNames=fieldnames(Data.Pwr_shaft_Hp);

% Delete any Word Doc files
fls2del=dir('Fig*.doc');
fls2del={fls2del.name};
delete(char(fls2del));

% Define Custom Font Size
TJHFontSize = 16;

% Conversion Factor
HP2kW=0.7459;
if 0
    figobj=figure
```

```matlab
    [C,h] = contourf(Data.Speed.RPM,
Data.Torque.percent,Data.Pwr_shaft_Hp.Machine1.ZValues*HP2kW)
    set(h,'ShowText','on','TextStep',get(h,'LevelStep')*1)
    % Set Font Size and Type
    textobj = findobj('type', 'text');
    set(textobj, 'fontsize', TJHFontSize);
    set(textobj, 'FontName','times');
    %       set(C, 'fontsize', TJHFontSize);
    %       set(C, 'FontName','times');
    % Write Axis Labels
    ylabel('Speed (RPM)','fontsize',TJHFontSize,'FontName','times')
    xlabel('Torque (%)','fontsize',TJHFontSize,'FontName','times')
    title([strcat('Machine1-2', '--','Pwr Shaft kW')])
    grid on
    colormap summer
    colorbar

    figure
    [C,h] = contourf(Data.Speed.RPM,
Data.Torque.percent,Data.Pwr_kW.Machine1.ZValues)
    set(h,'ShowText','on','TextStep',get(h,'LevelStep')*1)
    % Set Font Size and Type
    textobj = findobj('type', 'text');
    set(textobj, 'fontsize', TJHFontSize);
    set(textobj, 'FontName','times');
    %       set(spobj, 'fontsize', TJHFontSize);
    %       set(spobj, 'FontName','times');
    % Write Axis Labels
    ylabel('Speed (RPM)','fontsize',TJHFontSize,'FontName','times')
    xlabel('Torque (%)','fontsize',TJHFontSize,'FontName','times')
    title([strcat('Machine1', '--','Pwr kW')])
    grid on
    colormap summer
    colorbar

    figure
    [C,h] = contourf(Data.Speed.RPM,
Data.Torque.percent,Data.Pwr_kW.Machine2.ZValues)
    set(h,'ShowText','on','TextStep',get(h,'LevelStep')*1)
    % Set Font Size and Type
    textobj = findobj('type', 'text');
    set(textobj, 'fontsize', TJHFontSize);
    set(textobj, 'FontName','times');
    %       set(spobj, 'fontsize', TJHFontSize);
    %       set(spobj, 'FontName','times');
    % Write Axis Labels
    ylabel('Speed (RPM)','fontsize',TJHFontSize,'FontName','times')
    xlabel('Torque (%)','fontsize',TJHFontSize,'FontName','times')
    title([strcat('Machine2', '--','Pwr kW')])
    grid on
    colormap summer
    colorbar

    figure
    [C,h] =  contourf(Data.Speed.RPM,
Data.Torque.percent,Data.Pwr_kW.DCPwrSupply.ZValues)
    set(h,'ShowText','on','TextStep',get(h,'LevelStep')*1)
```

```matlab
    % Set Font Size and Type
    textobj = findobj('type', 'text');
    set(textobj, 'fontsize', TJHFontSize);
    set(textobj, 'FontName','times');
%       set(spobj, 'fontsize', TJHFontSize);
%       set(spobj, 'FontName','times');
    % Write Axis Labels
    ylabel('Speed (RPM)','fontsize',TJHFontSize,'FontName','times')
    xlabel('Torque (%)','fontsize',TJHFontSize,'FontName','times')
    title([strcat('DCPwrSupply', '--','Pwr kW')])
    grid on
    colormap summer
    colorbar

    figure
    [C,h] = contourf(Data.Speed.RPM,
Data.Torque.percent,Data.Pwr_kW.Inverter.ZValues)
    set(h,'ShowText','on','TextStep',get(h,'LevelStep')*1)
    % Set Font Size and Type
    textobj = findobj('type', 'text');
    set(textobj, 'fontsize', TJHFontSize);
    set(textobj, 'FontName','times');
%       set(spobj, 'fontsize', TJHFontSize);
%       set(spobj, 'FontName','times');
    % Write Axis Labels
    ylabel('Speed (RPM)','fontsize',TJHFontSize,'FontName','times')
    xlabel('Torque (%)','fontsize',TJHFontSize,'FontName','times')
    title([strcat('Inverter', '--','Pwr kW')])
    grid on
    colormap summer
    colorbar

    figure
    [C,h] = contourf(Data.Speed.RPM,
Data.Torque.percent,Data.Pwr_kW.VFD.ZValues)
    set(h,'ShowText','on','TextStep',get(h,'LevelStep')*1)
    % Set Font Size and Type
    textobj = findobj('type', 'text');
    set(textobj, 'fontsize', TJHFontSize);
    set(textobj, 'FontName','times');
%       set(spobj, 'fontsize', TJHFontSize);
%       set(spobj, 'FontName','times');
    % Write Axis Labels
    ylabel('Speed (RPM)','fontsize',TJHFontSize,'FontName','times')
    xlabel('Torque (%)','fontsize',TJHFontSize,'FontName','times')
    title([strcat('VFD', '--','Pwr kW')])
    grid on
    colormap summer
    colorbar

    figure
    [C,h] = contourf(Data.Speed.RPM,
Data.Torque.percent,Data.Pwr_kW.Xfmr.ZValues)
    set(h,'ShowText','on','TextStep',get(h,'LevelStep')*1)
    % Set Font Size and Type
    textobj = findobj('type', 'text');
    set(textobj, 'fontsize', TJHFontSize);
```

```matlab
    set(textobj, 'FontName','times');
    %     set(spobj, 'fontsize', TJHFontSize);
    %     set(spobj, 'FontName','times');
    % Write Axis Labels
    ylabel('Speed (RPM)','fontsize',TJHFontSize,'FontName','times')
    xlabel('Torque (%)','fontsize',TJHFontSize,'FontName','times')
    title([strcat('Xfmr', '--','Pwr kW')])
    grid on
    colormap summer
    colorbar

end


%% Calculate Effiency Data
% Add one for the total Power Losses and Efficiency
CatNames=fieldnames(Data.Pwr_shaft_Hp);


% for i=1:length(CatNames)+1


for i=1:length(CatNames)+1

    % If Statements
    if i==1||i==2
        Mat1 = Data.Pwr_kW.(CatNames[25]).ZValues;
        Mat2 = Data.Pwr_kW.(CatNames{i+1}).ZValues;

        CompName1 = (CatNames{i});
        CompName2 = (CatNames{i+1});
    elseif i==3
        Mat1 = Data.Pwr_kW.(CatNames{i}).ZValues;
        Mat2 = Data.Pwr_shaft_Hp.Machine1.ZValues*HP2kW;

        CompName1 = (CatNames{i});
        CompName2 = 'Shaft';
    elseif i==4
        Mat1 = Data.Pwr_shaft_Hp.Machine1.ZValues*HP2kW;
        Mat2 = -Data.Pwr_kW.(CatNames{i}).ZValues;

        CompName1 = (CatNames{i});
        CompName2 = 'Shaft';
    elseif i==5||i==6
        Mat1 = Data.Pwr_kW.(CatNames{i-1}).ZValues;
        Mat2 = Data.Pwr_kW.(CatNames{i}).ZValues;

        CompName1 = (CatNames{i});
        CompName2 = (CatNames{i-1});
    end


    % Plot Total Power Losses and Eff
    if i<=length(CatNames)
        % Call Calculation Function
        DataStructPath = ['Data.Eff.',(CompName1),'.ZValues'];
        [Data.Eff.(CompName1).ZValues,
Data.PwrLoss_kW.(CompName1).ZValues]=DetermineEff(Mat1,Mat2);
        % Calculate Average Eff
```

```matlab
        [Data.Eff.(CompName1).Avg] =
mean(mean([Data.Eff.(CompName1).ZValues]));
        [Data.Eff.(CompName1).Median] =
median(reshape([Data.Eff.(CompName1).ZValues].',1,[]));
        % Calculate Average PwrLoss_kW
        [Data.PwrLoss_kW.(CompName1).Avg] =
mean(mean([Data.PwrLoss_kW.(CompName1).ZValues]));
        [Data.PwrLoss_kW.(CompName1).Median] =
median(reshape([Data.PwrLoss_kW.(CompName1).ZValues].',1,[]));

        % Disp Avg Eff of Component
        disp([CompName1,' Eff Avg =
',num2str(mean(mean([Data.Eff.(CompName1).Avg])))]);
        disp([CompName1,' Eff Median =
',num2str(mean(mean([Data.Eff.(CompName1).Median])))]);
        disp([CompName1,' Power Loss Avg =
',num2str(mean(mean([Data.PwrLoss_kW.(CompName1).Avg]))),' kW']);
        disp([CompName1,' Power Loss Median =
',num2str(mean(mean([Data.PwrLoss_kW.(CompName1).Median]))),' kW']);
        disp(['-------------------']);


        % Write Eff values To Speadsheet

xlswrite(char(FileName),Data.Eff.(CompName1).ZValues,char(SheetNames(i)),'C59
:H64');

xlswrite(char(FileName),Data.Eff.(CompName1).Avg,char(SheetNames(i)),'I58');

xlswrite(char(FileName),Data.Eff.(CompName1).Median,char(SheetNames(i)),'J58'
);
        % Write Axis Values For Eff

xlswrite(char(FileName),Data.Speed.RPM',char(SheetNames(i)),'B59:B64');

xlswrite(char(FileName),Data.Torque.percent,char(SheetNames(i)),'C58:H58');
        xlswrite(char(FileName),{'Efficiency'},char(SheetNames(i)),'C56');
        xlswrite(char(FileName),{'Average'},char(SheetNames(i)),'I57');
        xlswrite(char(FileName),{'Median'},char(SheetNames(i)),'J57');

        % Write Power Loss values To Speadsheet

xlswrite(char(FileName),Data.PwrLoss_kW.(CompName1).ZValues,char(SheetNames(i
)),'C69:H74');

xlswrite(char(FileName),Data.PwrLoss_kW.(CompName1).Avg,char(SheetNames(i)),'
I68');

xlswrite(char(FileName),Data.PwrLoss_kW.(CompName1).Median,char(SheetNames(i)
),'J68');
        % Write Axis Values For Power Loss

xlswrite(char(FileName),Data.Speed.RPM',char(SheetNames(i)),'B69:B74');

xlswrite(char(FileName),Data.Torque.percent,char(SheetNames(i)),'C68:H68');
        xlswrite(char(FileName),{'Power Losses
(kW)'},char(SheetNames(i)),'C66');
        xlswrite(char(FileName),{'Average'},char(SheetNames(i)),'I67');
```

```matlab
        xlswrite(char(FileName),{'Median'},char(SheetNames(i)),'J67');

        % Plot Effiency Figure
        scrsz = get(0,'ScreenSize');
        ScrWidth=scrsz(3);   %
        ScrHeight=scrsz(4);
        FigWidth = ScrWidth*13/16;
        FigHeight = ScrHeight*9/16;
        FigWidthX1 = FigWidth*(1+1/2);
        FigWidthX2= FigWidth*(1-1/2);
        FigHeightY1 = FigHeight*(1+1/2);
        FigHeightY2 = FigHeight*(1-1/2);


        % Make New Figure
        fig=figure('Position',[FigWidthX1, FigHeightY2, FigWidth,
FigHeight]);
        % Set Text Size
        textobj = findobj('type', 'text');
        set(textobj, 'fontsize', TJHFontSize, 'FontName','times');

        % Plot Eff and Power Loss Same Figure next to each other
        spobj=subplot(1,2,1);
        [C,h] = contourf(Data.Speed.RPM,Data.Torque.percent,
Data.Eff.(CompName1).ZValues'*100,'LineWidth',1);
        set(h,'ShowText','on','TextStep',get(h,'LevelStep')*1)
        % Set Font Size and Type
        textobj = findobj('type', 'text');
        set(textobj, 'fontsize', TJHFontSize);
        set(textobj, 'FontName','times');
        set(spobj, 'fontsize', TJHFontSize);
        set(spobj, 'FontName','times');
        % Write Axis Labels
        xlabel('Speed (RPM)','fontsize',TJHFontSize,'FontName','times')
        ylabel('Torque (%)','fontsize',TJHFontSize,'FontName','times')
        % Write Title
        title([(CompName1), '--','Eff
(%)'],'fontsize',TJHFontSize,'FontName','times')
        grid on
        colormap summer

        % Plot Power Loss Figure
        spobj=subplot(1,2,2);
        [C,h] =
contourf(Data.Speed.RPM,Data.Torque.percent,Data.PwrLoss_kW.(CompName1).ZValu
es', 'LineWidth',1);
        set(h,'ShowText','on','TextStep',get(h,'LevelStep')*1)
        % Set Font Size and Type
        textobj = findobj('type', 'text');
        set(textobj, 'fontsize', TJHFontSize);
        set(textobj, 'FontName','times');
        set(spobj, 'fontsize', TJHFontSize);
        set(spobj, 'FontName','times');
        % Write Axis Labels
        xlabel('Speed (RPM)','fontsize',TJHFontSize,'FontName','times')
        ylabel('Torque (%)','fontsize',TJHFontSize,'FontName','times')
        % Write Title
```

90

```matlab
        title([strcat(CompName1, '--','PwrLoss
(kW)')],'fontsize',TJHFontSize,'FontName','times')
        grid on
        colormap summer


    elseif i==length(CatNames)+1
        % Calculate Total EFf
        Data.Eff.Total = Data.Eff.(CatNames{1}).ZValues.*...
            Data.Eff.(CatNames{2}).ZValues.*...
            Data.Eff.(CatNames{3}).ZValues.*...
            Data.Eff.(CatNames{4}).ZValues.*...
            Data.Eff.(CatNames{5}).ZValues.*...
            Data.Eff.(CatNames{6}).ZValues;

        Data.PwrLoss_kW.Total = Data.PwrLoss_kW.(CatNames{1}).ZValues+...
            Data.PwrLoss_kW.(CatNames{2}).ZValues+...
            Data.PwrLoss_kW.(CatNames{3}).ZValues+...
            Data.PwrLoss_kW.(CatNames{4}).ZValues+...
            Data.PwrLoss_kW.(CatNames{5}).ZValues+...
            Data.PwrLoss_kW.(CatNames{6}).ZValues;

        % Make New Figure
        fig=figure('Position',[FigWidthX1, FigHeightY2, FigWidth,
FigHeight]);
        % Set Text Size
        textobj = findobj('type', 'text');
        set(textobj, 'fontsize', TJHFontSize, 'FontName','times');

        % Plot Eff and Power Loss Same Figure next to each other
        spobj=subplot(1,2,1);
        [C,h] = contourf(Data.Speed.RPM, Data.Torque.percent,
Data.Eff.Total'*100,'LineWidth',1);
        set(h,'ShowText','on','TextStep',get(h,'LevelStep')*1)
        % Set Font Size and Type
        textobj = findobj('type', 'text');
        set(textobj, 'fontsize', TJHFontSize);
        set(textobj, 'FontName','times');
        set(spobj, 'fontsize', TJHFontSize);
        set(spobj, 'FontName','times');
        % Write Axis Labels
        xlabel('Speed (RPM)','fontsize',TJHFontSize,'FontName','times')
        ylabel('Torque (%)','fontsize',TJHFontSize,'FontName','times')
        % Write Title
        title(['Total', '--','Eff
(%)'],'fontsize',TJHFontSize,'FontName','times')
        grid on
        colormap summer

        % Plot Power Loss Figure
        spobj=subplot(1,2,2);
        [C,h] = contourf(Data.Speed.RPM, Data.Torque.percent,
Data.PwrLoss_kW.Total', 'LineWidth',1);
        set(h,'ShowText','on','TextStep',get(h,'LevelStep')*1)
        % Set Font Size and Type
        textobj = findobj('type', 'text');
        set(textobj, 'fontsize', TJHFontSize);
        set(textobj, 'FontName','times');
```

```matlab
        set(spobj, 'fontsize', TJHFontSize);
        set(spobj, 'FontName','times');
        % Write Axis Labels
        xlabel('Speed (RPM)','fontsize',TJHFontSize,'FontName','times')
        ylabel('Torque (%)','fontsize',TJHFontSize,'FontName','times')
        % Write Title
        title([strcat('Total', '--','PwrLoss
(kW)')],'fontsize',TJHFontSize,'FontName','times')
        grid on
        colormap summer
    end

    findfigs
    save2word('Figures.doc')
end
end

%-------------------------------------------------------------------------------

function [Eff,PLoss]=DetermineEff(PwrMat1,PwrMat2)
% Print Matrix
PwrMat1;          % PwrMat1
PwrMat2;
% Get Matrix Size
[rlen,clen]=size(PwrMat1);
DataSignOpp = sign(PwrMat1.*PwrMat2);  % Negative means the Signs are
opposite
% Pre allocated Size
Eff=zeros(rlen,clen);
Pin=zeros(rlen,clen);
Pout=zeros(rlen,clen);
PLoss=zeros(rlen,clen);
% Loop and check data
for i=1:rlen
    % Row

    for j = 1:clen
        % Column

        if DataSignOpp(i,j)>0
            % If the Pwr Mat Elements have same sign
            Pin(i,j)= max(abs(PwrMat1(i,j)),abs(PwrMat2(i,j)));
            Pout(i,j)= min(abs(PwrMat1(i,j)),abs(PwrMat2(i,j)));
        else
            % Other cases
            Pout(i,j)= 0;
            Pin(i,j)= abs(PwrMat2(i,j))+abs(PwrMat1(i,j));
        end
        Eff(i,j) = Pout(i,j)/Pin(i,j);          % Calc Eff Pout/Pin
        PLoss(i,j) = Pin(i,j)-Pout(i,j);          % Calc Eff Pout/Pin
        %disp(['Eff = ',num2str(Eff(i,j))]);

    end
end

end

%-------------------------------------------------------------------------------
```

```matlab
% Define Function to assemble Data
function[Data]=AssembleDataFunc(Data,FileName,SheetNames,Columns,NumSheets,NumCols,Torque_HeaderRow)

CatNames = {'VpHz','V_{rms} (V)','I_{rms}(A)','P (kW)', 'Q (kVAR)','S (kVA)','\lambda','\phi (\circ)','T_{shaft} (in-lbs)', 'P_{shaft} (Hp)'};
CatVarNames = {'VpHz','Vin_V','Iin_A','Pwr_kW', 'Q_kVAR','S_kVA','lambda','phi_deg','Trq_shaft_inlbs', 'Pwr_shaft_Hp'};

%For Loop for Components (1-6) and each category (ie. P, Vrms, Irms, ....)
for Cmp=1:NumSheets

    %Get Component Name from Sheets
    SheetName = char(SheetNames(Cmp));
    ParsedData=textscan(SheetName,'%s','delimiter','-');
    CompName = ParsedData{1,1}{2,1};

    %Assemble the Category Data (ie. P, Vrms, Irms, ....)
    for i=1:NumCols

        % Assemble Data

[ColName,DataMat]=AssembleDataSubFunc1(FileName,SheetName,Columns(i),Torque_HeaderRow);

        %Write Data Matrix to Appropaite Name (ie. Data.Inverter.P_kW)
        ['Data.',CatVarNames{i}];
        Data.(CatVarNames{i}).(CompName).('ZValues') = DataMat;
        Data.(CatVarNames{i}).(CompName).('Title') = [strcat(CompName, '--',CatNames(i))];


        if 1
            % Plot Data
            figure
            surf(Data.Torque.percent,Data.Speed.RPM,DataMat)
            ylabel('Speed (RPM)')
            xlabel('Torque (%)')
            title([strcat(CompName, '--',CatNames(i))])
            colormap hsv
            colorbar
        end

    end
end

%Save Assembled Data to a workspace file
save('Data_Assembled.mat')

end

% Define Function to assemble Data
function[ColName,num]=AssembleDataSubFunc1(FileName,SheetName,Column,Torque_HeaderRow)
clc
```

```matlab
%Read Column Name
Range=[Column,'3'];
[x,ColName,y] = xlsread(FileName,SheetName,Range);


%Actually Assembles Data into Matrix
for i=1:length(Torque_HeaderRow)
    %Defines the Range to be Assembled

Range=[Column,num2str(Torque_HeaderRow(i)+2),':',Column,num2str(Torque_Header
Row(i)+2+5)];
    Range;
    num(:,i) = xlsread(FileName,SheetName,Range);
    num;
end
end
```

```matlab
function save2word(filespec,prnopt)


% SAVE2WORD saves plots to Microsoft Word.
% function SAVE2WORD(filespec,prnopt) saves the current Matlab figure
%  window or Simulink model window to a Word file designated by
%  filespec.  If filespec is omitted, the user is prompted to enter
%  one via UIPUTFILE.  If the path is omitted from filespec, the
%  Word file is created in the current Matlab working directory.
%
%  Optional input argument prnopt is used to specify additional save
%  options:
%    -fHandle   Handle of figure window to save
%    -sName     Name of Simulink model window to save
%
%  Examples:
%  >> saveppt
%       Prompts user for valid filename and saves current figure
%  >> save2word('junk.doc')
%       Saves current figure to MS Word file called junk.doc
%  >> save2word('junk.doc','-f3')
%       Saves figure #3 to MS Word file called junk.doc
%  >> save2word('models.doc','-sMainBlock')
%       Saves Simulink model named "MainBlock" to file called models.doc
%
%  The command-line method of invoking SAVEPPT will also work:
%  >> save2word models.doc -sMainBlock
%
%  If the figure has to be pasted as a smaller size bitmap, go to
%  File->preferences->Figure Copy Template->Copy Options and
%  check "Match Figure Screen Size" checkbox.
%  Then make the figure small before by setting the position
%  of the figure to a smaller size using
%  set(gca,'Position',[xpos,ypos,width,height])
%
%  Check also saveppt in Mathworks fileexchange

%Suresh E Joel, Mar 6,2003
%Virginia Commonwealth University
```

94

```matlab
%Modification of 'saveppt' in Mathworks File Exchange
%and valuable suggestions by Mark W. Brown, mwbrown@ieee.org
%

% Establish valid file name:
if nargin<1 | isempty(filespec);
  [fname, fpath] = uiputfile('*.doc');
  if fpath == 0; return; end
  filespec = fullfile(fpath,fname);
else
  [fpath,fname,fext] = fileparts(filespec);
  if isempty(fpath); fpath = pwd; end
  if isempty(fext); fext = '.doc'; end
  filespec = fullfile(fpath,[fname,fext]);
end

% Capture current figure/model into clipboard:
if nargin<2
  print -dmeta
else
  print('-dmeta',prnopt)
end

% Start an ActiveX session with PowerPoint:
word = actxserver('Word.Application');
%word.Visible = 1;

if ~exist(filespec,'file');
   % Create new presentation:
  op = invoke(word.Documents,'Add');
else
   % Open existing presentation:
  op = invoke(word.Documents,'Open',filespec);
end

% Find end of document and make it the insertion point:
end_of_doc = get(word.activedocument.content,'end');
set(word.application.selection,'Start',end_of_doc);
set(word.application.selection,'End',end_of_doc);

% Paste the contents of the Clipboard:
invoke(word.Selection,'Paste');

if ~exist(filespec,'file')
  % Save file as new:
  invoke(op,'SaveAs',filespec,1);
else
  % Save existing file:
  invoke(op,'Save');
end

% Close the presentation window:
invoke(op,'Close');

% Quit MS Word
invoke(word,'Quit');
```

```matlab
% Close PowerPoint and terminate ActiveX:
delete(word);

return
```

APPENDIX D. MACHINE EQUIVALENT PARAMETERS

D.1 Machine Equivalent Circuit Parameters Data and Calculation

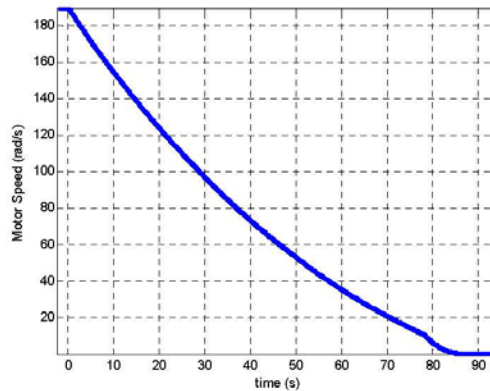# SB31 Machine Data Calculation
ABB 20HP Machine @ 230V
Configuration

Trever Hassell
June 9, 2012

_____

Init Stuff (✓)

- **Initialization Cells**

_____

Lab Data Calc (✓)

- **Sec 4.6- -- Motor Inertia Calc**
- **4.6 -- Matlab Data (✓)**

- **4.6 Solve for J (✓)**

97

$$J = \frac{-(T_f + B\omega_m)}{\frac{d\omega_m}{dt}}\Bigg|_{t=0^+} \approx \frac{-(K_m I_a)\big|_{t=0^-}}{\frac{d\omega_m}{dt}\Big|_{t=0^+}} \tag{10}$$

Ia(0) = 0.93673
ωm(0) = 507.1

J2 = $\frac{-\tau}{\frac{d\omega m}{dt}}$

ParamsJ = $\Big\{\tau \to 2 * \frac{1}{8.850745454}$, $d\omega m \to \Big(-(1797.) * \frac{\pi}{30}\Big)$, $dt \to 60 + 27.6\Big\}$
J2 /. ParamsJ // EngineeringForm

$-\dfrac{dt\,\tau}{d\omega m}$

$\{\tau \to 0.22597,\ d\omega m \to -188.181,\ dt \to 87.6\}$

105.191×10^{-3}

Number of Poles (✓)

■ **Problem Statement**

Find Number of Poles of the ABB 20 HP Induction Machines

Frequency (f_{out}) Hz	Speed (RPM)	Speed ($\frac{rads}{sec}$)	Mechincal Frequency (Hz)	Poles (~)
15.0	898	94.04	15.0	1.0
30.0	1797	188.18	30.0	1.0
45.0	2695	282.22	44.9	1.0
60.0	3592	376.15	59.9	1.0

No Load - Blocked Rotor Tests (✓)

■ **Problem Statement**

No load and blocked rotor test was performed on a three-phase, class A induction machine
and the following data was collected:

The dc phase resistance was found to be 0.3 Ω.

Find magnetizing reactance and the rotor resistance of this machine

No − Load	Blocked Rotor
$f_e = 60\,Hz$	$f_e = 15\,Hz$
$V_{an} = 220.04\,V_{rms}$	$V_{an} = 16.68\,V_{rms}$
$I_a = 7.463\,A_{rms}$	$I_a = 39.585\,A_{rms}$
$P_a = ??\,W$	$P_a = 138\,W$
$P_\Sigma = 723\,W$	$P_\Sigma = 719\,W$
$S_\Sigma = 2729\,VA$	$S_\Sigma = 1148\,VA$

No Load	-	Blocked Rotor

No Load	-	Blocked Rotor

99

■ **Initialization Cells**

■ **Define Functions and Variables (✓)**

```
ParamsGlobalValues = {nph → 3, Rdc → 0.3};
ParamsGlobalValuesNL = {feNL → 60, VlNL → 220.04, IaNL → 7.463, PNL → 723, SNL → 2808};
ParamsGlobalValuesBL = {feBL → 15, VlBL → 16.68, IaBL → 39.585, PBL → 719, SBL → 1148};
Grid[{ParamsGlobalValues, ParamsGlobalValuesNL, ParamsGlobalValuesBL}] // N //
  EngineeringForm
```

nph → 3.	Rdc → $300. \times 10^{-3}$			
feNL → 60.	VlNL → 220.04	IaNL → 7.463	PNL → 723.	SNL → 2.808×10^3
feBL → 15.	VlBL → 16.68	IaBL → 39.585	PBL → 719.	SBL → 1.148×10^3

The per-phase resistance is
$$R_1 = \frac{1}{2} R_{\text{measured}}$$

```
       1
R1 =  ─── Rdc /. ParamsGlobalValues
       2
```

```
0.15
```

■ Solution Approach

■ Find No Load Values

The core resistance is
$$R_c = 3 \frac{(V_{1,nl})^2}{P_{core}}$$

```
        3 V1NL²
Rc =  ─────────── /. ParamsGlobalValuesNL
          PNL
```

```
200.903
```

The total no-load Apperent Power is then
$$S_{nl} = n_{ph} V_{1,nl} I_{1,nl}$$

```
                V1NL
SNLCalc = nph  ─────── IaNL /. ParamsGlobalValuesNL /. ParamsGlobalValues
                √3
```

```
2844.3
```

The total no-load reactive power is then
$$Q_{nl} = \sqrt{S_{nl}^2 - P_{nl}^2}$$

```
QNL = √(SNL)² - (PNL)²  /. ParamsGlobalValuesNL // N
```

```
2713.33
```

The reactive is then found from
$$X_{nl} = \frac{Q_{nl}}{n_{ph} I_{1,nl}^2}$$

```
            QNL
XNL = ─────────────── /. ParamsGlobalValuesNL /. ParamsGlobalValues
        nph IaNL²
```

```
16.2388
```

■ Find Blocked Rotor Values

The total no-load Apperent Power is then
$$S_{nl} = n_{ph} V_{1,nl} I_{1,nl}$$

101

$$\text{SNLCalc} = \text{nph} \frac{\text{V1NL}}{\sqrt{3}} \text{ IaNL /. ParamsGlobalValuesNL /. ParamsGlobalValues}$$

> 2844.3

The total no-load reactive power is then

$$Q_{\text{bl}} = \sqrt{S_{\text{bl}}{}^2 - P_{bl}{}^2}$$

$$\text{QBL} = \sqrt{(\text{SBL})^2 - (\text{PBL})^2} \text{ /. ParamsGlobalValuesBL // N}$$

> 894.954

The reactive is then found from

$$X_{\text{bl}} = \frac{Q_{\text{bl}}}{n_{\text{ph}} \, I_{1,\text{bl}}^2}$$

$$\text{XBL} = \frac{\text{QBL}}{\text{nph IaBL}^2} \text{ /. ParamsGlobalValuesBL /. ParamsGlobalValues}$$

> 0.190379

The blocked-rotor resistance is

$$R_{\text{bl}} = \frac{P_{\text{bl}}}{n_{\text{ph}} \, I_{1,\text{bl}}^2}$$

$$\text{RBL} = \frac{\text{PBL}}{\text{nph IaBL}^2} \text{ /. ParamsGlobalValuesBL /. ParamsGlobalValues}$$

> 0.152949

The blocked-rotor reactance gives

$$X_2 = (X_{\text{bl}} - X_1)\left(\frac{X_{\text{bl}} - X_1}{X_{\text{bl}}' - X_{\text{bl}}}\right)$$

- **Find Equivalent Circuit Values**

  {XBL, XNL}

> {0.190379, 16.2388}

$$\text{Eq} = \text{X2} == (\text{XBL} - \text{X1}) \frac{(\text{XNL} - \text{X1})}{\text{XNL} - \text{XBL}}$$

> X2 = 0.0623115 (0.190379 − X1) (16.2388 − X1)

Class B Machine
See Table 6.1 on Page 335
$0.4\,X_1 + 0.6\,X_2 = 1$

```
Eq = Eq /. X1 → 0.6
              ─── X2
              0.4
```

$$X2 = 0.0623115 (0.190379 - 1.5 \, X2) (16.2388 - 1.5 \, X2)$$

```
SolEq = Solve[Eq, X2];
SolEq // N
X2 = X2 /. First[SolEq];
     0.6
X1 = ─── X2
     0.4
```

$$\{\{X2 \to 0.0762952\}, \{X2 \to 18.0091\}\}$$

```
0.114443
```

We can then find the magnetizing reactance
$X_m = X_{nl} - X_1$

```
XM = XNL - X1
```

```
16.1244
```

The rotor resistance is found from
$R_2 = (R_{bl} - R_1) \left(\dfrac{X_2 + X_m}{X_m} \right)^2$

```
R1
RBL
            ⎛ X2 + XM ⎞²
R2 = (RBL - R1) ⎜ ─────── ⎟
            ⎝  XM   ⎠
```

```
0.15
```

```
0.152949
```

```
0.00297687
```

103

$$L1 = \frac{X1}{2\,\pi\,feNL}\ /.\ ParamsGlobalValuesBL\ /.\ ParamsGlobalValuesNL$$

$$L2 = \frac{X2}{2\,\pi\,feNL}\ /.\ ParamsGlobalValuesBL\ /.\ ParamsGlobalValuesNL$$

$$LM = \frac{XM}{2\,\pi\,feNL}\ /.\ ParamsGlobalValuesBL\ /.\ ParamsGlobalValuesNL$$

```
0.000303569
```

```
0.000202379
```

```
0.0427712
```

- **Calculated Machine Parameters**

```
Sol1StrMatrix1 = Grid[{
    {StringForm["R₁ = `1` Ω", N[Round[R1, 10⁻⁴]]] // TraditionalForm,
     StringForm["R₂ = `1` Ω", N[Round[R2, 10⁻⁴]]] // TraditionalForm,
     StringForm["R_C = `1` Ω", N[Round[Rc, 10⁻⁴]]] // TraditionalForm},
    {StringForm["X₁ = `1` Ω", N[Round[X1, 10⁻⁴]]] // TraditionalForm,
     StringForm["X₂ = `1` Ω", N[Round[X2, 10⁻⁴]]] // TraditionalForm,
     StringForm["X_m = `1` Ω", N[Round[XM, 10⁻⁴]]] // TraditionalForm}
    }] // MatrixForm;
Sol1StrMatrix2 = Grid[{
    {StringForm["R₁ = `1` Ω", N[Round[R1, 10⁻⁴]]] // TraditionalForm // EngineeringForm,
     StringForm["R₂ = `1` Ω", N[Round[R2, 10⁻⁶]]] // TraditionalForm // EngineeringForm,
     StringForm["R_C = `1` Ω", N[Round[Rc, 10⁻⁴]]] // TraditionalForm // EngineeringForm},
    {StringForm["L₁ₛ = `1` Ω", N[Round[L1, 10⁻⁸]]] // TraditionalForm // EngineeringForm,
     StringForm["L₁ᵣ = `1` Ω", N[Round[L2, 10⁻⁸]]] // TraditionalForm // EngineeringForm,
     StringForm["L_m = `1` Ω", N[Round[LM, 10⁻⁸]]] // TraditionalForm // EngineeringForm}
    }] // MatrixForm;
```

- **Solution**

```
Sol1StrMatrix1
Sol1StrMatrix2
```

$$R_1 = 0.15\ \Omega \quad R_2 = 0.003\ \Omega \quad R_C = 200.903\ \Omega$$
$$X_1 = 0.1144\ \Omega \quad X_2 = 0.0763\ \Omega \quad X_m = 16.1244\ \Omega$$

$$R_1 = 150.\times 10^{-3}\ \Omega \quad R_2 = 2.977\times 10^{-3}\ \Omega \quad R_C = 200.903\ \Omega$$
$$L_{1s} = 303.57\times 10^{-6}\ \Omega \quad L_{1r} = 202.38\times 10^{-6}\ \Omega \quad L_m = 42.7712\times 10^{-3}\ \Omega$$

- **Extra Stuff**

No Load

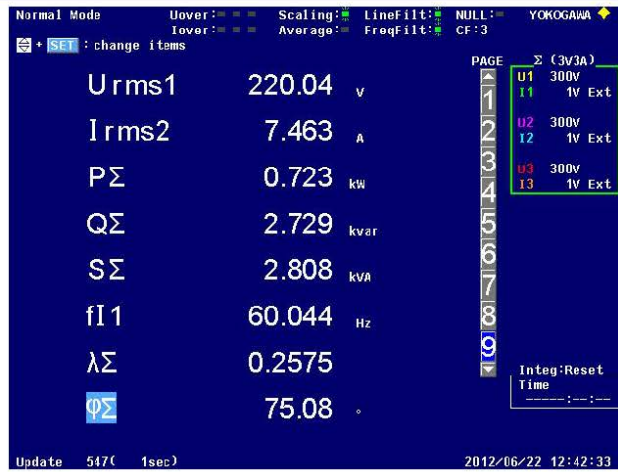$$R_1 = 0.15\ \Omega \quad R_2 = 0.003\ \Omega \quad R_C = 200.903\ \Omega$$
$$X_1 = 0.1144\ \Omega \quad X_2 = 0.0763\ \Omega \quad X_m = 16.1244\ \Omega$$

$$R_1 = 0.15\ \Omega \qquad R_2 = 0.003\ \Omega \qquad R_C = 200.903\ \Omega$$
$$L_{1s} = 300.\times10^{-6}\ \Omega \quad L_{1r} = 200.\times10^{-6}\ \Omega \quad L_m = 42.77\times10^{-3}\ \Omega$$

Blocked Rotor

$$R_1 = 0.15\ \Omega \qquad R_2 = 0.003\ \Omega \qquad R_C = 200.903\ \Omega$$
$$X_1 = 0.1144\ \Omega \quad X_2 = 0.0763\ \Omega \quad X_m = 16.1244\ \Omega$$

$$R_1 = 0.15\ \Omega \qquad R_2 = 0.003\ \Omega \qquad R_C = 200.903\ \Omega$$
$$L_{1s} = 1.21\times10^{-3}\ \Omega \quad L_{1r} = 810.\times10^{-6}\ \Omega \quad L_m = 171.08\times10^{-3}\ \Omega$$

105

APPENDIX E. DRAWING FILES

E.1 Electrical Schematic (SB31E001)

107
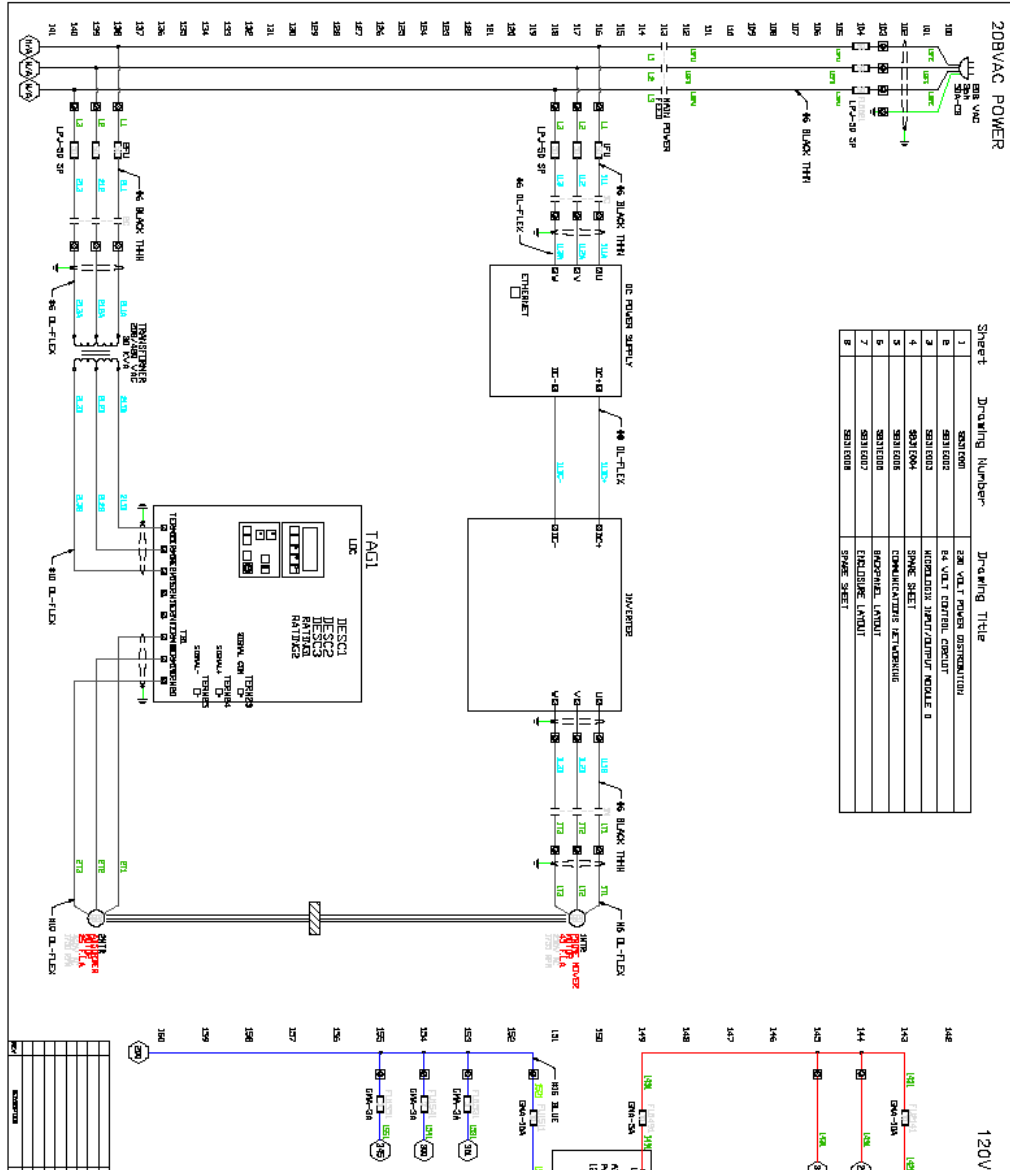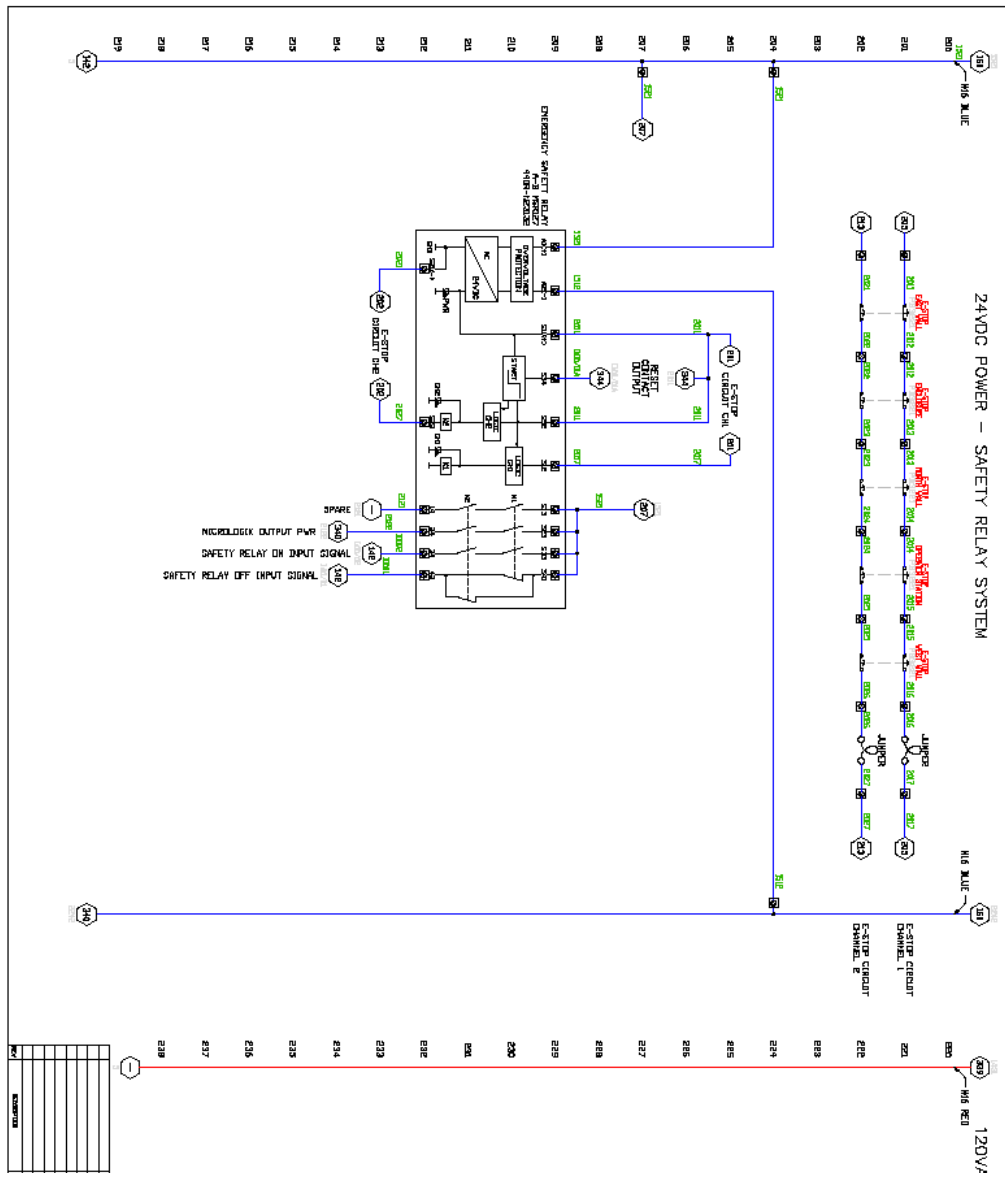
E.3 Electrical Schematic (SB31E003)
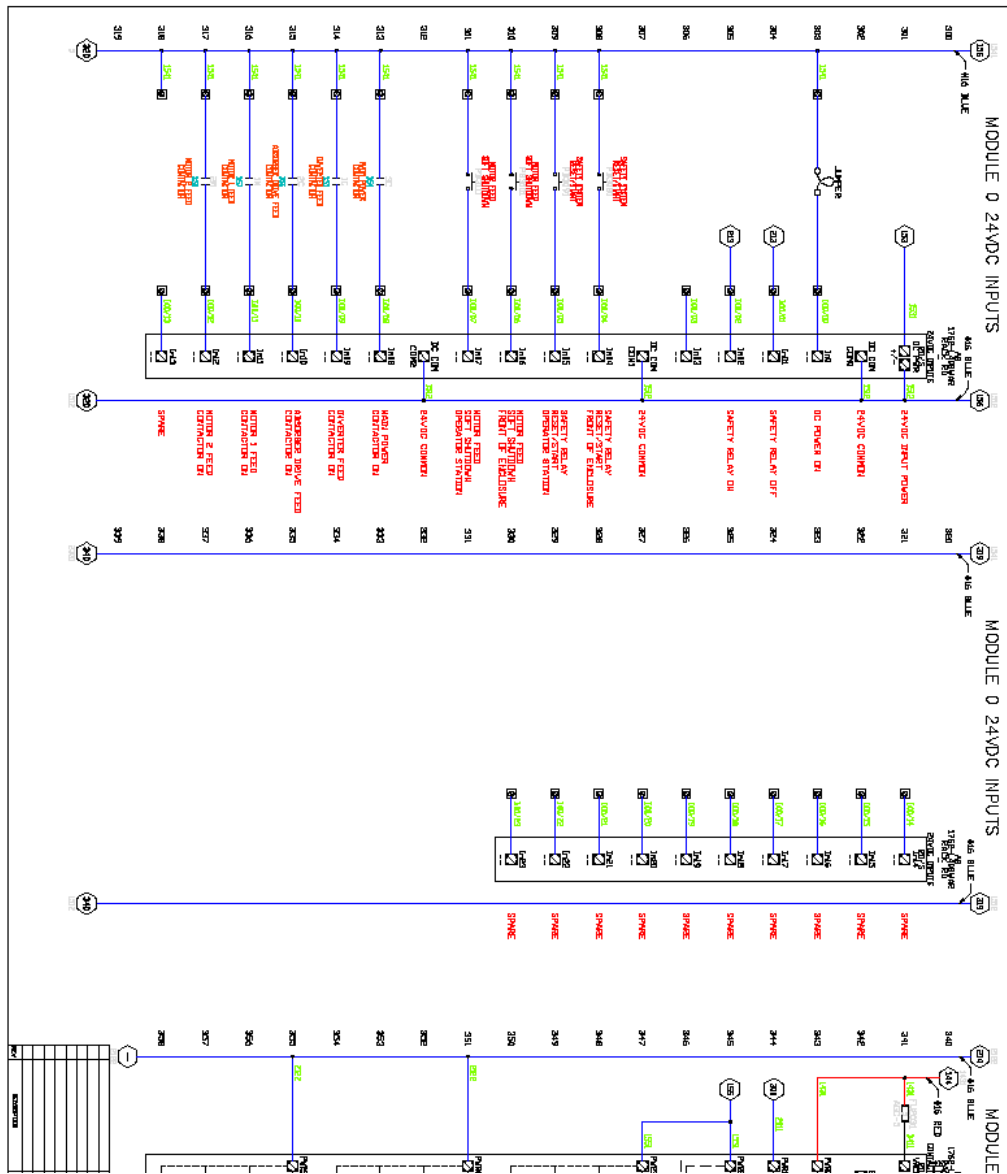
E.4 Electrical Schematic (SB31E004)

SPARE SHEET
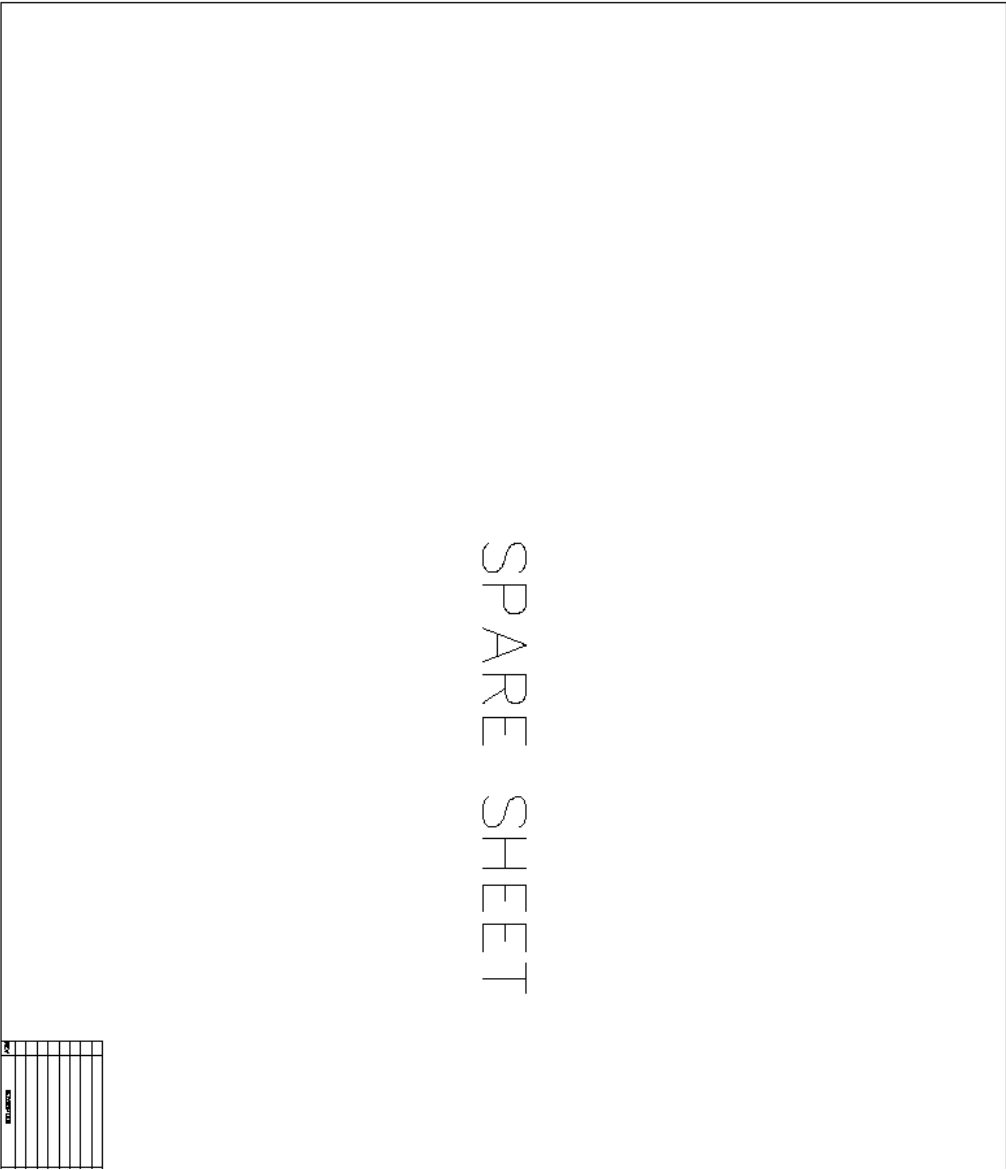
E.5 Electrical Schematic (SB31E005)
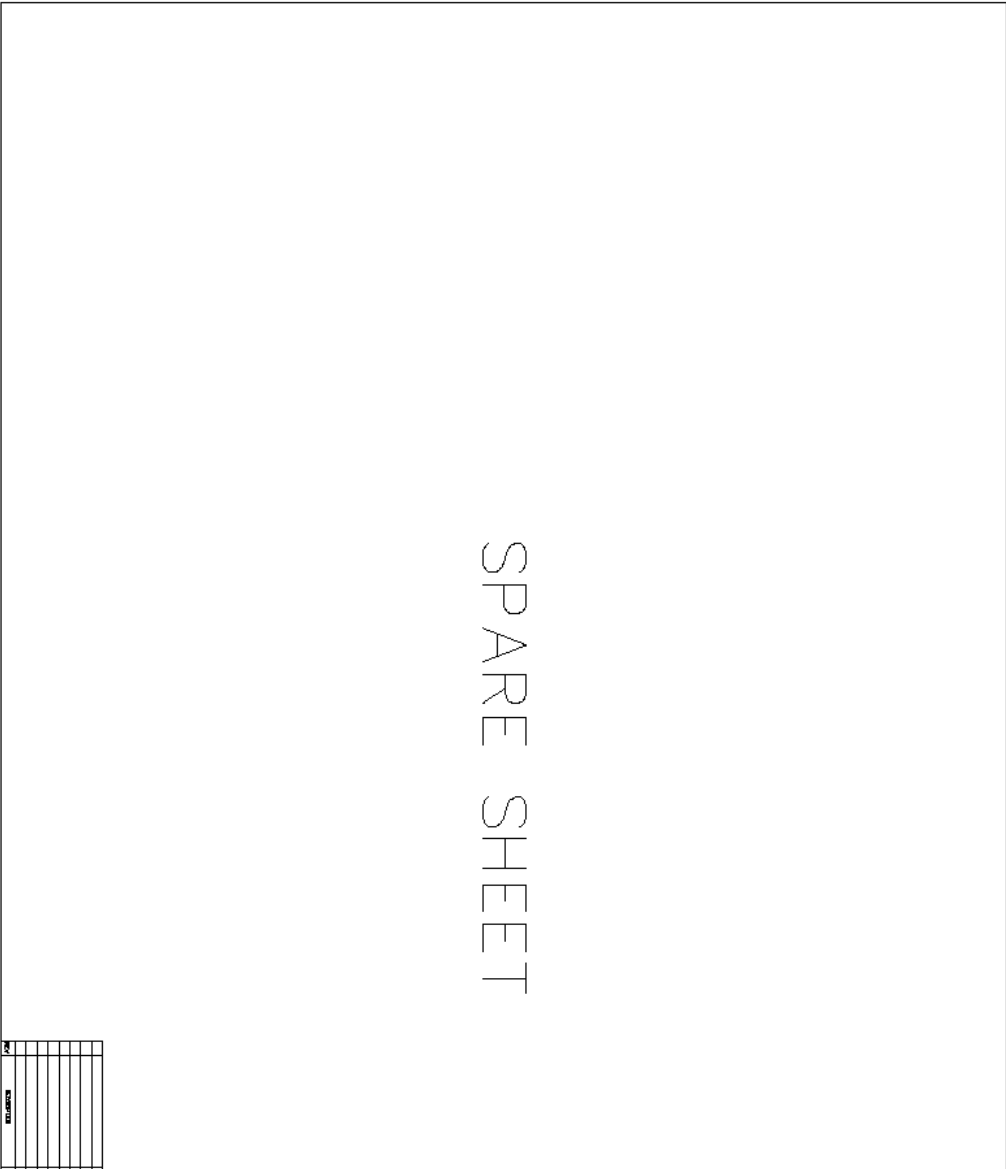
SPARE SHEET

E.6 Electrical Schematic (SB31E006)
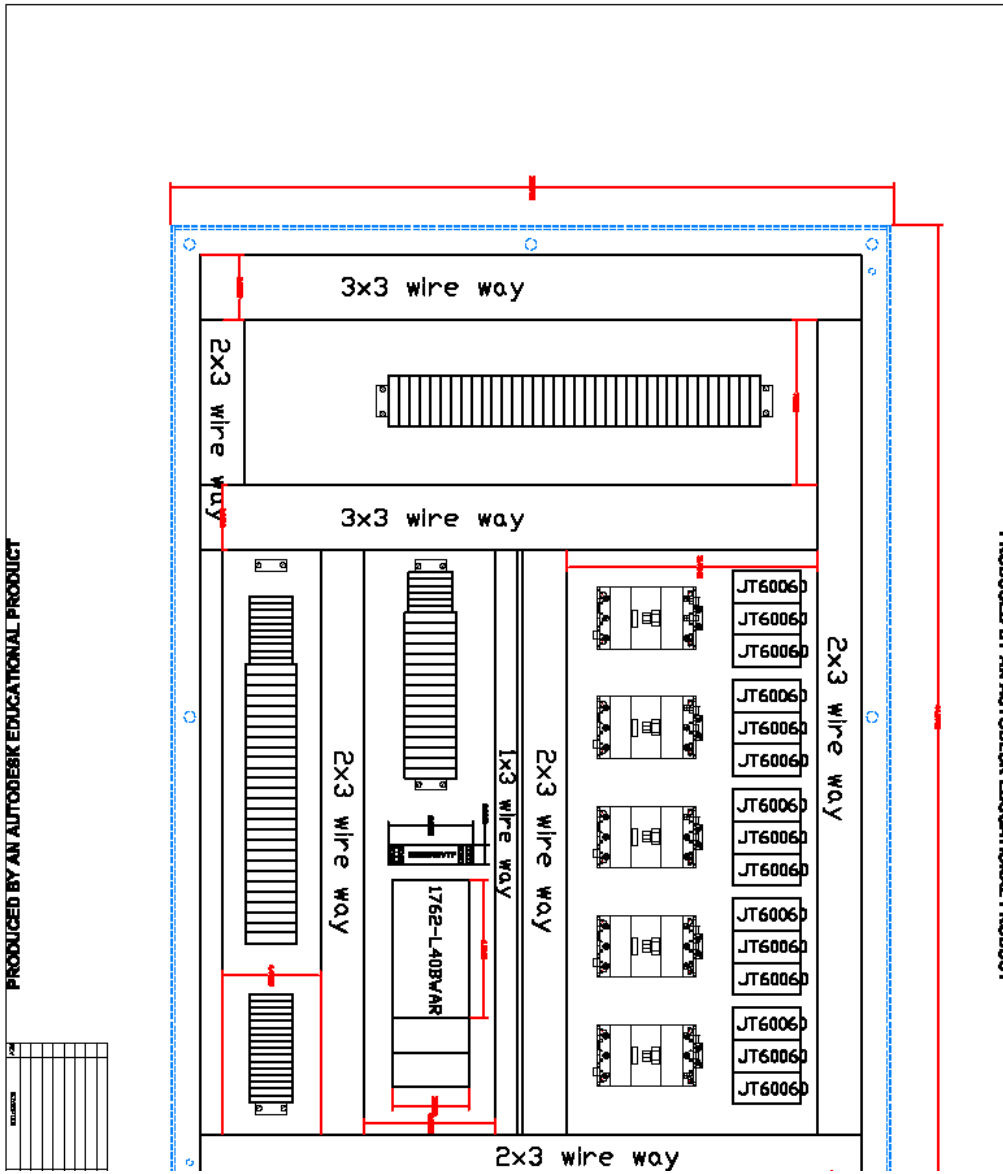
E.7 Electrical Schematic (SB31E007)
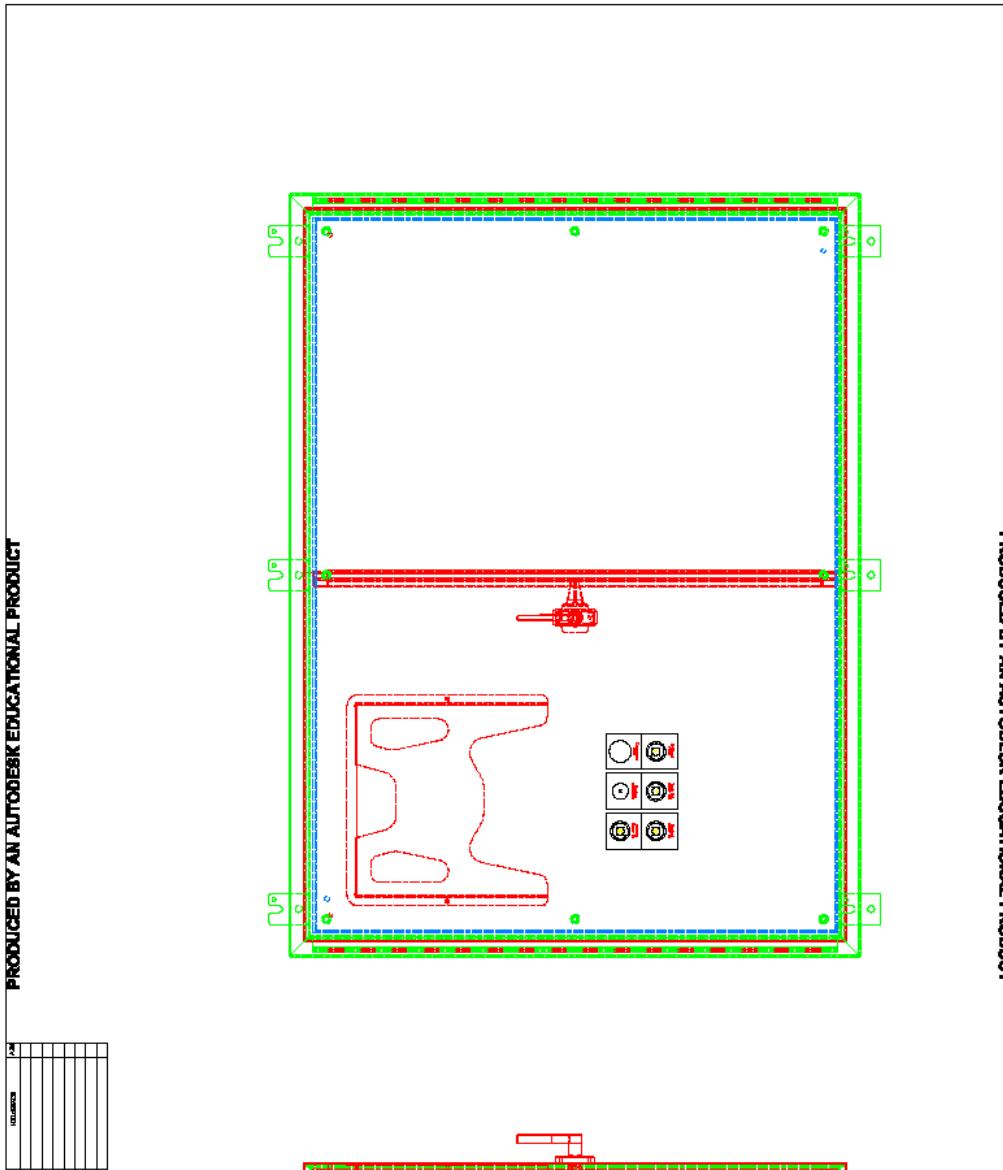
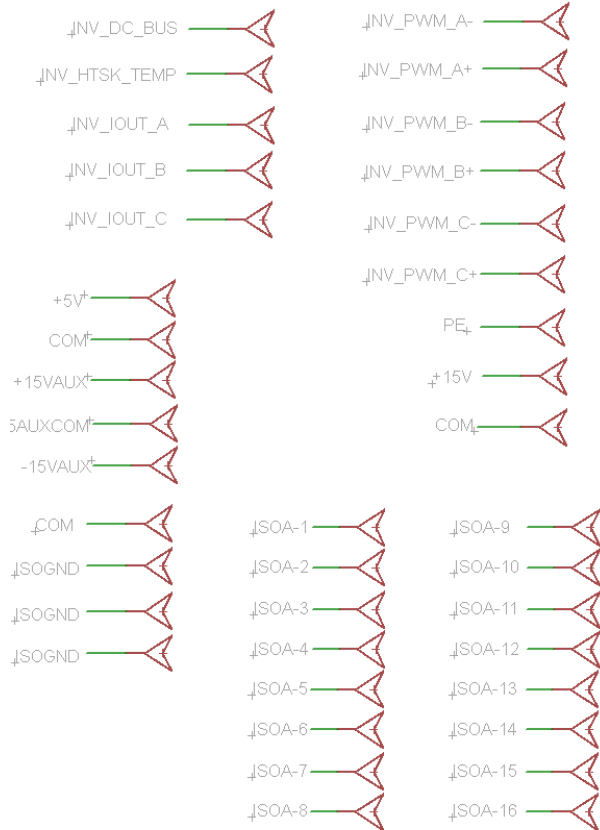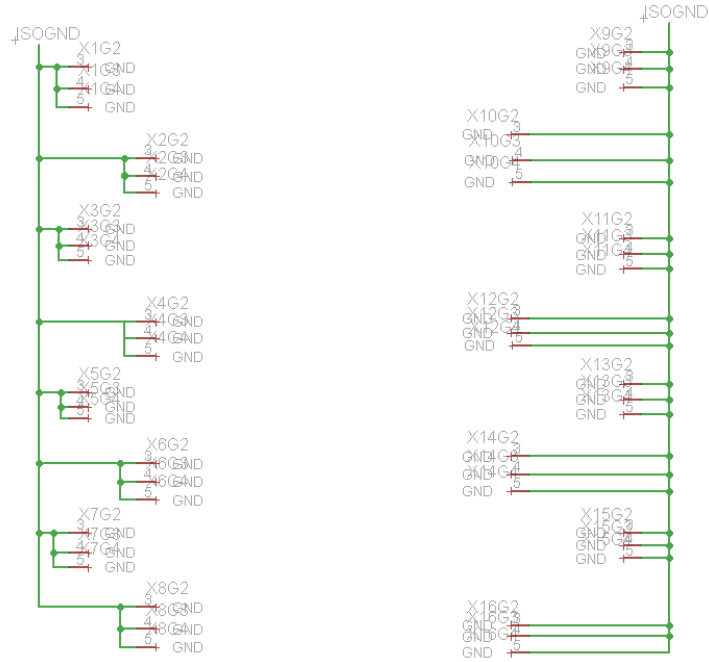**E.8 Electrical Schematic (SB31E008)**

SPARE SHEET
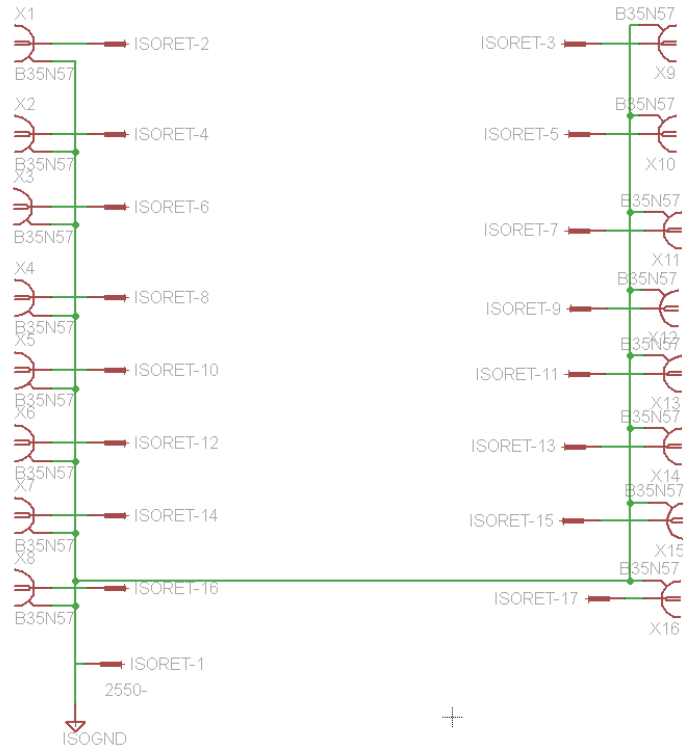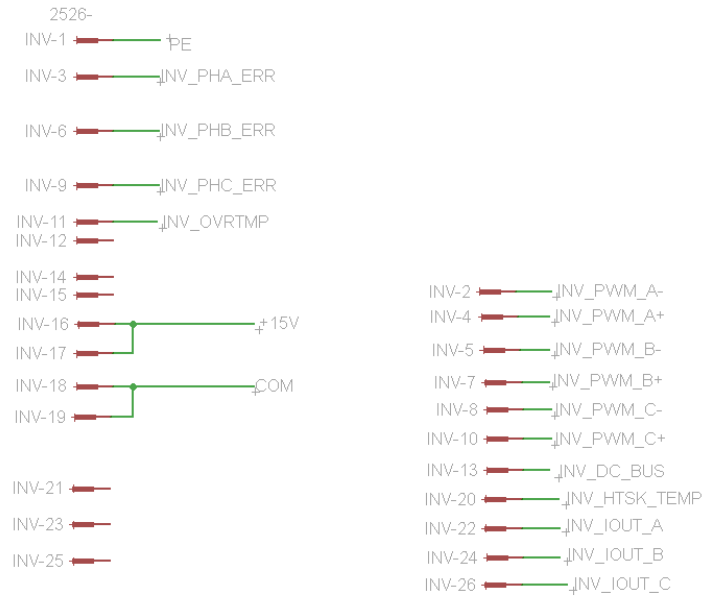
E.9 Induction Machine Rotor Blocking Fixture
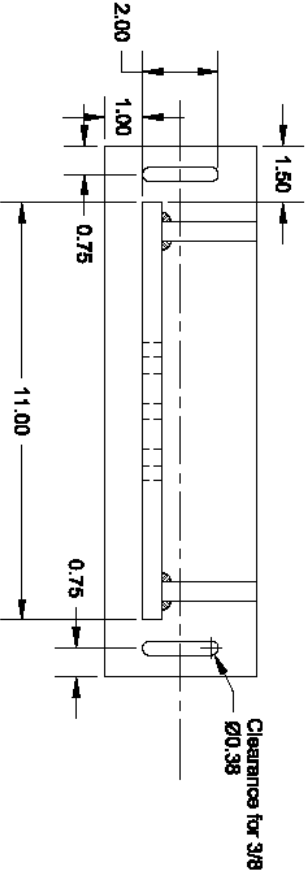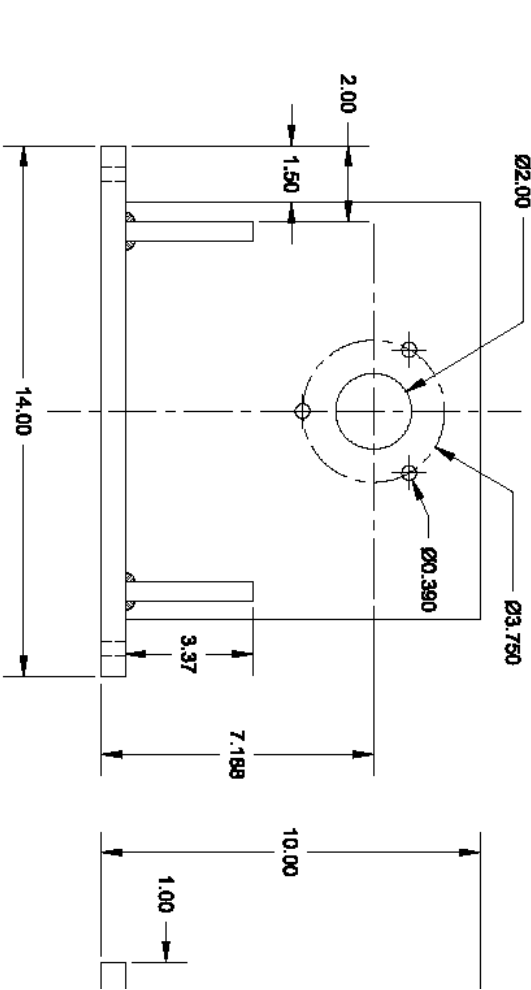
All material is 1/2" steel plate

APPENDIX F. SIGNAL ISOLATION BOARD

F.1 Electrical Schematic

X1
B35N57 — ISORET-2
X2
B35N57 — ISORET-4
X3
B35N57 — ISORET-6
X4
B35N57 — ISORET-8
X5
B35N57 — ISORET-10
X6
B35N57 — ISORET-12
X7
B35N57 — ISORET-14
X8
B35N57 — ISORET-16
— ISORET-1
2550-

ISOGND

B35N57
ISORET-3 —
X9
B35N57
ISORET-5 —
X10
B35N57
ISORET-7 —
X11
B35N57
ISORET-9 —
X12
B35N57
ISORET-11 —
X13
B35N57
ISORET-13 —
X14
B35N57
ISORET-15 —
X15
B35N57
ISORET-17 —
X16

Inverter Connector
2526-
INV-1 — PE
INV-3 — INV_PHA_ERR
INV-6 — INV_PHB_ERR
INV-9 — INV_PHC_ERR
INV-11 — INV_OVRTMP
INV-12 —

INV-14 —
INV-15 —
INV-16 — +15V
INV-17 —
INV-18 — COM
INV-19 —

INV-21 —

INV-23 —

INV-25 —

INV-2 — INV_PWM_A-
INV-4 — INV_PWM_A+
INV-5 — INV_PWM_B-
INV-7 — INV_PWM_B+
INV-8 — INV_PWM_C-
INV-10 — INV_PWM_C+
INV-13 — INV_DC_BUS
INV-20 — INV_HTSK_TEMP
INV-22 — INV_IOUT_A
INV-24 — INV_IOUT_B
INV-26 — INV_IOUT_C

Analog Out from Inverter

INV_DC_BUS — INV-ANAL-A-1
COM — INV-ANAL-A-2   MKDSN1,5/3-5,08
INV_HTSK_TEMP — INV-ANAL-A-3
COM — INV-ANAL-B-1
INV_IOUT_A — INV-ANAL-B-2   MKDSN1,5/3-5,08
COM — INV-ANAL-B-3
INV_IOUT_B — INV-ANAL-C-1
COM — INV-ANAL-C-2   MKDSN1,5/3-5,08
INV_IOUT_C — INV-ANAL-C-3

INV_PWM_A- — DIGA-1   MKDSN1,5/3-5,08
INV_PWM_A+ — DIGA-2
INV_PWM_B- — DIGA-3
INV_PWM_B+ — DIGB-1   MKDSN1,5/3-5,08
INV_PWM_C- — DIGB-2
INV_PWM_C+ — DIGB-3
PE — DIGC-1
F1   +15V — DIGC-2   MKDSN1,5/3-5,08
D4   COM — DIGC-3

C1   IC1P
+5V VCC   +   GND   COM

+15V   +5V
R1 1K   TP1   IC1A   R4 4.7K   ERR_C
INV_PHC_ERR   13   12   74LS14N   TP2   R3 750   COM

+15V   +5V
R2 1K   TP3   IC1B   R6 4.7K   ERR_B
INV_PHB_ERR   11   10   74LS14N   TP4   R5 750   COM

+15V   +5V
R7 1K   TP5   IC1C   R9 4.7K   ERR_A
INV_PHA_ERR   9   8   74LS14N   TP6   R8 750   COM

+15V   +5V
R10 1K   TP7   IC1D   R11 4.7K   OVRTMP
INV_OVRTMP   1   2   74LS14N   TP8   R12 750   COM

+15V
C3   C2   1.5K   +15V
COM   R14

+5V
C5   C4   500   +5V
COM   R13

+15VAUX
C7   C6   1.5K   +15V_AUX
+15VAUXCOM   R16

-15AUXCOM
C9   C8   1.5K   -15V_AUX
-15VAUX   R17

COM   0.   ISOGND
R15

+15VAUX   D1   MKDSN1,5/3-5,08   PWR_AUX-1
15AUXCOM   PWR_AUX-2
-15VAUX   D2   PWR_AUX-3

+5V   D3   MKDSN1,5/3-5,08   PWR_A-1
PWR_A-2
5VCOM   PWR_A-3
E-GND   PWR_B-1
PWR_B-2
5VCOM   PWR_B-3
MKDSN1,5/3-5,08
E-GND

22-23-2081
F2   AUXPWR-1
+5V   AUXPWR-2
COM   FUSEBLANK_5X20MM   AUXPWR-3
AUXPWR-4
F3   AUXPWR-5
+15VAUX   FUSEBLANK_5X20MM   AUXPWR-6
-15AUXCOM   AUXPWR-7
-15VAUX   F4   AUXPWR-8
FUSEBLANK_5X20MM

117

F.2 PCB Layout